Hydraulic traits and drought mortality risk of tree species

By

Ximeng Li (BSc, MSc)

A thesis submitted in fulfilment of the requirements

for the degree of Doctor of Philosophy

Hawkesbury Institute for the Environment

Western Sydney University

Acknowledgements

Upon the completion of the thesis, I would like to take this opportunity to express my sincere gratitude to my supervisor, Professor David Tissue, who has given me important guidance on the thesis. Without his help and encouragement, my thesis would have been impossible. Besides his help with my thesis, he has also given me much advice on the methods of doing research, which is of great value to my future academic life.

I also want to express my gratitude to my supervisory committee, Professor Belinda Medlyn, Professor Brendan Choat, Professor Remko Duursma and Dr. Chris Blackman for their inspirational help, advice and encouragement during my experiment and thesis writing.

I am also obliged to my lab members, Ms Renee Smith, Ms Chelsea Maier, Ms Anthea Challis, Dr Wen Shi, Dr. Jingting Bao, Ms Jennifer Peters, Ms Alice Gauthey and Ms Leah Koloadin for their support and assistance during my experiment.

I greatly appreciate members of HIE, Dr David Harland, Ms Patricia Hellier, Ms Jenny Harvey, Ms Lisa Davison, Mr Mr Gavin McKenzie, Mr Burhan Amiji, Mr Goran Lopaticki, Dr. Craig Barton, Dr. Andrew Gherlenda, Dr. Marcus Klein for facilitating my life and work in Australia.

I thank the financial support from HIE. Meanwhile, I gratefully acknowledge Prof. Kevin Griffin, Professor Jinchao Feng and Dr Chengyuan Xu, who had made my study at HIE finally happen.

Lastly, I am deeply indebted to my beloved parents and my wife Jing Xue, who have been supporting me in the last ten years. Their encouragement and support have accompanied me through the difficult course of the thesis and moments of my life.

Statement of Authentication

Statement of Authentication The work presented in this thesis is, to the best of my knowledge and belief, original except as acknowledged in the text. I hereby declare that I have not submitted this material, either in full or in part, for a degree at this or any other institution.

…… [redacted] ……..

Table of Contents

List of tables

List of figures

List of abbreviations

AI (dimensionless)	Aridity index
A_{max} (μmol m^{-2} s^{-1})	Maximum carbon assimilation rate under well-watered conditions
C (kg m^{-3} MPa^{-1})	Hydraulic capacitance
C^*_{FT} (mmol m^{-2} MPa^{-1})	Leaf hydraulic capacitance
C_{branch} (RWC MPa^{-1})	Hydraulic capacitance of whole branch
D (mm)	Plant basal diameter
g_{smax} (mol m^{-2} s^{-1})	Maximum stomatal conductance
H (cm)	Plant height
HSM_{HS} (MPa)	Hydraulic safety of hydraulic segmentation
HSM_{ST} (MPa)	Hydraulic safety of stomatal regulation
Hydroscape (MPa^2)	Hydroscape area
K_L (kg m^{-1} s^{-1} MPa^{-1})	Maximum leaf specific conductivity
K_{leaf} (kg m^{-1} s^{-1} MPa^{-1})	Leaf conductivity
K_s (kg m^{-1} s^{-1} MPa^{-1})	Maximum stem specific conductivity
MAP (mm)	Mean annual precipitation
MAT (^oC)	Mean annual temperature
P_{gs} (MPa)	Water potential threshold for stomatal closure
P_{gs50} (MPa)	Ψ_{leaf} at 50% of maximum stomatal conductance
P_{gs90} (MPa)	Ψ_{leaf} at 10% of maximum stomatal conductance
P_{L50} (MPa)	Ψ_{leaf} at 50% loss of xylem conductivity in leaves
PLC (%)	Percentage loss of conductivity

P_x (MPa)	Water potential threshold for xylem embolism in stems
P_{X12} (MPa)	Ψ_{stem} at 12% loss of xylem conductivity in stems
P_{X50} (MPa)	Ψ_{stem} at 50% loss of xylem conductivity in stems
P_{X88} (MPa)	Ψ_{stem} at 88% loss of xylem conductivity in stems
SLA (m^2 kg^{-1})	Specific leaf area
Slope (dimensionless)	Slope of Ψ_{pd} vs. Ψ_{md} relationship
TLP (MPa)	Leaf turgor loss point
VIGR (cm^3 day^{-1})	Stem volume index growth rate
VPD (KPa)	Vapor pressure deficit
WD (g cm^3)	Sapwood density
$\Delta\Psi_{max}$ (MPa)	Maximum range of daily leaf water potential variation
ε (MPa)	Modulus of elasticity
Ψ_{leaf} (MPa)	Leaf water potential
Ψ_{md} (MPa)	Midday leaf water potential
Ψ_{pd} (MPa)	Predawn leaf water potential
Ψ_{stem} (MPa)	Stem water potential

Abstract

Increased drought frequency and severity associated with global climate changehas contributed to large scale forest dieback on all vegetated continents. Forest dieback may alter community composition, leading to cascading negative impacts on ecosystem function and service, and creating a positive feedback loop between biosphere and atmosphere. Traits-based approaches have emerged as a promising way to accurately predict the impacts of climate change on vegetation dynamics. Yet predicting the forest mortality pattern resulting from drought stress remains challenging, largely because of a lack of knowledge of the plant traits determining the risk and modulating the process of drought-induced mortality, and how these traits vary across and within species. Hydraulic traits define species distributions along local or regional gradients of water availability, and recent advances in modelling forest dynamics highlight the critical role of hydraulic traits in improving model predictive power with respect to mortality events. Using various ecologically and economically important tree species from New South Wales, Australia, my PhD thesis was designed to examine inter-specific variation of various hydraulic traits across a wide range of species native to five different vegetation types: Rainforest (*Acmena smithii*), Wet sclerophyll forest (*Eucalyptus grandis*, *E. viminalis*), Dry sclerophyll forest (*Angophora costata*, *Corymbia gummifera*, *E. sideroxylon*), Grassy woodland (*E. blakelyi*, *E. macrorhyncha*, *E. melliodora*) and Semi-arid woodland (*Acacia aneura*, *E. largiflorens*, *E. populnea*). In addition, intra-specific variation of key hydraulic traits was examined for *Banksia serrata*. The primary objective of my work was to provide trait values that will help to predict the dynamics of tree species upon climate change with vegetation models. Furthermore, the correlative relationships among hydraulic traits and between traits and climate presented in this study broaden our understanding of plant hydraulic strategies and plant adaptation to low-rainfall environments.

In the first experimental chapter (Li et al. 2018a), a suite of hydraulic and carbon traits were examined on 12 ecologically important species representing five different vegetation types (Rainforest, Wet sclerophyll forest, Dry sclerophyll forest, grassy woodland and semiarid woodland) in New South Wales. Plants were grown in ambient environmental conditions in a poly-tunnel facility under well-watered conditions and then were exposed to two drought cycles. In the first drought cycle, plants were dried until leaves were visually wilting and were then rewatered for two weeks to allow for recovery. In the second drought cycle, plants were dried down to mortality by completely withholding irrigation. Plants were harvested progressively, and physiological status was monitored during this drought cycle. The results showed that drought response and key hydraulic traits varied markedly across species. In addition, a strong correlation was found between the water potential thresholds inducing stem embolism (P_x) and stomatal closure (P_{gs}). Importantly, P_{gs} was consistently less negative than P_x, indicating stomatal closure prevented the occurrence of xylem embolism during drought. Furthermore, there were trade-offs among P_x, hydraulic efficiency (K_s), whole branch hydraulic capacitance (C_{branch}) and wood density (WD), while P_{gs} and P_x were also negatively correlated with plant growth rate. Moreover, both P_{gs} and P_x were correlated with annual precipitation and aridity index of species' climate of origin. The findings of this experiment demonstrate that plant hydraulic traits are highly coordinated. The strong linkage between species' traits and their climate of origin suggest strong adaptation of stomatal behaviour and embolism resistance to the environment.

In the second experimental chapter (Li et al. 2019b), different metrics quantifying plant water regulation strategy were calculated and evaluated. Ten species from contrasting climates were grown in a polytunnel facility under well-watered conditions. A drought treatment similar to

that described in the first experimental chapter was applied to the plants, with predawn and midday leaf water potentials (Ψ_{pd} and Ψ_{md}) being measured during the second drought phase. Species' water regulation strategies were quantified either based on the degree of homeostasis of water potential during dry down or hydraulic traits defining stomatal behaviour and embolism resistance upon drought stress. Hydraulic traits were either measured on well-watered plants or sourced from the first experiment. Results showed that different metrics generated distinct rankings in terms of species response to drought. Among these, a newly developed metric, Hydroscape (i.e. the landscape over which stomata effectively regulate leaf water potential), correlated well with a wide range of plant hydraulic traits characterizing drought resistance and performance under well-watered conditions. In addition, species' Hydroscapes were related to home-climate representing water availability. Along the continuum of water regulation strategy, species with larger Hydroscape had higher stomatal conductance under well-watered conditions, more negative water potential thresholds at stomatal closure, turgor loss and onset of xylem embolism, and tended to occupy arid regions. It was concluded that Hydroscape appears a good metric that not only describes how plants regulate water potential during drought, but also summarises the overall drought response strategy.

In the third experimental chapter (Li et al. 2019a), the intraspecific variation of functional traits was investigated for Banksia serrata. Plant materials were collected from three sites with different local climates (Warm-Wet, Warm-Dry, and Cool-Wet). Xylem embolism threshold of leaves and stems, leaf pressure-volume characteristics, sapwood density, Huber value and specific leaf area were measured. Results showed that key traits including thresholds of xylem embolism in leaves and stems as well as leaf turgor loss point did not differ across sites despite the contrasting mean annual precipitation and temperature.

However, physiological and morphological adjustments were found for plants from the Warm-Dry environment, including higher stem specific conductivity, lower leaf hydraulic capacitance, modulus of elasticity and sapwood density. Overall, key hydraulic traits were generally conserved across populations despite differences in mean site water availability, and the safety-efficiency trade-off was absent in this species. These results suggest that B. serrata has limited ability to adjust its hydraulic architecture in response to environmental change and thus may be susceptible to climate change-type drought stress.

In the fourth experimental chapter (Li et al. 2018b), the leading hypothesis of drought related tree mortality, namely hydraulic failure, was tested on a field population of Eucalyptus piperita Sm. by taking advantage of a Winter-Spring drought event in 2017. Branch samples from healthy trees (non-dieback) and trees showing signs of dieback were collected one month after drought-induced leaf and branch dieback was observed in field populations of E. piperita in the Blue Mountains (Australia). Levels of native embolism were measured on tertiary branchlets. Additionally, xylem vulnerability to embolism was determined for leaves and stems using samples collected from healthy trees. The level of native embolism in dieback trees was significantly higher than that in healthy trees on average (26% vs. 11%). Importantly, there was a significant positive correlation (R^2=0.51) between the level of leaf death and the level of native embolism recorded in branchlets from dieback-affected trees. Moreover, a narrow hydraulic safety margin for hydraulic segmentation was found for this species. This retrospective study suggests that hydraulic failure was the primary mechanism of leaf and branch dieback in response to a natural drought event in the field. It also suggests that post-drought embolism refilling is minimal or absent in this species of eucalypt.

In summary, my PhD research addresses inter- and intra-specific variation as well as the coordination of a wide range of hydraulic traits for woody species from contrasting habitats across New South Wales, Australia. These findings demonstrate that hydraulic traits vary remarkably and systematically across species distributed along environmental gradients characterized by rainfall and aridity. Compared with mesic zone species, species occupying arid regions have more negative water potential thresholds of hydraulic dysfunction, and therefore are physiologically more resistant to drought. However, difference in the levels of water deficit occurring in their natural habitats may expose them to similar risk of mortality. Additionally, results from this study suggest that hydraulic traits are highly coordinated, indicating that traits conferring drought resistance are co-selected by the environment. The water potential threshold for stomatal closure was consistently less negative than that for the onset of xylem embolism, implying that stomata closure protects the integrity of xylem water transport during drought. Within species, key hydraulic traits are generally conserved, although some physiological and morphological adjustments may occur in response to site-specific water availability. Moreover, this research confirms the leading role of hydraulic dysfunction in causing drought related mortality in trees. Collectively, these results suggest that risk of drought-related mortality is similar across NSW tree species, and physiological adjustments may not be sufficient to alleviate the impacts of rapid global climate change. Therefore, increased mortality events are expected if climate becomes warmer and drier in the future.

Chapter 1

General introduction

1.1 Background

Large scale forest collapse has been observed in every vegetated continent in the past decades and may accelerate in the near future due to the increased frequency, severity and duration of drought stress resulting from rapid global climate change (Allen et al. 2010, Allen et al. 2015). Forests cover approximately 30% of land surface area and provide numerous ecological, economic as well as social benefits (Bonan 2008). Globally, forests store *ca*. 45% carbon of terrestrial ecosystems and sequester one-fourth of annual anthropogenic carbon emission each year (Bonan 2008, Pan et al. 2011). In addition, forests can strongly modify the terrestrial energy budget and hydrological cycle by altering surface albedo and evaporation. Climate change induced forest mortality can therefore influence ecosystem structure and composition, generating multiple negative effects on global carbon, energy and water balance, and will eventually lead to a positive feedback to the climate (Anderegg et al. 2013b).

Motivated by the urgent need to ameliorate the potential increase in forest dieback, efforts have been made worldwide to unravel the mechanisms underlying tree death and enhance the predictability of forest dynamics under drought stress (McDowell et al. 2008, Anderegg et al. 2012a, Adams et al. 2013, Allen et al. 2015, Anderegg et al. 2016). Early studies have documented two physiologically distinct, while mutually related, mechanisms (McDowell et

al. 2008, McDowell 2011a) and experimental evidence is now converging on the critical role of hydraulic dysfunction in drought related tree mortality (Adams et al. 2017). Despite mounting knowledge regarding this mechanism, predicting how trees respond to and eventually die from drought remains challenging (McDowell et al. 2013a, Powell et al. 2013) as current vegetation models either incorporate mechanisms implicitly or group multiple species into *a priori* defined plant functional types (PFTs), making it difficult to capture inter- and intra-specific variation in response to drought.

Plant functional traits exert strong control on organismal performance (Soudzilovskaia et al. 2013, Li et al. 2015a, Skelton et al. 2015). Viewing the plant community as a continuum of interrelated functional traits instead of PFTs can greatly improve model performance (Xu et al. 2016). Moreover, functional traits are mechanistically informative and can provide a simple algorithm for models (McDowell et al. 2011b, Brodribb et al. 2017). The trait-based approach is emerging as a promising alternative to forecast plant dynamics in response to environmental perturbation. Past success in explaining plant demography using plant functional traits demonstrates that traits are able to robustly capture the impacts of global climate change on vegetation abundance (Soudzilovskaia et al. 2013). Recent studies have highlighted the capability of traits-based models in characterizing dynamics of trees in response to water deficit (McDowell et al. 2013a, Xu et al. 2013, McDowell and Allen 2015, Xu et al. 2016). Likewise, plant water use strategy defined by functional traits shows good agreement with observed drought response, further underscoring the predictive power of trait-based approaches (Skelton et al. 2015).

Predicting how plants will respond to the environment using a traits-based approach requires knowledge of species-specific trait values. Global databases of functional traits are becoming

increasingly available, but are often constrained to a few traits and species (Bartlett et al. 2012, Choat et al. 2012a, Klein 2014). This poses a major obstacle to the application of the trait-based approach, especially when predicting drought-induced tree mortality, which is a function of multiple hydraulic traits (Klein et al. 2014, Blackman et al. 2016b, Choat et al. 2018a). In addition, the variation of traits over space and time further complicates the model algorithm. A better understanding of the variation and coordination of traits involved in plant water relations will significantly advance our ability to predict the response of plants to drought stress.

1.2 Literature review

1.2.1 The history of tree mortality research: physiological mechanisms

More than three decades ago, Manion et al. (1981) proposed a slow decline hypothesis to explain the progress of tree mortality. In this theory, tree death is initialized with a moderate long-term stress that predisposes trees to mortality risk, is intensified by a short-term severe stress and eventually occurs due to a contributing factor. Later works often build on this original theory, with particular emphasis on the role of carbon balance in tree mortality (Sevanto and Xu 2016). Based on previous work, McDowell et al. (2008) proposed three hypotheses that explain and generalize mechanisms underlying this phenomenon. The *carbon starvation hypothesis* suggests that down-regulated stomatal conductance during drought stress will lead to reduced carbon assimilation. As plants still require photosynthate to maintain metabolic processes such as respiration and osmoregulation, limited carbon supply and continued demand will eventually deplete carbon storage, which in turn induces carbon starvation or lowers the ability of plants to fend off biotic attack, and subsequently leads to tree death (Anderegg and Anderegg 2013a, O'Brien et al. 2014). Alternatively, the *hydraulic failure hypothesis* suggests that when xylem water transport is under greater tension due to

high evaporative demand and/or decreased soil water availability, air bubbles will be aspirated into functional vessels through inter-conduit pits, consequently creating emboli that break the continuity of water transport in xylem. Embolized conduits are unable to transport water to distal organs, eventually leading to decreased photosynthesis and organ/plant level desiccation (Breshears et al. 2009, Anderegg et al. 2015). It is worth noting that hydraulic failure can also occur in the rhizosphere when root-soil contact is blocked by air (Sperry et al. 1998). The third candidate is biotic attack, including insects and pathogens. However, biotic attack does not always result in tree death. In addition, the occurrence of biotic attack usually requires stressed trees to facilitate population growth (McDowell 2011a). Here I primarily focus on hydraulic failure, which has been identified as a key process resulting in tree death during drought.

It has now been widely recognised that hydraulic failure and carbon starvation are not mutually exclusive. Rather, the two mechanisms are interdependent, as plant carbon dynamics and water relations are tightly coupled (McDowell 2011a, McDowell et al. 2011b), and therefore the two processes can co-occur. For example, Sevanto et al. (2014) reported that *Pinus edulis* trees can die from carbon depletion or hydraulic failure when exposed to severe drought stress. These authors further concluded that hydraulic failure occurs when there is insufficient carbohydrate available to maintain hydraulic integrity. Similarly, using a novel experimental design that separates the effects of carbon dynamics and water relations, Hartmann et al. (2011) observed that hydraulic failure killed *Picea abies* more rapidly than carbon starvation unless carbohydrates cannot be utilized. Those results highlight the critical role of phloem functioning in the survival of trees and imply the interdependency between carbon starvation and hydraulic failure. An integrated mechanism was posed by McDowell (2011a) suggesting that protracted stomatal closure reduces photosynthesis while respiration

continues for maintenance during drought stress. Carbohydrate availability further declines due to the carbon demands of hydraulic processes such as turgor maintenance and xylem refilling. Embolized conduits increase because refilling is no longer possible due to inadequate carbohydrate availability, resulting in further declines in photosynthesis. Mortality can occur when one or more processes involved exceed their critical threshold. Therefore, carbon starvation and hydraulic failure represent two endpoints of the complicated mortality spectrum, indicating that the carbon-hydraulic dichotomy is oversimplified.

1.2.2 Hydraulic dysfunction underpins tree mortality during drought

Loss of stem and/or root hydraulic conductivity in dead trees has been reported in many species, with little or no change in tissue carbohydrate concentration (Hoffmann et al. 2011, Anderegg et al. 2012b, Anderegg et al. 2013a, Duan et al. 2014). In other studies, although carbohydrate content is not measured, near-complete loss of hydraulic conductivity is observed in dead individuals (Brodribb and Cochard 2009, Urli et al. 2013). On the other hand, observations supporting carbon starvation are relatively scarce and direct evidence showing that insufficient carbon supply kills trees is currently lacking (Sala et al. 2010). Indeed, few studies have directly tested the role of carbohydrate in drought-induced mortality, and it appears carbohydrate depletion may not be a contributing factor that leads to tree mortality. For example, O'Brien et al. (2014) demonstrated a positive relationship between non-structural carbohydrate availability and survival time. However, in this work, prolonged time-to-mortality was attributed to the maintenance of hydraulic function that was facilitated by carbohydrate availability. In another work, increased temperature shortened the survival time of *Pinus edulis* by one-third due to carbon loss from enhanced respiration, implying that carbon starvation may lead to tree death (Adams et al. 2009). Carbohydrate content, however, was not monitored in this work, making this conclusion equivocal. It

appears that instead of playing a direct role in delaying mortality during drought, carbohydrate facilitates prolonged survival time by aiding osmoregulation, turgor maintenance and increasing rooting depth. A recent multi-species synthesis shows that trees dying from drought typically exhibit >60% embolism with various degree of carbon depletion, indicating hydraulic failure is a general phenomenon for trees exposed to lethal drought stress (Adams et al. 2017). Additionally, a global meta-analysis conducted by Anderegg et al. (2016) showed that patterns of tree mortality can be well explained by traits such as xylem water potential and hydraulic safety margin. Taken together, these results strongly suggest that plant hydraulic traits hold the promise to predict patterns of forest dieback during drought stress.

1.2.3 Modelling the dynamics of forest under lethal drought stress

Ecosystem models are the only tools that allow for prediction of plant dynamics at large scales (e.g. regional and global) (McDowell et al. 2013a). Terrestrial biosphere models (TBMs) are models that simulate growth, mortality and reproduction of the major vegetation, and are often coupled with general circulation models (GCMs) to predict the dynamics of plant community under climate change (Fisher et al. 2014). Drought-induced mortality events have been incorporated into TBMs in response to the urgent need for better forecasting of the fate of vegetation in the future (Adams et al. 2013, McDowell et al. 2013a). However, the predictability of drought-related tree mortality of TBMs remains limited. Indeed, current TBMs often fail to precisely capture physiological variation (carbon and hydraulics) of plants during drought stress. For example, using five terrestrial biosphere models, Powell et al. (2013) simulated the response of Amazon forest to drought stress and further evaluated their predictive power by comparing model outcomes against observations. Their results showed that estimated carbon flux was in line with observations in well-watered control plots but not

in drought stressed plots. Likewise, an inter-model comparison conducted by McDowell et al. (2013a) showed that all models predicted depletion of carbon pools and reduced xylem conductivity and in turn tree mortality in a time-dependent manner, but none of these processes were accurately simulated.

Tree mortality can also be predicted using empirical models, which rely heavily on correlative relationships with implicit mechanistic understanding (Adams et al. 2013). Although empirical models have been criticized for not being applicable under future novel conditions, this approach provides a powerful tool for assessing and appreciating the complex plant response to changing climate. Furthermore, empirical models often require less data and flexible spatial scale for initialization calibration, making them more straightforward to implement (McDowell et al. 2011b, McDowell et al. 2013b). For example, Williams et al. (2013) reported that drought-induced forest mortality pattern in southwestern US was well correlated with forest drought stress index (FDSI), which was derived from long timescale tree-ring data. This strongly suggests the significant role of empirical models in simulating forest dynamics, especially in the early stage of model development when both available dataset and mechanistic understanding are limited. However, building empirical models need records of forest death events. In Australia, large scale tree death due to drought has only been recorded in a few regions (Matusick et al. 2013, Mitchell et al. 2014, Li et al. 2018b). In the case of NSW, only a handful of drought-induced mortality events have ever been reported (Mitchell et al. 2014, Li et al. 2018b).

Process-based models will be very valuable if greater comprehensive understanding of drought-induced tree mortality can be attained. Though experimental evidence strongly supports the role of plant hydraulic failure in mortality events, detailed information is still

limited in terms of model parameterization, which in turn forces modellers to use logical but largely untested algorithms to simulate mortality. For instance, in a recent model modified by Xu et al. (2016), the authors assumed xylem conductivity decreases sigmoidally as xylem water potential declines, and conductivity recovers following the same pattern as the mitigation of water stress. This assumption holds only if xylem refilling can occur, which is not broadly supported by experimental evidence (Choat et al. 2015b, Charrier et al. 2016, Choat et al. 2018b). Further, it is known that hydraulic traits can vary markedly within species over space and time (Anderegg 2015), the variation of which is often ignored in models. Further studies are needed to elucidate the detailed physiological processes during drought if we are to better predict the fate of forest in the future.

1.2.4 Hydraulic failure occurs in two phases

It has been suggested that the development and progression of hydraulic failure can be divided into two major phases (Choat et al. 2018a). During the initial phase of drought stress (phase I), soil water availability progressively decreases due to reduced precipitation in combination with increased soil-atmosphere moisture gradient (i.e. VPD). Xylem tension starts to increase due to the decline in water supply. As drought progresses, the leaf mesophyll cells lose turgor, leading to decreased stomatal aperture until full stomatal closure. During this phase, the xylem water transport system remains intact with little or no embolism (Figure 1b). It has been shown in many studies that complete stomatal closure typically occurs prior to the inception of xylem embolism (Martin-StPaul et al. 2017, Li et al. 2018a). Stomatal closure during drought stress can greatly reduce water loss. On the other hand, carbon assimilation is compromised due to stomatal closure, in turn leading to increased risk of carbon starvation. To balance the competing demands for assimilating carbon and

conserving water, plants can postpone stomatal closure, with the timing being dependent on the species-specific stomatal regulation strategy.

As soil water availability further decreases, roots can no longer extract water from soil either due to low soil water potential and/or loss of root-soil contact. During this phase (phase II), stomata are completely closed, and water loss from the plant occurs via the cuticle or leaky stomata (Blackman et al. 2016b). Water is no longer taken up from the soil, but the plant gradually loses the water stored in intercellular space, apoplast, living tissues or xylem (i.e. hydraulic capacitance). In some species, leaves begin to shed and become hydraulically isolated from branches to further minimize water loss (Figure 1c). This phenomenon, terms as hydraulic segmentation, has been observed in some species, but not in others, suggesting that leaf shedding during drought is not a universal strategy (Zhu et al. 2016). The mechanism underpinning this strategy is thought to be the different vulnerability to embolism between leaves and stems (Tsuda and Tyree 1997, Pivovaroff et al. 2014, Charrier et al. 2016), although recent studies showed that leaf shedding due to drought can occur in species with similarly vulnerable organs (Klepsch et al. 2018, Wason et al. 2018). In addition, hydraulic segmentation may have limited ability to prevent the occurrence of xylem embolism in branches, as embolism thresholds of leaves can be close to those of stems in some species (Li et al. 2019b). As xylem water potential continues to decrease, exceeding the embolism threshold, an increasing number of vessels become air-filled and therefore lose the ability to conduct water (Figure 1a). The percentage loss of conductivity (PLC) of the xylem increases following a sigmoidal curve until 100% (Figure 1b). The complete loss of water transport capacity results in desiccation of living tissue, including meristem and cambium (Li et al. 2016a), causing whole tree death.

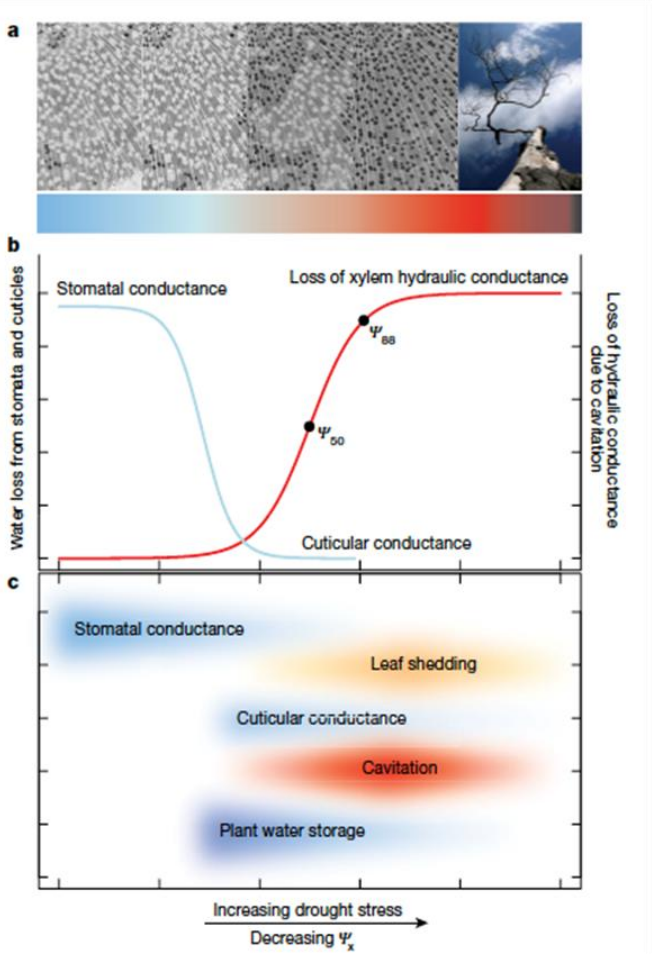

Figure 1-1 A hypothetical scheme of the development of hydraulic failure. See main text of detailed description (taken from Choat et al. 2018a).

1.2.5 Towards a better prediction of tree death: what traits matter?

The point at which drought-induced tree death occurs depends on multiple morphological and physiological traits. Early works assessed the probability of tree death using vigour, which is characterized by relative growth rate and abnormal growth that are related to a suite of traits associated with carbon and nutrient acquisition as well as hydraulic transport (Sevanto et al. 2016). For example, differences in growth rates among individual is in association with functional traits such as photosynthetic rate and light use efficiency, and also with morphological traits such as total leaf area and above/below ground biomass, which collectively determine both plant performance under favourable conditions and response to

environmental perturbations (Binkley et al. 2010, Ryan et al. 2010). It is thought that trees with higher vigour are generally more resistant and resilient to drought. In support of this view, Garcia-Forner et al. (2016) showed that trees with higher rates of photosynthesis and carbohydrate content (i.e. high vigour) tend to have longer survival times during drought stress.

According to the two-phase development of xylem embolism, stomata play a pivotal role in regulating plant water status during moderate water stress (i.e. phase I). Stomatal regulation strategy exerts strong control during this stage. At whole plant level, rooting depth is an important trait; species with deeper roots can access a larger soil moisture store, and are potentially able to reach groundwater, giving them a higher overall water availability compared to shallow-rooted species (Fan et al. 2017). In addition, total leaf area (LA) is fundamentally important as it determines the quantity of water loss from canopy at given driving force (i.e. VPD). Taken together, these traits characterize the water balance of plants, which in turn determines the time at which plants move into phase II.

Functional traits during phase II can be well described by the hydraulic model proposed by Blackman et al. (2016b), which highlights the crucial role of hydraulic traits after stomata close. Here, time to mortality (t_{crit}, s) can be estimated by the following equation:

$$t_{crit} = \frac{(\theta_0 - C \cdot \Psi_{crit})V_W}{A_L g_0 D} \quad (1)$$

where θ_0 (%) is the branch relative water content (RWC) at the point where stomata have just closed; C (RWC MPa^{-1}) is the stem water capacitance; Ψ_{crit} (MPa) is the xylem water potential associated with lethal levels of drought stress; V_W (kg) is the total amount of water available to the branch; A_L (m^2) is the total leaf area ; g_0 (mmol m^{-2} s^{-1}) is the canopy conductance after stomatal closure (i.e. cuticular conductance); and D (kPa) is the vapour

pressure deficit of the atmosphere. According to this model, a longer survival time can be achieved by increasing water storage (i.e. higher $C \times V_w$), decreasing water loss (lower g_0 and A_L) and increasing cavitation resistance (more negative P_{50} or P_{88}) or the combination of all of the above. Note this model is developed based on excised branches, and distal part death (e.g. leaf, branch) does not equate to whole plant mortality.

Hydraulic capacitance (C) is defined as the mass of water that can be extracted per unit change in water potential (Richards et al. 2014). C varies widely across species and habitats. Studies suggest that C may buffer the daily fluctuation of xylem tension by discharging water to transpiration upstream in many species, but not all (Meinzer et al. 2004, Chapotin et al. 2006, Scholz et al. 2007). In some species, water stored in plant tissues has been estimated contribute up to 50% of daily evaporation (Meinzer et al. 2004, Gleason et al. 2014). An advantage of using stored water in plant tissue is that the steep drop in xylem water potential during water deficit can be mitigated, therefore lowering the risk of catastrophic xylem embolism. Furthermore, it is proposed that high C can also facilitate xylem refilling, thereby enhancing plants' drought resilience (Richards et al. 2014). However, species with higher capacitance may also be more vulnerable to xylem cavitation. Ψ_{crit} represents the minimum recoverable water potential, which equates to the xylem water potential at which 50% and 88% to 100% conductivity is lost in gymnosperms and angiosperm, respectively (Brodribb et al. 2009, Urli et al. 2013, Li et al. 2016a). It is generally believed that species with more negative Ψ_{crit} are more drought resistant as cavitation will be unlikely to happen until xylem water potential becomes extremely negative. However, species with more negative Ψ_{crit} also tend to have more negative daily minimum water potential (Ψ_{min}). Given the climatic conditions differ substantially across species provenance Ψ_{crit} alone may provide limited insights in the mortality risk. Hydraulic safety margin (HSM) describes the distance of plants

water status from a critical threshold, therefor offering a normalized metric for the comparison of drought sensitivity among species. HSM can be defined in different ways, but perhaps the most common definition is Ψ_{min}-Ψ_{crit}, which quantify the embolism risk under the context of species' climatic envelope. For example, Ψ_{min}-Ψ_{crit} is found to be highly convergent across globe, indicating that plants are equally vulnerability to drought induced embolism regardless

of the annual mean precipitation (Choat et al. 2012a). HSM can also be defined as the distance between species-specific Ψ_{crit} and hydraulic behaviour, thereby providing additional information with respect to plant drought response (Blackman 2018). Although the role of HSM in assessing plant vulnerability to drought stress has been questioned, and substantial interspecies variation in Ψ_{crit} has been observed at local scale (Nardini et al. 2013, Klein et al. 2014), such results strongly imply that most plants will be exposed to drought risk in a drier and warmer world.

1.2.6 Expanding the trait database using easily-measured proxies

Using easily-measured traits as proxies of traits which are time and labour consuming to measure has been widely adopted by the ecological community when parameterizing TBMs. This approach is built on the co-ordination of various plant functional traits, although some traits can be decoupled in some cases (Wright et al. 2004, Li et al. 2015a, Blackman et al. 2016a). Sap wood density (WD), which is thought to integrate a suite of plant functional traits, has been shown to be a strong indicator of xylem vulnerability to embolism (Hacke et al. 2001a, Hoffmann et al. 2011). It is generally observed that species with high wood density are more resistant to drought induced xylem embolism. A positive relationship between wood density and desiccation time is therefore expected across species growing in the same environment. The mechanism behind this phenomenon might be that the reinforced structure

can resist xylem implosion and cavitation. However, caution should be taken when extrapolating this correlation to drought induced mortality in field-grown trees as mortality risk is also dependent on the attributes of drought stress in species' natural habitats, as well as other hydraulic traits other than vulnerability to embolism. Indeed, some species characterized by high WD tend to exhibit higher mortality ratio. This inconsistency is attributed to different stomatal regulation strategies between dense wood and light wood species (Hoffmann et al. 2011). In addition, woody density is correlated with sapwood hydraulic capacitance, which may underpin both drought resistance and resilience (Meinzer et al. 2009). If this is widespread, woody density provides an easily-measured proxy for physiological traits such as P_{x50} or C. Another valuable trait is the leaf water potential at turgor loss (TLP), which has been used to assess drought tolerance in plant physiology for decades. A global meta-analysis showed that TLP is correlated with site water availability within and across biomes (Bartlett et al. 2012). Furthermore, TLP has been found to be linked to the water potential thresholds triggering stomatal closure and xylem embolism, highlighting the coordination between leaf and stem (Li et al. 2016a). Recent findings also suggest that TLP integrates a wide range of hydraulic traits, therefore informing the overall water use strategy of plants (Meinzer et al. 2016, Hochberg et al. 2018, Fu and Meinzer 2018).Together, these easily-measured traits provide proxies for other physiological traits and a rapid tool for assessing plant drought vulnerability. This is of significance for modelling, especially at large scales where detailed physiological data are unavailable for a large number of species.

1.3 Thesis Overview

1.3.1 Thesis objectives

The overarching objective of my thesis is to examine how hydraulic traits vary within and across tree species of NSW, and how these traits inform the risk of drought-related tree mortality. To achieve this goal, four experiments were conducted. The first two experiments investigated the interspecific variation of key hydraulic traits. Tree species originating from five different vegetation types across NSW (Rainforest, Wet sclerophyll forest, Dry sclerophyll forest, grassy woodland and semiarid woodland) were selected for the first experiment. Using a common-garden approach, a wide range of leaf and stem physiological traits (e.g. xylem vulnerability to drought, stomatal closure point, turgor loss point), as well as carbon (e.g. photosynthetic rate, stomatal conductance) and morphological traits (e.g. Huber value) were assessed. In the third experiment, I examined the intraspecific variation of plant hydraulics. *Banksia serrata* was selected for this study based on the local availability. Several key hydraulic traits were compared among three climatically distinct sites (Warm-Dry, Warm-Wet and Cool-Wet). Finally, I took the advantage of a natural Winter-Spring drought event in the Blue Mountain region of 2017. *Eucalyptus piperita* (Sydney peppermint), which is endemic within this region and was severely affected by the drought stress, was chosen to investigate the relationship between canopy dieback and xylem embolism. Collectively, these experiments were designed to answer the following questions:

1. How do hydraulic traits vary and coordinate across species, and how do they relate to species climate-of-origin?
2. To what degree do key hydraulic traits vary within species?
3. Is hydraulic failure responsible for canopy dieback of field grown trees?

1.3.2 Outline of my thesis

Chapter 1 presents a general introduction of my thesis.

Chapter 2 aimed to examine the variation of coordination of key hydraulic traits across species. I investigated key hydraulic and carbon traits of 12 woody species in Australia from a broad climatic gradient. The influence of environmental variation was minimized by a common garden approach, allowing the influence of environment on phenotypic variation across species to be factored out. I found that hydraulic traits (leaf turgor loss point (TLP), stomatal sensitivity to drought (P_{gs}), xylem vulnerability to embolism of stem (P_x) and branch capacitance (C_{branch})) were highly coordinated across species and strongly related to rainfall and aridity in the species native distributional range. In addition, trade-offs between drought tolerance and plant growth rate were observed across species. Results of this chapter provide critical insight into the coordination among hydraulic traits in modulating drought adaptation, and will significantly advance our ability to predict drought vulnerability in these dominant trees species.

Chapter 3 compared four metrics used for quantifying the plant water use strategy. A subset comprising ten eucalypts from experiment Chapter 2 were selected and investigated in a common garden experiment. The results showed that species rankings of water use strategy were inconsistent across metrics. A newer metric (Hydroscape) was strongly linked to various plant traits, including the leaf turgor loss (TLP), water potential at stomatal closure (P_{gs90}), leaf and stem hydraulic vulnerability to embolism (P_{L50} and P_{x50}), safety margin of hydraulic segmentation (HSM_{HS}), maximum stomatal conductance (g_{smax}) and Huber value (HV). In addition, Hydroscape was correlated with climatic variables representing the water availability at the seed source site. Along the continuum of water regulation strategy, species with samller Hydroscapes tended to occupy mesic regions and exhibit less negative TLP, P_{L50} and P_{x50} values and narrow HSM_{HS}. High g_{smax} recorded in species with broad Hydroscapes were also associated with high HV. Despite a 4-fold difference in Hydroscape area, all

species closed their stomata prior to the onset of hydraulic dysfunction, suggesting a common stomatal response across species that minimises embolism risk during drought. It was concluded that Hydroscape area is useful in bridging stomatal regulation, hydraulic architecture and species drought tolerance, thus providing insight into species water relations strategies.

Chapter 4 examined the within species variation of key hydraulic traits along an environmental gradient. *Banksia serrata* (L.f.) was sampled from three sites characterized by contrasting climates (Warm-Wet, Warm-Dry, and Cool-Wet). Hydraulic characteristics, including vulnerability to embolism, hydraulic conductance, pressure-volume traits and key morphological traits were measured. Vulnerability to embolism in leaf and stem, defined by the water potential inducing 50% and 88% loss of hydraulic conductivity (P_{50} and P_{88}, respectively), did not differ across sites. However, plants from the Warm-Dry environment exhibited higher stem conductivity (K_s) than the Cool-Wet environment. Leaf turgor loss point (TLP) did not vary among sites, but Warm-Dry site plants showed lower leaf capacitance (C^*_{FT}) and higher modulus of elasticity (ε) than the other two sites. Plants from the Cool-Wet site had lower specific leaf area (SLA) and plants from the Warm-Dry site had lower sapwood density (WD). Overall, key hydraulic traits were generally conserved across populations despite differences in mean site water availability, and the safety-efficiency trade-off was absent in this species. These results suggest that *B. serrata* has limited ability to adjust hydraulic architecture in response to environmental change and thus may be more susceptible to drought stress induced by climate change. Results of study indicate that most hydraulic traits were highly conservative across populations, therefore lack the ability to acclimate to local environment.

Chapter 5 investigated the relationship between canopy dieback and levels of native embolism on E. *piperita* during a natural drought event. One month after drought-induced leaf and branch dieback was observed in field populations of *Eucalyptus piperita* in the Blue Mountains (Australia), we measured the level of native stem embolism and characterised the extent of leaf death in co-occurring dieback and healthy (non-dieback) trees. I found that canopy dieback-affected trees showed significantly higher levels of native embolism (26%) in tertiary order branchlets than healthy trees (11%). Furthermore, there was a significant positive correlation ($R^2 = 0.51$) between the level of leaf death and the level of native embolism recorded in branchlets from dieback-affected trees. This retrospective study suggests that hydraulic failure was the primary mechanism of leaf and branch dieback in response to a natural drought event in the field. It also suggests that post-drought embolism refilling is minimal or absent in this species of eucalypt. Results of this chapter corroborate the notion that hydraulic dysfunction underpins drought related tree mortality.

Chapter 6 synthesizes the major findings of this research. In this research, key hydraulic traits varied significantly among species from contrasting climates across NSW. Arid zone species were generally less vulnerable to drought stress when grown in common garden due to their more negative water potential thresholds for xylem embolism and turgor loss, as well as hydraulic strategies such as early stomatal closure and hydraulic segmentation, which will enable longer time-to-mortality during protracted drought stress. However, these species could be at equal risk of mortality depending on the frequency, duration and severity of drought stress in their natural habitats. Across species, various hydraulic traits were highly coordinated, suggesting that plant hydraulics were highly coordinated and therefore can be predicted from each other if species-specific trait values are unavailable. On the other hand, intraspecific variation in hydraulic traits was minimal, suggesting plant hydraulic traits are

under genetic control and thus have limited capacity to undergo rapid physiological adjustments in response to different hydrological environments. Furthermore, this study confirmed the fundamental role of hydraulic dysfunction in triggering drought related tree mortality, providing further evidence for the promise of plant hydraulic traits in predicting trees respond to drought.

Experiments in **Chapter 2** were designed by David Tissue, Belinda Medlyn, Brendan Choat, Remko Duursma and Paul Rymer, and were conceived by David Tissue, Belinda Medlyn, Brendan Choat, Chris Blackman and Ximeng Li for **Chapter 3**, **4** & **5**. Data collection was carried out by Ximeng Li and Chris Blackman. Ximeng Li performed data analysis and led the writing of all chapters.

All experimental chapters of this thesis have been published in peer-reviewed journals:

Chapter 2: **Li X**, Blackman CJ, Choat B, Duursma RA, Rymer PD, Medlyn BE and Tissue DT, 2018. Tree hydraulic traits are coordinated and strongly linked to climate-of-origin across a rainfall gradient. *Plant, Cell & Environment*, 41(3): 646-660.

Chapter 3: **Li X**, Blackman CJ, Peters JMR, Choat B, Rymer PD, Medlyn BE and Tissue DT. More than iso/anisohydry: Hydroscapes integrate plant water-use and drought tolerance traits in ten eucalypt species from contrasting climates. *Functional Ecology* (published)

Chapter 4: **Li X**, Blackman CJ, Choat B, Rymer PD, Medlyn BE and Tissue DT. Drought tolerance traits do not vary across sites differing in water availability in *Banksia serrata* (Proteaceae). *Functional Plant Biology* (published)

Chapter 5: **Li X**, Blackman CJ, Rymer PD, Quintans D, Duursma RA, Choat B, Medlyn BE and Tissue DT. 2018. Xylem embolism measured retrospectively is linked to canopy dieback in natural populations of *Eucalyptus piperita* following drought. *Tree Physiology*, 38(8): 1193-1199.

I also contributed to a submitted paper based on the experiments described in Chapters 2 & 3:

Blackman CJ, **Li X,** Choat B, Rymer PD, Kauwe MGD, Duursma RA, Tissue DT and Medlyn BE. Desiccation time during drought is highly predictable across tree species from contrasting climates (in review).

Additionally, I have written or co-authored the following published articles:

Li, X, C Xu, Z Li, J Feng, DT Tissue and KL Griffin. 2019. Late growing season carbon subsidy in native gymnosperms in a northern temperate forest. *Tree Physiology* (published).

Patterson AE, Arkebauer R, Quallo C, Heskel MA, **Li X**, Boelman N and Griffin KL, 2018. Temperature response of respiration and respiratory quotients of 16 co-occurring temperate tree species. *Tree Physiology*, 38(9): 1319–1332.

Li Z, **Li X**, Rubert-Nason KF, Yang W, Fu W, Feng J and Shi S, 2018. Photosynthetic acclimation of an evergreen broadleaved shrub (*Ammopiptanthus mongolicus*) to seasonal climate extremes on the Alxa Plateau, a cold desert ecosystem. Trees, 32(2): 603-614.

Chapter 2

Tree hydraulic traits are coordinated and strongly linked to climate-of-origin across a rainfall gradient

2.1 Introduction

Plant functional traits are typically well-correlated with the physical environment and are important in determining plant performance under environmental stress (Soudzilovskaia et al. 2013). Drought-induced hydraulic dysfunction may strongly limit the distribution of species along environmental gradients of water availability (Pockman and Sperry 2000, Choat et al. 2007, Kursar et al. 2009, Larter et al. 2017), define critical drought tolerance thresholds (Brodribb et al. 2009, Urli et al. 2013), and be used to predict drought-induced tree mortality (Xu et al. 2016, Tai et al. 2017). However, determining species overall drought susceptibility will depend on a more thorough understanding of the suite of traits that define plant water use and drought response strategies (Gleason et al. 2014, Blackman et al. 2016a, Brodribb et al. 2017), and their relationship to traits regulating growth and productivity.

Drought-related hydraulic impairment primarily occurs via cavitation induced embolism (Choat 2013). During drought stress, embolism spreads through the xylem primarily via 'air seeding', a process by which gas penetrates pit membranes connecting water-filled and air-filled conduits seeding new cavitation events (Zimmermann and Brown 1971, Brodersen et al. 2013). Embolism reduces the capacity of xylem to conduct water and, if unrepaired, may eventually lead to whole plant dehydration and mortality (Brodribb et al. 2009, Urli et al. 2013). The ability to resist xylem embolism (i.e. P_x) has emerged as a key trait in assessing

plant drought tolerance and is generally defined as the xylem water potential generating a 50% loss of conductance (P_{50}) (Maherali et al. 2004, Choat et al. 2012a, Powell et al. 2017). The P_{50} is often correlated with habitat water availability (Pockman et al. 2000, Blackman et al. 2014, Bourne et al. 2017, Larter et al. 2017, Trueba et al. 2017), and has been shown to coincide with drought-induced mortality in gymnosperms (Brodribb et al. 2009), while in angiosperms lethal water potentials are typically associated with greater losses of conductance, e.g. P_{88} or P_{99} (Kursar et al. 2009, Urli et al. 2013, Li et al. 2016). However, P_{50} is not a magic number determining drought tolerance in plants, and its importance must be viewed within the suite of traits controlling water uptake and water loss (Brodribb et al. 2017).

While xylem cavitation resistance is defined by the lower bounds of water potential that a plant may tolerate without risking serious drought injury, the likelihood of reaching these water potentials is controlled by a complex interaction of structural, physiological and phenological traits (Skelton et al. 2015, Martin-StPaul et al. 2017). Stomata regulate water and carbon exchange and respond to water deficit by gradual closure, thereby minimizing water loss and slowing further decreases in xylem water potential (Tyree and Sperry 1988, Brodribb and Holbrook 2003b, Nolf et al. 2015). In theory, stomatal sensitivity to drought should be linked to hydraulic safety to balance the competing requirements of water conservation and carbon gain. Indeed, evidence is emerging that the water potential at 90% stomatal closure (i.e. P_{gs90}) is coordinated with embolism thresholds across species at both community and global scales (Klein 2014, Bartlett et al. 2016, Martin-StPaul et al. 2017), though stomata may also respond to other biochemical and/or biophysical signals (Salleo et al. 2000), including leaf turgor loss. Nevertheless, the safety margin between the leaf water potential at stomatal closure and critical embolism thresholds (e.g. P_{50}), vary widely across

species and are important to determining species risk of significant hydraulic dysfunction during drought (Klein 2014, Skelton et al. 2015). Despite the significant implication of this metric, there are relatively few studies measuring these traits on the same plants (but see Skelton et al. 2015).

Studies of plant structure and function across species and habitats often identify trait trade-offs that are informative of species ecological strategy (Westoby 1998). For a given individual, trait trade-offs originate from the uneven allocation of limited resources, and, as a corollary, success in one trait must come at the cost of the competitive ability of another trait (Reich 2014). With regard to plant water relations, the trade-off between hydraulic safety (P_{50}) and efficiency (K_s) has been intensively studied. Although this trade-off has been observed in many studies (Lens et al. 2011, Markesteijn et al. 2011, Bourne et al. 2017, Zhang et al. 2017), a meta-analysis of diverse species across a global dataset suggests that the trade-off between these two traits is significant but weak (Gleason et al. 2016). Another important facet of xylem structure and function is a proposed trait trade-off between storage and biomechanical strength and support (Scholz et al. 2007, McCulloh et al. 2011). Water stored in living cells can be released into the transpiration stream as water potential increases during drought, thereby mitigating the development of xylem embolism (Pfautsch et al. 2015) and delaying the onset of critical drought stress (Meinzer et al. 2009, Gleason et al. 2014). High capacitance (C), however, may come at the cost of decreased biomechanical strength, as determined by sapwood density (WD, McCulloh et al. 2011). Collectively, traits related to efficiency, safety, storage and support constitute fundamental axes of trait variation in plant hydraulics. However, the number of studies that measure all of these traits on the same plants is relatively limited (Pratt and Jacobsen 2017).

A recently developed “fast-slow” traits spectrum proposes that trade-offs exist between plant carbon economy, growth and hydraulics (Reich 2014), though validation of this single axis across species is still unknown. Carbon and hydraulic traits can be decoupled due to structural or evolutionary divergence (Li et al. 2015a, Blackman et al. 2016a), while multidimensional trait variation (Powell et al. 2017), plant economic and hydraulic traits are interrelated, but operate independently. Nonetheless, it is unclear whether stem hydraulic traits are coordinated with leaf economic traits and plant growth.

A principal driver of species variation in hydraulic traits is climate. In xeric regions, the environment will select traits conferring drought tolerance (e.g. cavitation resistance) and/or avoidance (e.g. early stomatal closure). Given the importance of cavitation resistance and stomatal regulation in determining drought tolerance, site aridity is often observed to correlate with water potential thresholds inducing cavitation and stomatal closure (e.g. P_x, P_{gs}), as well as being related to traits such as leaf turgor loss point (Bourne et al. 2017, Trueba et al. 2017). These trends are often characterized based on field studies, with species growing along moisture availability gradients. Under field conditions, however, it is impossible to separate the relative contribution of genetics and environment to the observed phenotypic variation (Nicotra et al. 2010). Furthermore, species might be exposed to variable environmental conditions even when growing in a common site, resulting in phenotypic shifts unrelated to genetic composition (de Villemereuil et al. 2016). Consequently, field-based trait variance may be misleading if applied to conservation and breeding efforts. Common garden experiments, which minimise environmental variation and phenotypic plasticity, can yield valuable insight into the genetic constraints of plant traits.

Using a common garden type design we examined the level of coordination among a wide range of structural and functional traits in 12 tree species from five major woody vegetation types (rainforest, wet sclerophyll forest, dry sclerophyll forest, grass woodland, and semi-arid woodland) across a strong rainfall gradient in New South Wales, Australia. We also examined whether trait variation across species was genetically constrained and related to climate-of-origin. We investigated carbon, economic, leaf and stem hydraulic traits, in order to gain a comprehensive view of plant water use, growth and drought response strategies. Specifically, we hypothesized that: (1) leaf turgor loss point, stomatal closure and xylem cavitation thresholds are coordinated (i.e. traits are correlated); (2) there are trade-offs among traits that represent hydraulic efficiency, safety, support and storage, that is, negative correlation exists among K_s, P_{50}, WD and C; (3) there is an economic-hydraulic trade-off such that traits conferring drought resistance are negatively correlated with carbon economy traits; and (4) trait variation across species is correlated with climate-of-origin, and in particular, site water availability at the home climate of each species.

2.2 Materials and methods

2.2.1 Plant material and experimental design

Twelve dominant tree species, representing five major woody vegetation types in NSW, Australia, were chosen for the present study (Table 2-1). Species vary markedly in climate-of-origin, with mean annual temperature (MAT) ranging from 10 ºC to 20.5 ºC, and mean annual precipitation (MAP) ranging from 188 mm to 1125 mm. Aridity index (AI), calculated as the ratio of MAP and potential evaporation (PET), varies between 0.1 (most arid) for *Acacia aneura* and 1.1 (least arid) for *Eucalyptus viminalis*. Differences in climate-of-origin across species reflect differences in their native geographical distribution range (Figure A-1). Rainforest and wet sclerophyll forest species are distributed along the eastern coastline of

Australia, with the distribution of *E. viminalis* extending south to Tasmania. Semi-arid woodland species occur in the drier inland areas and *A. aneura* (Mulga) has the widest distribution range of the 12 species, occurring across much of outback Australia.

Table 2-1 Summary of species, abbreviations, vegetation types, mean annual temperature (MAT, ^{o}C), mean annual precipitation (MAP, mm) and aridity index (AI) for all species, averaged across each species distributional range.

Species	Abbreviation	Vegetation type	MAT	MAP	AI
Acmena smithii	Asm	Rainforest	14.9	837.4	0.9
Eucalyptus grandis	Egr	Wet sclerophyll forest	18.6	1124.5	0.9
Eucalyptus viminalis	Evi		10	751.5	1.1
Angophora costata	Aco	Dry sclerophyll forest	17.2	877.8	0.8
Corymbia gummifera	Cgu		16.8	880.3	0.8
Eucalyptus sideroxylon	Esi		16.4	478.1	0.4
Eucalyptus blakelyi	Ebl	Grassy woodland	15.1	550.2	0.5
Eucalyptus macrorhyncha	Ema		13.8	546.5	0.7
Eucalyptus melliodora	Eme		14.7	526.1	0.5
Acacia aneura	Aan	Semi-arid woodland	20.5	188.2	0.1
Eucalyptus largiflorens	Ela		17.4	250.2	0.2
Eucalyptus populnea	Epo		18.8	370.6	0.3

Seeds were obtained from Mount Annan Botanic Garden (Mount Annan, NSW, Australia, Table A-2) and sown in forestry tubes in a sun-lit poly-tunnel provided by Greening Australia (Richmond, NSW, Australia). On 15th Mar 2016, when seedlings were approximately 15 cm tall, plants were moved to the poly-tunnel facility of Western Sydney University (33^{o}33'S, 150^{o}44'E, Richmond, NSW, Australia) and transplanted into 25 litre bags filled with roughly 20 kg of loamy sand soil. The bags were isolated from the ground by palettes to prevent roots spreading beyond the pots. Each species was represented by 24 individuals, with the exception of *E. populnea* and *E. macrorhyncha*, which were represented by 17 and 18 individuals, respectively. All plants were fertilized 3 days after transplanting with soluble fertilizer and fertilized fortnightly until May 2016. Thereafter, plants were provided with commercial controlled release fertilizer (Osmocote, All purpose, Scotts, Australia) to ensure that they were not nutrient limited. All plants were watered for 10 mins every other day using an irrigation system to maintain soil water content at field capacity.

A randomized block design was adopted to minimize climatic variation in the poly-tunnel, which was divided into six blocks. Three or four plants of each species were randomly allocated to each block. Four individuals of each species were assigned to a well-watered treatment, and were watered daily over the experimental period. The remaining individuals were assigned to a drought treatment. The unbalanced allocation of individuals to treatments enabled drought plants to be destructively sampled across a range of xylem water potentials during soil drying. Due to differences in growth rate between species, the drought treatment was applied separately to three groups of 3-5 species at different time periods. The drought treatment was implemented by withholding irrigation during two drought cycles. In the first drought cycle, plants were dried until leaves were visually wilting. Thereafter, irrigation

resumed and plants were watered daily for ten days to allow full recovery. In the second drought cycle, irrigation was discontinued and the plants were allowed to dry-down. During this phase, leaf gas exchange characteristics and corresponding leaf water potential (Ψ_{leaf}, MPa) were measured periodically until positive net photosynthesis (A_{max}, μmol m^{-2} s^{-1}) was no longer detectable. Stem water potential (Ψ_{stem}, MPa) was monitored daily using leaf water potential (Ψ_{leaf}) as a proxy. To achieve maximum equilibrium between Ψ_{leaf} and Ψ_{stem}, leaves were covered with plastic wrap and aluminium foil in the evening prior to measurement. Plants were harvested when the desired Ψ_{stem} was attained. For each harvest, pots were bagged and sealed at the base of the plant stem. Subsequently, pots were submerged in a 75 litre bin filled with water and the stem excised within 5 cm above soil level. Stems were quickly transferred to another bin filled with clean water and covered with an opaque plastic bag to minimise water loss and transported to the lab for hydraulic measurements. Photosynthetic photon flux density (PPFD, μmol m^{-2} s^{-1}), air temperature (T_{air}, ^{o}C) and relative humidity (RH, %) were monitored in the poly-tunnel at 1.5 m height using a temperature/humidity probe (HMP60-L, Campbell Scientific Inc., Logan, UT, USA) and PPFD sensor (Decagon Devices Inc., Pullman, WA, USA), and were logged every 15 minutes with a data-logger (CR300, Campdell Scientific Inc.). Mean daily PPFD during the experimental period (i.e. Dec 2017 to May 2017) was 6.24 mol day^{-1}. Average T_{air} and RH were 20.2 ^{o}C and 65%, respectively.

2.2.2 Gas exchange measurements

Gas exchange measurements were conducted on recent, fully expanded leaves. During drought stress, the healthiest fully expanded leaf on each individual plant was chosen. Leaf gas exchange was measured using a portable infrared gas analyzer (Model 6400XT, Li-Cor, Lincoln, NE, USA) equipped with the red-blue LED light source (6400-02B) and external

CO_2 injector. Leaf net carbon assimilation rate (A_n), stomatal conductance (g_s mol m^{-2} s^{-1}) and leaf transpiration rate (E, mmol m^{-2} s^{-1}) were measured by placing the leaf into a 2 x 3 cm cuvette supplied with saturating light (1500 μmol m^{-2} s^{-1}) and ambient CO_2 concentration (420 μmol mol^{-1}). Parameters were logged when readings were visually stable (total coefficient of variation <1) which was typically achieved within five minutes. During these measurements, cuvette temperature was maintained at 25 ºC, flow rate was set at 500 ml min^{-1} and relative humidity in the cuvette was maintained between 60-70%. A leakage correction was applied on Li-Cor 6400XT data according to the manual, assuming a constant ambient CO_2 concentration (420 μmol mol^{-1}). Immediately after each gas exchange measurement, leaves were excised and placed in a zip-lock bag humidified with moist paper towel and transported to the lab in an ice filled container for Ψ_{leaf} measurements. Ψ_{leaf} was measured using a Scholander-type pressure chamber (PMS Instruments, Corvalis, OR, USA).

2.2.3 Stem vulnerability curves

Stem vulnerability curves were constructed for each species by slowly dehydrating whole plants in 25L pots (Sperry et al. 1988, Martorell et al. 2014). Stem samples were prepared for hydraulic measurement following Wheeler et al. (2013) and Torres-Ruiz et al. (2015). Excising stem segments under high xylem tension may allow air bubbles to enter the stem xylem even if performed under water, consequently leading to an overestimation of the level of embolism. To avoid this 'cutting' artefact, stem samples were rehydrated for at least 2 h before sample preparation by placing plants in darkness with the cut surface submerged in water. Xylem tension was considered sufficiently relaxed when Ψ_{leaf} was higher than -1 MPa; thereafter, a 10-15 cm stem segment was targeted for xylem hydraulic conductivity measurements. Side branches were removed and the cut surfaces sealed with para-film, if necessary. The first cut was made to the upstream end of the branch, at least 30 cm from the

targeted segment, and then left to rehydrate for 10 minutes. Subsequent cuts were made at approximately two minute intervals, alternating between upstream and downstream ends of the segment. Once the desired stem length was achieved, the sample was labelled and connected to a pressure head (0.002 MPa) generated gravitationally and the initial flow rate ($K_{initial}$) was measured using a digital liquid flow meter (Liqui-Flow L10, Bronkhorst High-Tech BV, Ruurlo, Gelderland, Netherlands) connected to flow analysis programs FlowDDE and FlowPlot (Version 4.69 and 3.34, respectively, Bronkhorst, FlowWare, http://downloads.bronhorst.com). Thereafter, the stem segment was attached to a water tank filled with 2 mmol KCL solution. The segment was flushed with a pressure of 200 kPa for at least 30 mins to remove any embolism and then connected again to the flow meter to measure final flowrate (K_{final}). K_{final} was normalized by the pressure gradient, sapwood area and stem length to obtain initial and final xylem specific hydraulic conductivity (K_s, kg m^{-1} s^{-1} MPa^{-1}). Percentage loss of xylem conductivity (PLC, %) was calculated as PLC = $(1-K_{initial}/K_{final})\times 100$.

2.2.4 Pressure volume analysis

For each species, one leaf per well-watered plant was collected for leaf pressure volume determination; for species with reduced leaf petioles, a terminal shoot was used instead. Leaves were excised under water in the early morning and transported to the lab with the petiole kept under water. Samples were placed in opaque plastic bags for up to 3 hours to ensure maximum rehydration. Leaf pressure volume (PV) curves were generated following Maréchaux et al. (2015). Briefly, Ψ_{leaf} was measured using the Scholander pressure chamber and fresh weight (FW) was measured with a digital balance (weighed to 0.1 mg). Then, leaves were bench-dried with Ψ_{leaf} and FW measured periodically. Finally, leaves were oven-dried at 70 ^{o}C for at least 48 h to obtain dry weight (DW). Leaf PV traits were estimated as

described by Lenz et al. (2006). The inverse of leaf water potential ($1/\Psi_{leaf}$) was plotted against leaf relative content (RWC_{leaf}, %) to facilitate calculation. Leaf turgor loss point (TLP, MPa) was taken as the point where the line became non-linear.

2.2.5 Hydraulic capacitance

Whole branch hydraulic capacitance (C_{branch}) was measured on well-watered plants using the bench dehydration method. The aboveground portion of the plant was excised at predawn (when xylem tension was minimal), covered by an opaque plastic bag, and transported to the lab where branch FW and Ψ_{leaf} were immediately measured. Samples were allowed to slowly dehydrate under lab conditions, during which time Ψ_{stem} and branch fresh mass were regularly measured. Before each measurement, the branch was placed into a sealed plastic bag for roughly 1 hour to ensure equilibration between Ψ_{leaf} and Ψ_{stem}. Afterwards, branch samples were oven-dried at 70 ^{o}C until mass was constant. Branch relative water content (RWC_{branch}, %) at each measurement period was calculated and plotted against Ψ_{stem}. C_{branch} was estimated as the slope of the second linear portion of the water release curve, expressed as $\Delta RWC/\Delta\Psi$ (RWC MPa^{-1}).

2.2.6 Morphological traits

Plant height (H, cm) and basal diameter (D, mm) were measured monthly from May to November 2016. Basal diameter was measured at 3 cm above soil level. A stem volume index was calculated as $H \times D^2$ (cm^3), and a volume index growth rate (VIGR, cm^3 day^{-1}) was calculated as the incremental increase in stem volume between measurement periods divided by the number of days between measurements.

Following stem hydraulic measurements, plants were separated into leaves and stems. Leaf samples were further divided according to leaf position relative to the stem segment used for

hydraulic measurement. A representative subsample of fresh leaves was collected from four per plants per species and leaf area was measured using a leaf area meter (LI-3100A, Li-Cor Inc. USA). In addition, an approximately 4 cm long segment was collected from the basal region of the stem. Bark was carefully removed with a razor blade and sapwood fresh volume was determined using the water displacement method (Markesteijn et al. 2011). Then, all samples were oven-dried at 70 ^{o}C for 48 h to constant mass and then weighed. Specific leaf area (SLA m^2 kg^{-1}) was calculated as the ratio of leaf area to dry mass. Sapwood density was calculated as the ratio of dry mass to fresh volume (WD, g cm^{-3}).

2.2.7 Statistical analyses

The geographic and climate details for each species distribution were obtained from Atlas of Living Australia within Mapping & analysis channel (http://spatial.ala.org.au/, accessed in May 2016) and plotted using R (R Development Core Team, 2014). Stem vulnerability curves were fitted using the Weibull function, and key traits (i.e. P_{12}, P_{50}, P_{88}; Table 2) were statistically tested by comparing bootstrap confidence intervals. Similarly, stomatal conductance was plotted against leaf water potential, and fitted with a weighted polynomial regression to extract P_{gs50} and P_{gs90} (Table 2). All curve fittings were performed using R with the *fitplc* package (Duursma and Choat 2017). For other traits, data normality and equality were tested and values were log-transformed if necessary. Statistical differences across species were examined using Tukey HSD test. Correlation among traits and climatic variables was tested using linear regression. Principle component analysis (PCA) was conducted in R using the *prcomp* function.

Table 2-2 Acronym of traits, units, definitions, and their significance in plant carbon and hydraulic strategies.

Traits	Units	Definition	Significance
Ψ_{leaf}, Ψ_{stem}	MPa	Leaf and stem water potential	Potential energy of water; indicators of organ water status
P_{x12}	MPa	Ψ_{stem} at 12% loss of conductivity	Inception of stem embolism; closely linked to leaf gas exchange
P_{x50}	MPa	Ψ_{stem} at 50% loss of conductivity	Index of hydraulic safety and drought tolerance across species
P_{x88}	MPa	Ψ_{stem} at 88% loss of conductivity	Hypothetical maximum water stress level in angiosperms beyond which recovery is very unlikely
K_s	kg m^{-1} s^{-1} MPa^{-1}	Water flow per unit conduit area at given time and pressure gradient	Water transport capacity of stem; index of hydraulic efficiency and may trade off with hydraulic safety
P_{gs50}	MPa	Ψ_{leaf} at 50% of maximum stomatal conductance	Early decline of stomatal conductance; proxy of Ψ_{leaf} at which stomata initiate closure
P_{gs90}	MPa	Ψ_{leaf} at 10% of maximum stomatal conductance	Maximum water stress while still maintaining minimal photosynthesis; proxy of complete stomatal closure
TLP	MPa	Bulk leaf water potential at which turgor pressure is zero	Ψ_{leaf} when leaf losses turgor and wilts, while leaf becomes physiologically dysfunctional
C_{branch}	RWC MPa^{-1}	Amount of releasable water of living cells as xylem tension increases	Total releasable water following the reduction of plant water potential, which may facilitate recovery from embolism
HSM	MPa	Hydraulic safety margin, defined as difference between P_{gs90} and P_{50}	HSM integrating leaf and stem hydraulics, reflecting the coordination between different organs and putatively linked to drought resistance
SLA	m^2 kg^{-1}	Ratio of leaf area to dry mass	Leaf area produced by given biomass investment; may affect leaf carbon assimilation and plant drought tolerance
A_{max}	μmol m^{-2} s^{-1}	Maximum carbon assimilation rate under well-watered conditions	Index of leaf photosynthetic capacity

g_{smax}	mol m^{-2} s^{-1}	Maximum stomatal conductance under well-watered conditions	Pivotal trait bridging carbon and water exchange
VIGR	cm^3 day^{-1}	Stem volume index growth rate	Surrogate of plant growth rate
WD	g cm^3	Sapwood density	Highly integrative trait of wood anatomical features

2.3 Results

2.3.1 Coordination between leaf and xylem hydraulics

Water potentials inducing 50% loss of xylem conductivity (P_{x50}) and 90% stomatal closure (P_{gs90}) varied considerably among species (Figure 2-1), as did most hydraulic and carbon economy traits (Tables 2-3 and 2-4). Strong correlation was observed between stomatal closure and key xylem embolism thresholds (Figure 2-2). P_{gs90} was correlated with P_{12}, and all species resided approximately on the 1:1 line (Figure 2-2a, R^2=0.869, $p<0.001$). P_{gs90} and P_{50} were also tightly correlated across species (Figure 2-2b, R^2=0.911, $p<0.001$). For all species, stomatal closure occurred at higher (less negative) water potentials than P_{50}, indicating that the hydraulic safety margin (HSM, defined as P_{gs90}-P_{50}) was always positive. The HSM increased with increasing P_{50} with the highest HSM (3.46 MPa) found in *A. aneura*. By contrast, the difference between P_{gs90} and P_{50} was smallest in *C. gummifera*, resulting in a narrow HSM of 0.14 MPa.

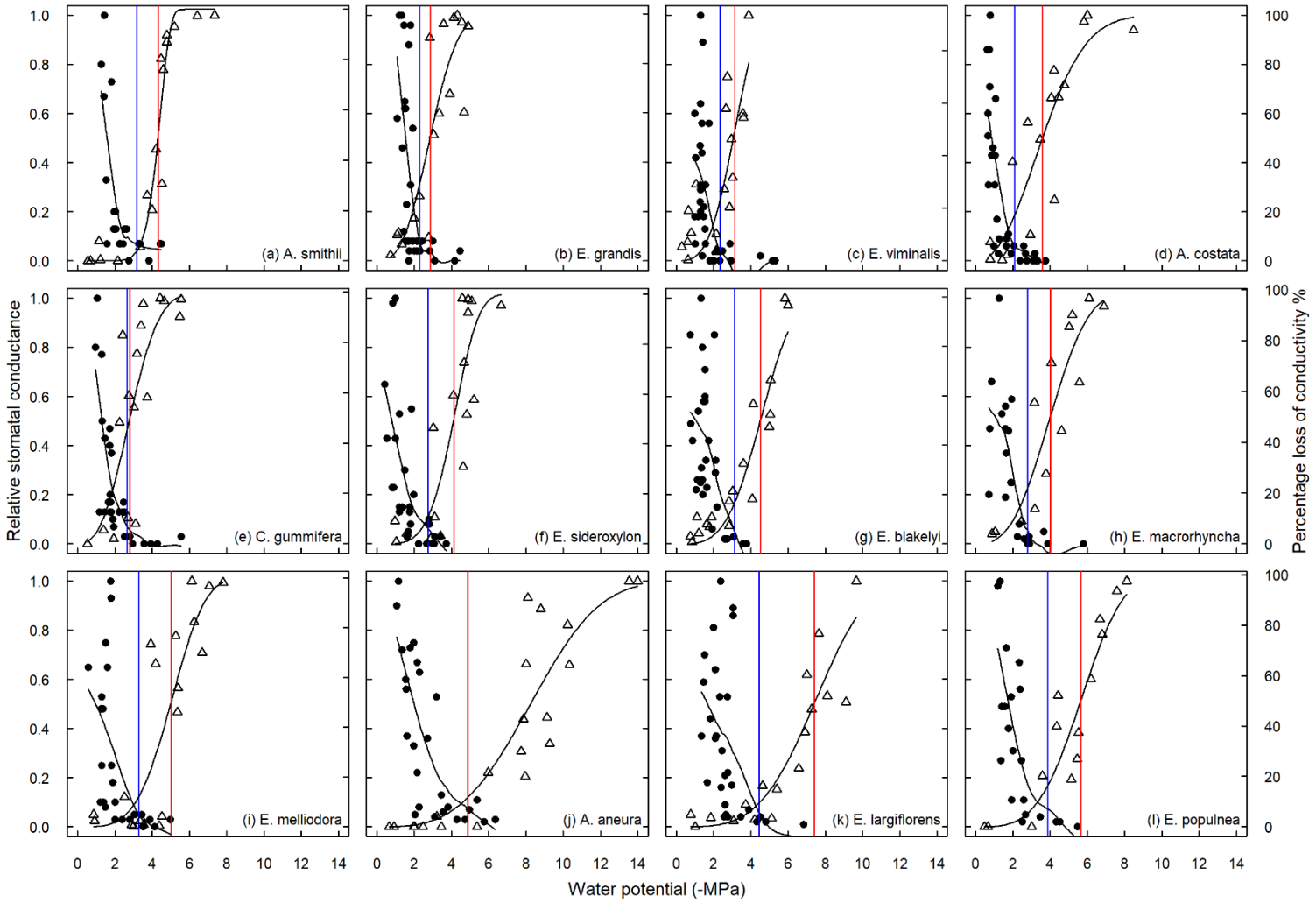

Figure 2-1 Percentage loss of xylem conductivity (PLC, open triangle) and relative leaf stomatal conductance (closed circle) response to water potential of twelve woody species. Red and blue vertical lines indicate xylem water potential inducing 50% loss of conductivity (P_{x50}) and leaf water potential at 90% stomatal closure (P_{gs90}), respectively; distance between lines denotes the hydraulic safety margin (HSM).

Table 2-3 Xylem cavitation (P_{x12}, P_{x50}, P_{x88}), stomatal closure threshold (P_{gs50}, P_{gs90}), branch capacitance (C_{branch}), leaf turgor loss point (TLP) and xylem specific conductivity (K_s) of twelve tree species. Numbers in brackets are lower and upper bound of 95% confidence interval. C_{branch}, TLP, and K_s are shown in mean ± standard error (SE). Different letters following SE indicate statistically significant at $P \leq 0.05$ level. Cross species comparison was conducted using Tukey HSD *post hoc*.

Vegetation type	Species	P_{x12} -MPa	P_{x50} -MPa	P_{x88} -MPa	P_{gs50} -MPa	P_{gs90} -MPa	C_{branch} RWC MPa^{-1}	TLP -MPa	K_s kg m^{-1} s^{-1} MPa^{-1}
Rainforest	*A. smithii*	3.61 [3.35,4.15]	4.33 [4.15,4.57]	4.88 [4.61,5.21]	1.85 [1.65,2.02]	3.12 [2.23,]	0.08± 0.01e	1.84± 0.04b	0.73± 0.08g
Wet sclerophyll forest	*E. grandis*	1.57 [1,2.81]	2.85 [2.36,3.34]	4.24 [3.02,5.22]	1.66 [1.44,2.12]	2.27 [1.95,]	0.34± 0.03a	1.54± 0.03bc	2.31± 0.11a
	E. viminalis	1.89 [0.67,2.46]	3.15 [2.7,4.32]	4.43 [3.77,]	1.79 [1.49,3.79]	2.37 [1.87,]	0.23± 0.02b	1.51± 0.09bc	2.17± 0.13ab
Dry sclerophyll forest	*A. costata*	1.69 [0.97,2.83]	3.59 [2.91,4.28]	5.9 [4.86,7.98]	1.28 [1.1,1.47]	2.09 [1.65,]	0.19± 0.03bcde	1.46± 0.04c	1.19± 0.16efg
	C. gummifera	1.47 [0.8,2.67]	2.81 [2.15,3.34]	4.29 [3.32,5.35]	1.56 [1.4,1.72]	2.66 [2.17,]	0.12± 0.01cde	1.87± 0.07b	1.75± 0.11abcde
	E. sideroxylon	2.81 [1.8,4.16]	4.12 [3.5,4.66]	5.3 [4.6,6.63]	1.34 [0.97,1.69]	2.72 [1.76,]	0.17± 0.02bcde	1.52± 0.09bc	1.62± 0.11bcde
Grass woodland	*E. blakelyi*	2.84 [2.17,3.92]	4.51 [4.11,5.01]	6.12 [5.49,8.1]	2.14 [1.83,2.7]	3.11 [2.39,]	0.21± 0.02bc	1.67± 0.05bc	1.86± 0.15abcd
	E. macrorhyncha	2.2 [1.31,3.29]	4.01 [3.32,4.59]	5.95 [4.84,7.37]	2.02 [1.78,2.78]	2.79 [2.36,]	0.24± 0.03b	1.5± 0.06bc	1.95± 0.2abc
	E. melliodora	3.28 [2.22,4.69]	5.02 [4.23,5.52]	6.65 [5.49,7.58]	2.05 [1.16,3.02]	3.26 [2.31,]	0.19± 0.01bcd	1.52± 0.03bc	1.85± 0.08abcd
Semi-arid woodland	*A. aneura*	4.89 [3.74,7.55]	8.24 [7.25,9.29]	11.63 [8.15,13.27]	2.25 [1.91,2.67]	4.78 [3.16,]	0.1± 0de	1.68± 0.14bc	0.93± 0.1fg
	E. largiflorens	4.73 [3.85,5.87]	7.4 [6.89,8.3]	9.95 [7.95,12.95]	2.59 [2.15,4.7]	4.26 [3.12,]	0.08± 0e	2.26± 0.03a	1.33± 0.14cdef
	E. populnea	3.53 [2.5,4.72]	5.64 [4.99,6.06]	7.7 [6.99,9.07]	2.13 [1.8,2.84]	3.87 [2.53,]	0.09± 0e	2.34± 0.13a	1.26± 0.16defg

Leaf TLP was positively, but weakly, correlated with P_{gs90} (Figure 2-3b, R^2=0.309, p=0.035) and was not correlated with other key stomatal indices including P_{gs50} (Figure 2-3a). Furthermore, the water potential at P_{gs90} was consistently lower (i.e. more negative) than TLP.

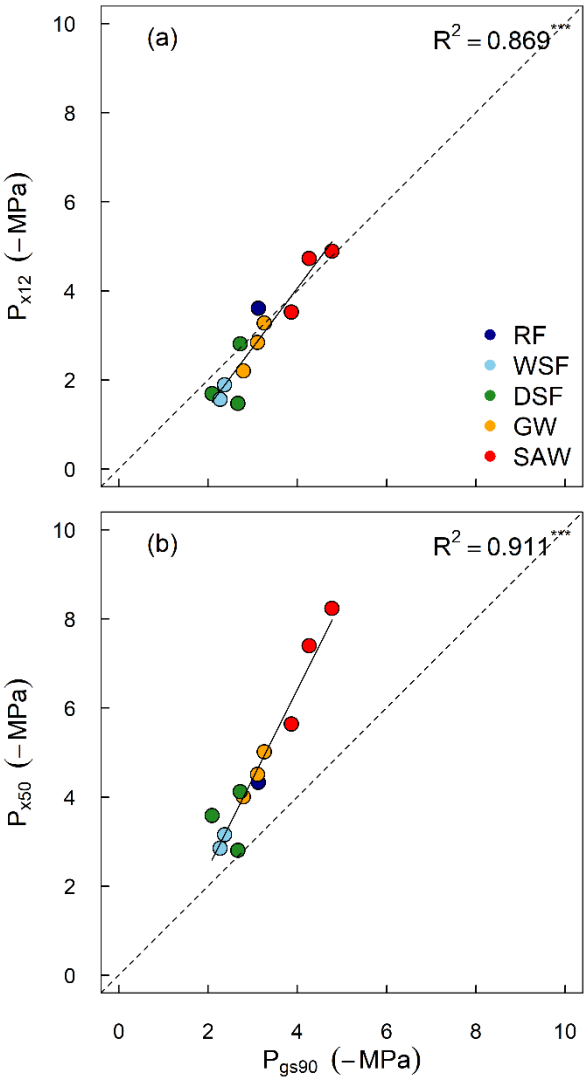

Figure 2-2 The relationship between xylem water potential at 90% stomatal closure (P_{gs90}) and xylem water potential at the inception of xylem cavitation (P_{x12}; Figure 2-2a), and 50% loss of conductivity (P_{x50}; Figure 2-2b). Adjusted R^2 of linear regressions (solid lines) are provided. Statistical significance is indicated by asterisk (***, P<0.001; **, P<0.01; *, P<0.05; ns, not significant). Five vegetation types (rainforest (RF), wet sclerophyll forest (WSF), dry

sclerophyll forest (DSF), grass woodland (GW), and semi-arid woodland (SAW)) are represented by different colours. Dashed lines indicate 1:1 relationship.

Table 2-4 Species values of maximum photosynthetic rate (A_{max}), maximum stomatal conductance (g_{smax}), sapwood density (WD), specific leaf area (SLA) and stem volumetric growth rate (VIGR). See Table 2-2 for units and definitions. Data are shown as mean ± SE. Different letters stand for statistical significance at P≤0.05 level.

Vegetation type	Species	A_{max}	g_{smax}	WD	SLA	VIGR
		μmol m^{-2} s^{-1}	mol m^{-2} s^{-1}	g cm^{-3}	m^2 kg	cm^3 day^{-1}
Rainforest	*A. smithii*	8.4±	0.12±	0.54±	9.27±	0.08±
		0.71e	0.01c	0.02c	0.48c	0.01f
Wet sclerophyll forest	*E. grandis*	16.68±	0.22±	0.35±	18.34±	0.55±
		1.27d	0.02bc	0.01f	1.44b	0.03a
	E. viminalis	15.86±	0.26±	0.36±	25.87±	0.51±
		0.82de	0.04bc	0.01f	3.16a	0.03a
Dry sclerophyll forest	*A. costata*	16.26±	0.21±	0.42±	7.56±	0.31±
		1.16de	0.02bc	0.01ef	0.43c	0.03bc
	C. gummifera	14.57±	0.21±	0.45±	10.98±	0.19±
		0.75de	0.03bc	0.02de	0.79c	0.02de
	E. sideroxylon	23.89±	0.31±	0.51±	11.14±	0.25±
		1.95bc	0.06bc	0.01cd	1.35c	0.03cd
Grass woodland	*E. blakelyi*	19.41±	0.58±	0.45±	18.14±	0.37±
		1.19cd	0.07bc	0.02de	1.89b	0.03b
	E. macrorhyncha	16.15±	0.36±	0.42±	12.83±	0.27±
		0.57de	0.06abc	0.02ef	1.69bc	0.03bcd
	E. melliodora	13.39±	0.3±	0.54±	12.59±	0.25±
		0.94de	0.03bc	0.02c	1.04bc	0.02cd
Semi-arid woodland	*A. aneura*	32.22±	0.64±	0.56±	8.1±	0.11±

		1.24a	0.06a	0.01bc	0.69c	0.01ef
	E. largiflorens	27.2±	0.58±	0.65±	9.88±	0.1±
		3.09ab	0.07a	0.01a	0.42c	0.01ef
	E. populnea	20.21±	0.4±	0.63±	11.57±	0.1±
		1.61bcd	0.08ab	0.02ab	0.86c	0.02ef

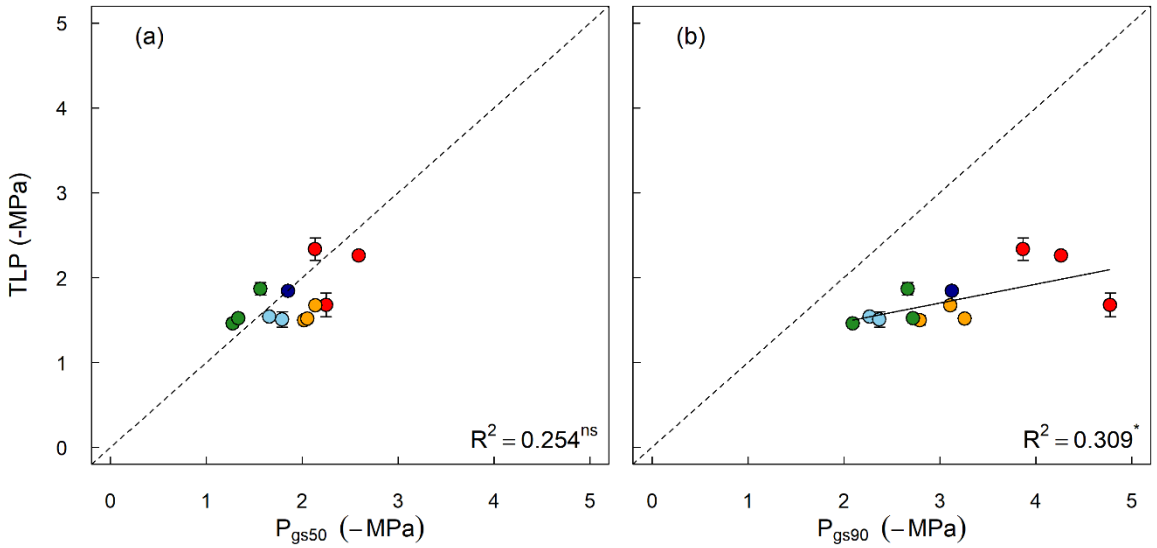

Figure 2-3 The relationship between leaf turgor loss point (TLP) and leaf water potential inducing 50% stomatal closure (P_{gs50}, Figure 2-3a) and 90% stomatal closure (P_{gs90}, Figure 2-3b). Error bars indicate standard error of mean. Adjusted R^2 of linear regression are shown. Statistical significance is indicated by asterisk (***, P<0.001; **, P<0.01; *, P<0.05; ns, not significant).

2.3.2 Trade-offs between hydraulic traits

Relationships among traits representing hydraulic safety (P_{x50}), efficiency (K_s, kg m^{-1} s^{-1} MPa^{-1}), storage (C_{branch}, RWC MPa^{-1}) and mechanical support (WD, g cm^{-3}) are shown in Figure 2-4. A positive relationship was found between WD and P_{x50} (Figure 2-4a; R^2=0.603, p<0.001). P_{x50} and K_s displayed a significant, but weak negative relationship (Figure 2-4b; R^2=0.266, p=0.049), indicating an overall weak trade-off. Notably, *A. smithii*, the only rainforest species in this study, was positioned furthest away from the regression line. We also found a strong trade-off between C_{branch} and WD across species (Figure 2-4c; R^2=0.646, p<0.001).

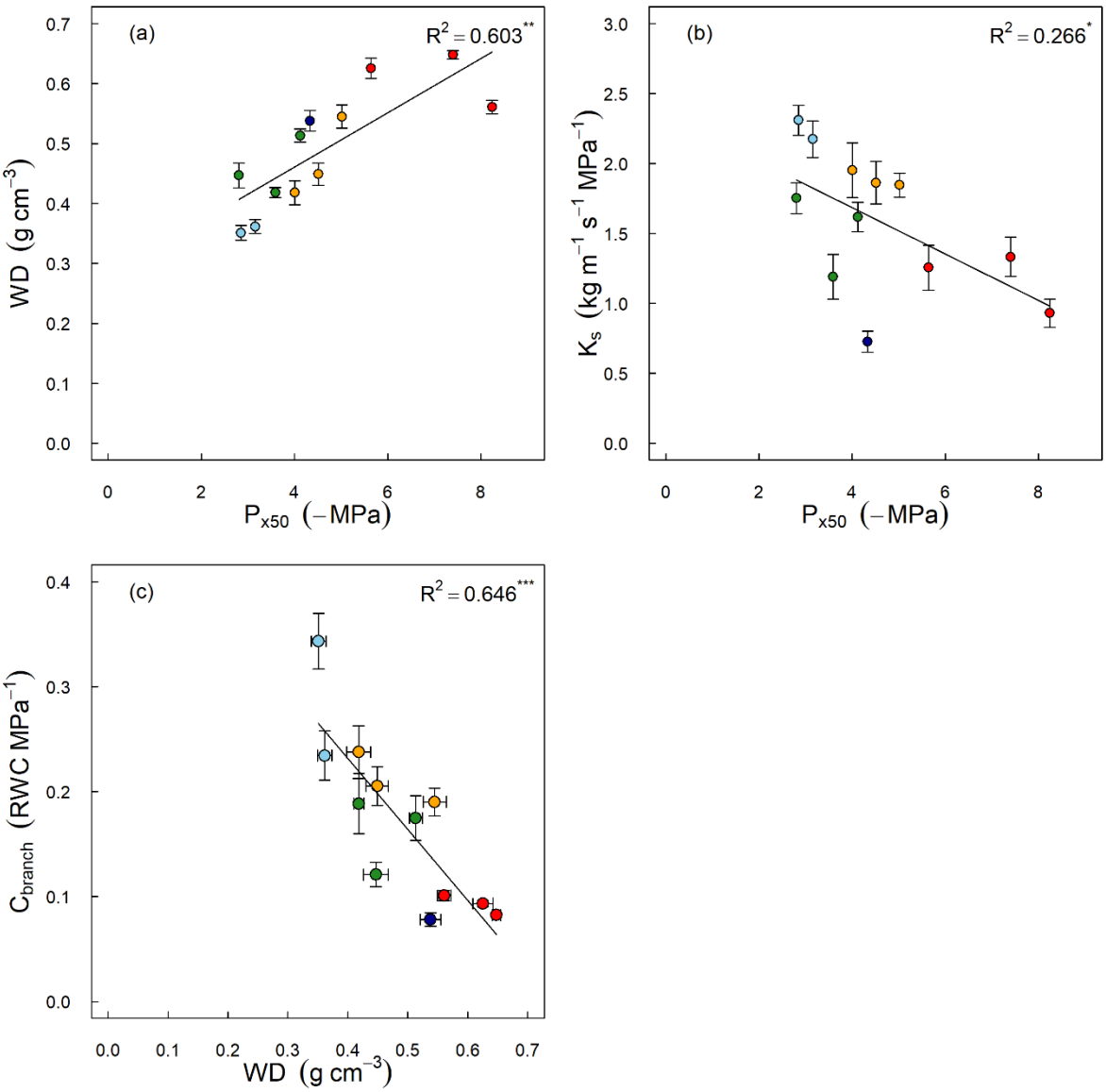

Figure 2-4 Correlations among xylem cavitation resistance (P_{x50}) and sap wood density (WD, Figure 2-4a) as well as xylem specific conductivity (K_s, Figure 2-4b), and between WD and whole branch capacitance (C_{branch}, Figure 2-4c) across species. Error bars indicate standard error of mean. Regression lines and corresponding adjusted R^2 are given. Statistical significance is indicated by asterisk (***, P<0.001; **, P<0.01; *, P<0.05; ns, not significant). Colour scheme for data points is same as Figure 2-1.

2.3.3 Relationship between carbon and hydraulic traits

Correlations between key carbon economy and hydraulic traits (Figure 2-5) indicated some trade-offs in these traits. Negative correlations between P_{gs90} and VIGR (Figure 2-5e; R^2=0.441, p=0.011), and between P_{x50} and VIGR (Figure 2-5f; R^2=0.348, p=0.026), indicate a trade-off between hydraulic safety and carbon economy traits related to growth. No trade-off was detected between hydraulic traits and leaf-level carbon economic traits. However, both maximum photosynthetic rate (A_{max}, μmol m^{-2} s^{-1}) and maximum stomatal conductance (g_{smax}, mol m^{-2} s^{-1}) showed a positive correlation with P_{x50} and P_{gs90} (Figure 2-5a-d). Furthermore, we observed a positive relationship between A_{max} and HSM (Figure A-2).

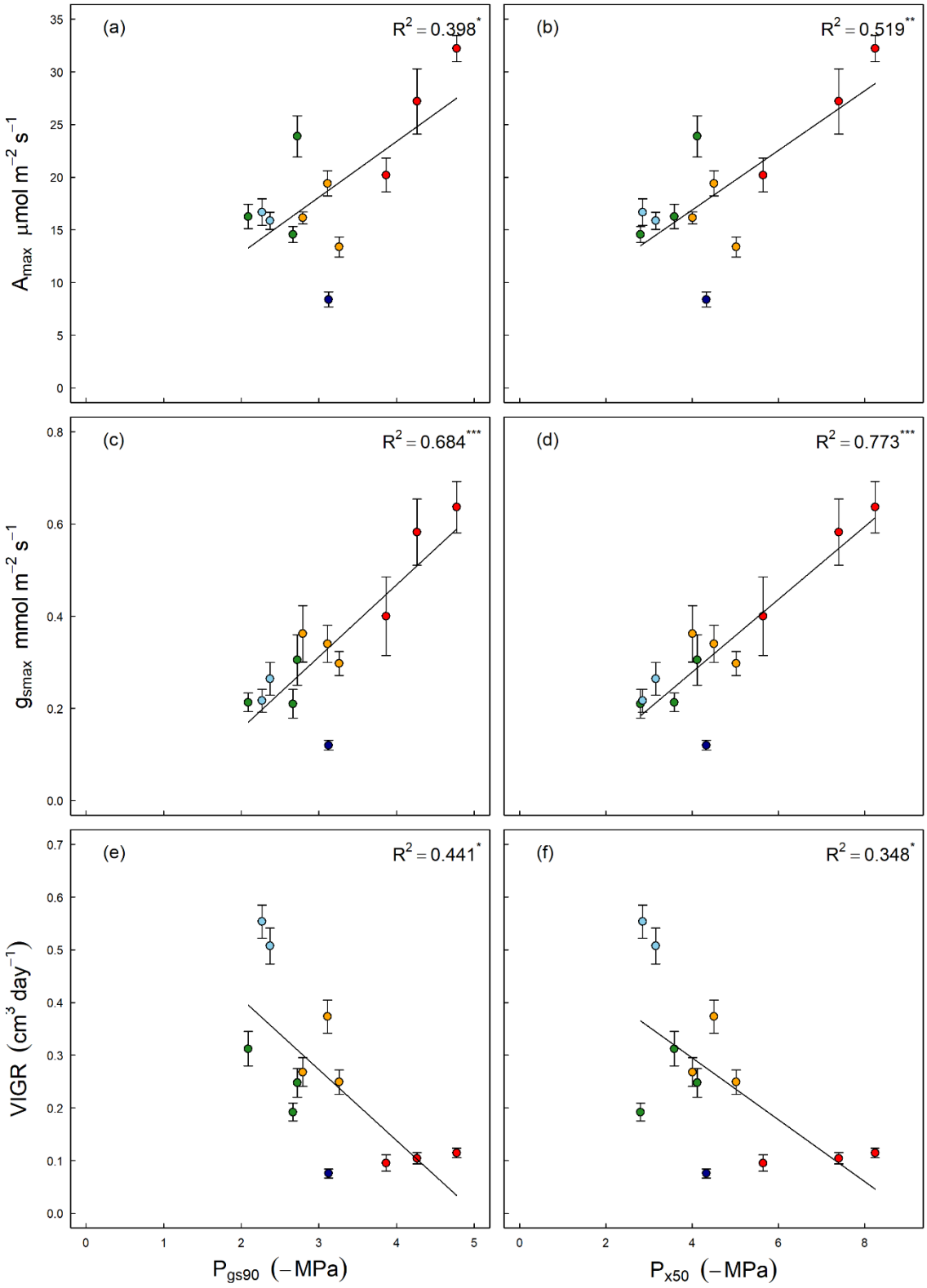

Figure 2-5 Correlations among xylem water potential at 90% stomatal closure (P_{gs90}), xylem cavitation resistance (P_{x50}), maximum photosynthetic rate (A_{max}, Figure 2-5a,b), maximum stomatal conductance (g_{smax}, Figure 2-5c,d) and volume index growth rate (VIGR, Figure 2-

5e,f). Error bars indicate standard error of mean. Regression lines and corresponding adjusted R^2 are given. Statistical significance is indicated by asterisk (***, P<0.001; **, P<0.01; *, P<0.05; ns, not significant).

We used principal component analysis (PCA) to examine the level of coordination among selected traits across species (Figure 2-6). PCA identified two primary axes of variation (principal components) that cumulatively explained 89.1% of total variation. The first axis (PC1), which explained 68.5% of total variation, was positively associated with traits related to carbon-use (VIGR, SLA) and hydraulic efficiency (K_s) and negatively associated with WD. The second axis (PC2), which explained 18.8% of total variation, was associated with water-use (g_{smax}) and hydraulic safety (P_{gs90}, P_{x50}).

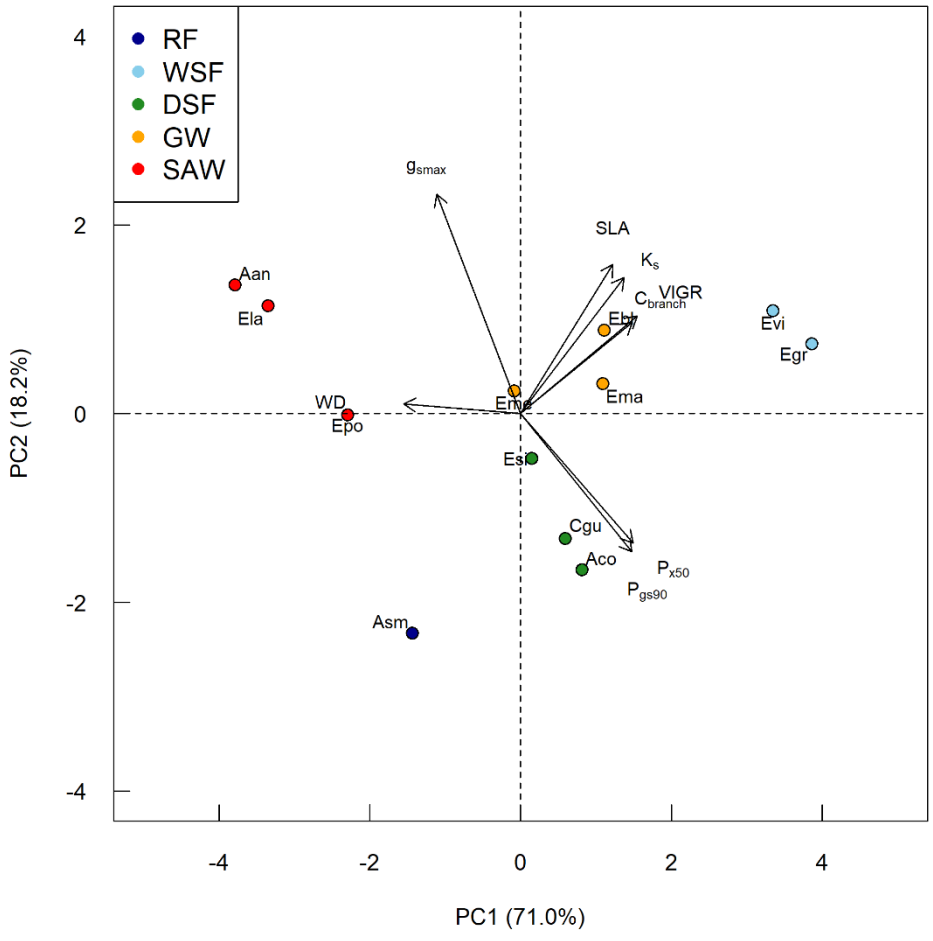

Figure 2-6 Bi-plot of principal component analysis (PCA) of the trade-offs between hydraulic and carbon economy traits. Traits used for PCA analysis were xylem water potential at 50% loss of conductivity (P_{x50}), water potential at 90% stomatal closure (P_{gs90}), xylem specific conductivity (K_s), sap wood density (WD), maximum stomatal conductance (g_{smax}), specific leaf area (SLA), branch capacitance (C_{branch}) and volume index growth rate (VIGR) for the five vegetation types: rainforest (RF), wet sclerophyll forest (WSF), dry sclerophyll forest (DSF), grass woodland (GW), and semi-arid woodland (SAW).

2.3.4 Correlation between hydraulic traits and climatic variables

To test the potential genetic constraint of leaf and xylem hydraulic traits, key characteristics were plotted against MAT, MAP and AI averaged across each species' distribution (Figure 2-7). P_{gs90} was strongly related to climate-of-origin across species, as indicated by the significant inverse correlations between P_{gs90} and MAP, as well as AI (Figure 2-7d, f; R^2=0.691 and 0.69 for MAP and AI, respectively). Likewise, inverse relationships were found between P_{50} and habitat water availability (Figure 2-7g,i; R^2=0.735 and 0.721 for MAP and AI, respectively), and HSM (Figure 2-7j,l; R^2=0.665 and 0.641 for MAP and AI, respectively). By contrast, some species with remarkably different site water availability showed somewhat similar TLP, resulting in a decoupling between TLP and climate. For example, *E. grandis* and *E. sideroxylon* had contrasting MAP and AI, but showed no difference in TLP (Table A-1). No significant correlation was found between MAT and hydraulic traits.

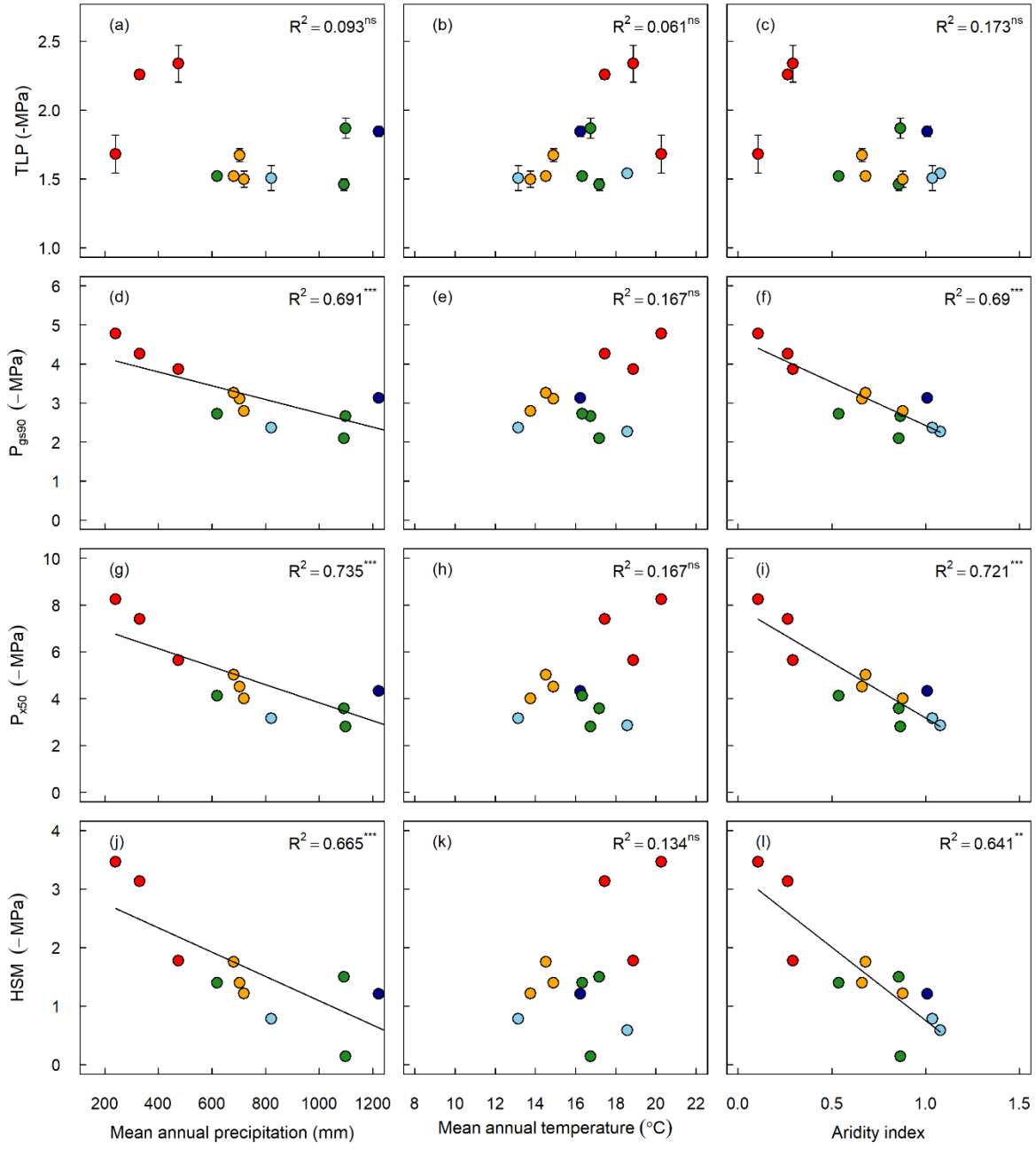

Figure 2-7 Effect of provenance water availability, characterized by mean annual precipitation (MAP) and aridity index (AI), and mean annual temperature (MAT) on leaf turgor loss point (TLP, Figure 7a-c), water potential at 90% stomatal closure (P_{gs90}, Figure 7d-f), xylem cavitation resistance (P_{x50}, Figure 7g-i) and hydraulic safety margin (HSM, Figure 7j-l). Adjusted R^2 of linear regressions are shown for each correlation, but regression

lines are only drawn for statistically significant cases. Statistical significance is indicated by asterisk (***, P<0.001; **, P<0.01; *, P<0.05; ns, not significant).

2.4 Discussion

We quantified key hydraulic and carbon economy traits of 12 woody species from a broad climatic gradient, with the aim of examining the level of coordination among these traits and the role of climate in shaping cross-species trait variation. The influence of environmental variation was minimized by the uniform growth condition, allowing us to factor out the influence of environment on phenotypic variation across species. We found that hydraulic traits were highly coordinated across species and strongly related to rainfall and aridity of the species native distributional range. In addition, trade-offs between drought tolerance and plant growth rate were observed. Collectively, these results provide critical insight into the coordination among hydraulic traits in modulating drought adaptation, and will significantly advance our ability to predict drought vulnerability in these dominant trees species.

2.4.1 Leaf and xylem hydraulics are highly coordinated

Consistent with other studies, the significant correlation between P_{12} and P_{gs90} indicates that stomatal behaviour in response to decreasing water potential was highly coordinated with the beginning of stem xylem cavitation (Brodribb et al. 2003a, Li et al. 2016, Bourne et al. 2017). It has been hypothesized that coordination exists between stomatal and xylem traits because increased cavitation resistance enables prolonged stomatal opening during drought, thereby maximizing carbon gain (Klein 2014, Bartlett et al. 2016). Furthermore, the observation that all species were located close to the 1:1 line was consistent with other studies (Brodribb et al. 2003b, Li et al. 2016), indicating that stomatal closure is timed to prevent the occurrence of significant xylem cavitation in the stem (Delzon and Cochard 2014, Nolf et al. 2015). Some studies suggest that interrupted water flow *per se* resulting from cavitation events may act as

a rapid signal that triggers stomatal closure (Nardini and Salleo 2000, Salleo et al. 2000). However, it is difficult to evaluate the mechanistic linkages between xylem cavitation and stomatal closure unless both processes are monitored simultaneously. Of note, Hochberg et al. (2017) concurrently visualized the progress of xylem cavitation and stomatal closure in grapevine, wherein complete stomatal closure always preceded xylem cavitation, thus suggesting that these two events are interrelated, but operate independently.

Additionally, the occurrence of significant levels of embolism prior to stomatal closure would require that embolised conduits be readily repaired following the relief of drought stress (Hochberg et al. 2017). While the occurrence of xylem refilling after drought induced cavitation has been documented in a number of plant species (Brodersen et al. 2010, Ogasa et al. 2013, Trifilò et al. 2015), recent studies suggest that xylem refilling post-drought is not widespread in tree species and is unlikely to occur in the absence of positive xylem pressure (Delzon et al. 2014, Choat et al. 2015b, Charrier et al. 2016). If embolism repair is not common in trees, the relationship between stomatal closure and early embolism formation observed in our study species may arise from functional convergence rather than a mechanistic linkage. Establishing the relationship between stomatal closure and early embolism thresholds is of critical significance for modelling, as information regarding species-specific stomatal and cavitation thresholds is limited (Choat et al. 2012a, Klein 2014, Martin-StPaul et al. 2017).

Leaf TLP was positively (but weakly) correlated with P_{gs90}, indicating that species with more negative TLP maintain stomatal opening across a wider range of water potentials. Recent studies also found a positive correlation between leaf TLP and P_{gs90} in a broad range of tree and shrub species (Brodribb et al. 2003a, Li et al. 2016, Bourne et al. 2017, Farrell et al.

2017). It has been proposed that guard cells can perceive alterations in leaf or epidermis water potential, and directly translate it into stomatal movement (Brodribb et al. 2003a). If so, leaf turgor loss and stomatal closure should occur synchronously. However, in the current study, although TLP and P_{gs90} were significantly correlated, P_{gs90} was consistently lower than TLP, indicating that stomata remained open even after bulk leaf turgor was lost. A similar observation has been reported for some tree and shrub species (Brodribb et al. 2003a, Farrell et al. 2017), and is interpreted as a decoupling between guard cell and bulk leaf water potential (Mott and Franks 2001). Indeed, stomatal behaviour is governed by numerous biophysical and biochemical (i.e. abscisic acid) factors (Salleo et al. 2000, Brodribb et al. 2003b, Brodribb and McAdam 2011). Given the weak correlation between these two parameters in our study, care should be taken when using TLP as the proxy of stomatal closure point, which has been adopted in some recent studies (Christoffersen et al. 2016, Xu et al. 2016).

2.4.2 Trade-offs among hydraulic traits

We found evidence supporting key trade-offs among hydraulic traits. P_{50} and K_s were negatively correlated across species, reflecting the trade-off between hydraulic safety and efficiency. Theoretically, this trade-off is derived from variation in the anatomy of vessels because safety and efficiency share the same structural basis (Gleason et al. 2016). Decreased K_s and increased cavitation resistance are often correlated with reduced vessel diameter and length, as well as increased vessel frequency for a given conducting area. Ultimately, control of cavitation resistance occurs at the pit level and can be achieved via changes in pit membrane thickness and porosity (Choat et al. 2008, Lens et al. 2011). Trade-offs also exist at the pit level; while thicker and less porous pit membranes result in higher cavitation resistance, they may also lower xylem conductivity because resistance of inter-vessel pits

account for more than 50% of total resistance in the xylem vessel network (Wheeler et al. 2005, Choat et al. 2006). However, the generality of the safety efficiency trade-off was recently challenged by a global data synthesis that showed a significant, but very weak, relationship between P_{50} and K_s (Gleason et al. 2016). In our study, the strength of the trade-off between P_{50} and K_s is likely due to the close phylogenetic relationship of our study species (11 of 12 species are in *Myrtaceae*) and uniform methodology.

C_{branch} and WD were inversely related, corroborating the proposed trade-off between storage and mechanical support. The functional significance of capacitance in plants has been well documented (Meinzer et al. 2009). Among the proposed mechanisms, capillary and elastic water release account for a significant portion of internal water storage and play a critical role in delaying dehydration (Richards et al. 2014). Furthermore, features favouring high storage capacity such as low fibre wall area can lead to lower mechanical support of xylem cavitation resistance (Jacobsen et al. 2005), which may help explain the observed relationship between P_{50} and WD. During drought, the strong tension generated in the xylem water column increases the risk of vessel implosion and wall collapse, with theoretical collapse pressures being correlated with embolism resistance (Hacke et al. 2001b, Cochard et al. 2004, Blackman et al. 2010). Increased resistance to cell wall collapse is dependent on having thicker vessel walls relative to lumen diameter, which may contribute to higher WD. As such, WD is often correlated with embolism resistance across species (Lens et al. 2011, Markesteijn et al. 2011), as was found in this study. These findings highlight the important role WD plays in plant ecological strategy.

2.4.3 Co-ordination between carbon and water traits

We found that P_{gs90} and P_{50} were inversely related to plant growth rate as estimated by VIGR, suggesting that increased embolism resistance may only be possible at the expense of reduced growth potential. Few studies have investigated the potential trade-off between hydraulic and carbon economic traits, particularly with regard to growth (Hajek et al. 2014). A negative correlation between P_{50} and aboveground biomass production has been observed among several *Populus* and *Salix* clones by Cochard et al. (2007). Likewise, *Eucalyptus* species with more negative TLP tended to exhibit lower growth rates (Bourne et al. 2017). The relationship between P_{50} and growth rate could be connected by WD, with higher construction costs of dense and rigid woody tissue being coupled to lower growth rates and increased cavitation resistance.

The positive correlations between hydraulic traits related to drought (e.g. P_{50}, P_{gs90} and HSM) and leaf carbon economy traits (e.g. A_{max} and g_{smax}) were somewhat unexpected. Intuitively, high g_{smax} potentially gives rise to rapid carbon assimilation at the expense of high rates of water loss. Species with such traits typically close stomata early during drought (i.e. less negative P_{gs}) and are relatively vulnerable to cavitation (i.e. less negative P_x) (Skelton et al. 2015). Yet, for species from dry regions, higher g_{smax} and A_{max} are beneficial for maximizing the utilization of unpredictable and rare precipitation events. Meanwhile, to endure protracted drought periods, higher drought resistance (e.g. high P_{gs}, P_x and HSM) is required.

2.4.4 Hydraulic strategy as defined by leaf and xylem traits

The use of trait combinations, instead of single traits, may yield crucial information on plant hydraulics. HSMs based on both xylem and leaf traits integrates key aspects of plant water balance, thus allowing the water regulation strategy and the likelihood of survivorship during drought to be identified (Delzon et al. 2014, Skelton et al. 2015, Martin-StPaul et al. 2017).

For instance, by examining P_{50} and P_{gs12}, Skelton et al. (2015) assessed the hydraulic conservatism of several co-occurring species and their likelihood of mortality under drought, such that species with positive HSM are more likely to die from carbon starvation, while species with negative HSM are more likely to die from hydraulic failure. Contrary to this finding, all species examined in the current study recorded positive HSM values, indicating that stomatal closure occurred prior to the occurrence of significant embolism formation, which is consistent with a recent global meta-analysis by Martin-St. Paul et al. (2017). Notably, in their synthesized dataset, P_{50} and the point of stomatal closure were linearly correlated until P_{50} became very negative (< -6 MPa), suggesting that early stomatal closure is of critical importance in facilitating drought adaptation in more arid environments. This pattern is in part supported by our findings, as indicated by the progressive deviation from the 1:1 line in more drought resistant species.

2.4.5 Cross species traits variation is driven by site water availability

Our hypothesis that variation of traits across species is related to climate-of-origin is strongly supported by the observation that P_{gs90} and P_{50} were negatively correlated with climatic indices of site water availability. Previous studies examining natural populations show that P_{50} is strongly related to site moisture across species, suggesting that cavitation resistance is a key determinant of species distribution (Brodribb and Hill 1999, Maherali et al. 2004). However, interspecific variation becomes larger as rainfall decreases as a result of within-site variation in water access or exposure to water stress (Choat et al. 2012a). In our common garden experiment the relationship between traits conferring drought tolerance and species climate-of-origin provides further evidence of strong genetic control over the development of these traits. Genetic constraint of P_{50} and P_{gs90} indicate a limited capacity for short-term acclimation in novel climate scenarios, which is supported by recent work showing limited

intra-specific variation in cavitation resistance across aridity gradients (Lamy et al. 2014, López et al. 2016).

2.5 Conclusion

Knowledge of hydraulic traits is essential to predict plant drought tolerance and species distributions with respect to water availability. Our data on plant hydraulic strategies of evergreen angiosperm species may be used to improve hydraulic modules of dynamic vegetation models to assess forest function under varying water availability. Leaf and xylem hydraulic traits were highly coordinated, collectively facilitating plant drought adaptation. Importantly, key hydraulic traits such as P_{gs} and P_x might be predicted from other traits, when data are otherwise unavailable. The trade-offs between plant hydraulic and carbon economy traits are indicative of plant growth strategy, in that slow-growers are more drought resistant and fast-growers are less drought resistant. Overall, species drought tolerance was linked to climate-of-origin, suggesting strong genetic constraints on these traits and indicating that some species may lack the capacity for short-term acclimation to increasing aridity.

Chapter 3

More than iso/anisohydry: Hydroscapes integrate plant water-use and drought tolerance traits in ten eucalypt species from contrasting climates

3.1 Introduction

Formulated eighty years ago, the iso/anisohydry remains the most popular terminology to describe stomatal regulation strategy during drought (Berger-Landefeldt 1936, Hochberg et al. 2018). Species with isohydric behaviour adopt a conservative water use strategy, with the stomata closing early during drought, thereby maintaining relatively constant leaf water potential with declining soil water content. Anisohydric species, on the other hand, maintain stomata open despite decreasing leaf water potential as soil water availability declines (Garcia-Forner et al. 2016a, Meinzer et al. 2016, Pivovaroff et al. 2018). The revival of this terminology in recent years largely lies in its simplicity, nicely contrasting plant carbon and hydraulic mechanisms of plant response to drought. In the recent literature, species' water use strategy has been described in terms of their position along a continuum, with isohydric and anisohydric stomatal behaviour representing two extremes (Klein 2014, Martínez-Vilalta et al. 2014). The iso/anisohydry continuum has been incorporated into the "carbon-hydraulic framework" of tree mortality, suggesting that species with contrasting degrees of isohydricity may die from either of two mechanisms, i.e., carbon starvation and hydraulic failure (McDowell et al., 2008) . However, recent meta-analyses suggest that tree death occurs mainly through hydraulic dysfunction (Adams et al. 2017), and that vulnerability to hydraulic failure might be related to traits other than water potential regulation (Fu and Meinzer 2017;

Martínez-Vilalta and Garcia-Forner 2017). Hence, the iso/anisohydry categorization might be too simplistic to identify which species are more or less vulnerable to mortality from drought stress (Garcia-Forner et al. 2016b).

Nonetheless, it is useful to have a summary metric to describe plant performance during drought. Various metrics have emerged that attempt to quantify the species drought response strategies, most of which incorporate some aspect of stomatal regulation (Meinzer et al. 2016). Generally speaking, the quantification of these metrics fall into two categories. The first type of metric highlights stomatal control of water loss and is based on the degree of homeostasis in plant water potential during drought. Examples of this kind of metric include (i) the slope of the relationship between midday leaf water potential (Ψ_{md}) and predawn leaf water potential (Ψ_{pd}; Martínez-Vilalta et al. 2014) , and (ii) the 'hydroscape' area over which plants are able to regulate leaf water potential (Meinzer et al. 2016). However, species rankings are highly variable using this type of metric (Martínez-Vilalta and Garcia-Forner 2017, Hochberg et al. 2018), partly because stomatal regulation during drought can be influenced by other environmental factors in addition to water availability (Hochberg et al. 2018). Alternatively, species drought response strategies can be defined based on the stringency of stomatal regulation within the bounds of critical thresholds of hydraulic failure due to embolism (Skelton et al. 2015). Examples of this kind of metric include the maximum range of daily leaf water potential variation ($\Delta\Psi_{max}$; Klein, 2014) , and the stomatal-hydraulic safety margin, which is defined as the difference in water potential at stomatal closure and xylem cavitation threshold (HSM_{ST}, P_{gs90}-P_{L50}; Skelton et al. 2015) . Although both types of metrics have been adopted (Johnson et al. 2018a, Pivovaroff et al. 2018), it remains unclear which metric best characterises plant water regulation strategy under common conditions during drought.

Characterising the overall water relations strategy of a species requires knowledge of a number of stomatal and hydraulic traits that contribute to plant water use and drought tolerance. Leaf traits such as turgor loss point (TLP) and leaf water potential at stomatal closure (P_{gs90}) represent the minimum water potential at which carbon assimilation is operational, and therefore are among the most fundamental traits when assessing species' drought resistance. However, the effectiveness of having drought resistant stomata (i.e. more negative P_{gs90}) depends on the water potential threshold beyond which significant xylem embolism occurs (Skelton et al. 2015, Choat et al. 2018a). Indeed, early stomatal closure relative to the onset of xylem cavitation has been shown to be an important strategy in boosting plant drought resistance (Martin-StPaul et al. 2017). Moreover, embolism thresholds have been shown to be responsible for organ and whole plant death (Blackman et al. 2009, Brodribb et al. 2009, Urli et al. 2013, Li et al. 2016). These hydraulic traits characterizing plant vulnerability to embolism are often well correlated with climatic factors across species, therefore informing the evolutionary drivers shaping the adaptation of drought response strategies (Choat et al. 2012a, Blackman et al. 2014, Bourne et al. 2017, Trueba et al. 2017, Li et al. 2018a, Skelton et al. 2018). In addition, significant differences between leaf and stem vulnerability provides evidence for hydraulic vulnerability segmentation (HSM_{HS}), a strategy that minimises water loss during drought *via* leaf shedding (Pivovaroff et al. 2014, Zhu et al. 2016a, Zhang et al. 2017). Given their functional significance, examining how different metrics are related to these key drought tolerance traits will advance our understanding on species life history strategies, as well as helping to identify species at risk of drought mortality and clarifying the underlying mechanisms providing drought tolerance.

In addition to traits related to drought tolerance, plant water use strategies also depend on stomatal and hydraulic traits that influence rates of plant water use under non-stressful

conditions. Photosynthetic capacity, maximum hydraulic conductance (k_{max}) and maximum stomatal conductance (g_{smax}) are often correlated (Brodribb and Feild 2000, Santiago et al. 2004, Choat et al. 2011), while many studies find a trade-off between embolism resistence and hydraulic conductivity (Markesteijn et al. 2011, Li et al. 2018a). It might therefore be expected that species with greater drought tolerance that operate across a broader range of water potentials would exhibit lower leaf conductance under non-stressful conditions, which is consistent with an overall more conservative growth strategy (Reich et al. 2014). In agreement with this expectation, Maherali et al. (2006) reported increased stomatal conductance in species with high vulnerability in a study of 14 co-occurring temperate tree species. However, we found the opposite correlation for eucalypt species from contrasting climate-origins: Li et al. (2018a) showed that g_{smax} is positively correlated with embolism resistance. Furthermore, Meinzer et al. (2017) showed that the velocity of stomatal open under light and g_{smax} were positively correlated with increasing stomatal regulation in 10 woody species. It is as yet unclear how this relationship contributes to species water potential regulation and water-use strategies.

Here, we examined the water-use strategy of ten eucalypt species from four major forest types (wet sclerophyll forest, dry sclerophyll forest, grassy woodland and semi-arid woodland) across NSW, Australia. These ten species were studied in a previous experiment (Li et al. 2018a) and found to have strongly contrasting stomatal and hydraulic traits, which were closely correlated with climate-of-origin. Growth conditions were normalized by using a common garden approach, thus minimising confounding environmental effects on plant water use. We assessed different drought response metrics, as well as key stomatal and hydraulic traits related to plant water use and drought tolerance. Specifically, we asked: (1) Is species ranking consistent using different metrics for plant water use strategy? (2) What

insight do the different metrics provide into overall water use strategy? and (3) How do the metrics correlate with plant performance and drought tolerance traits?

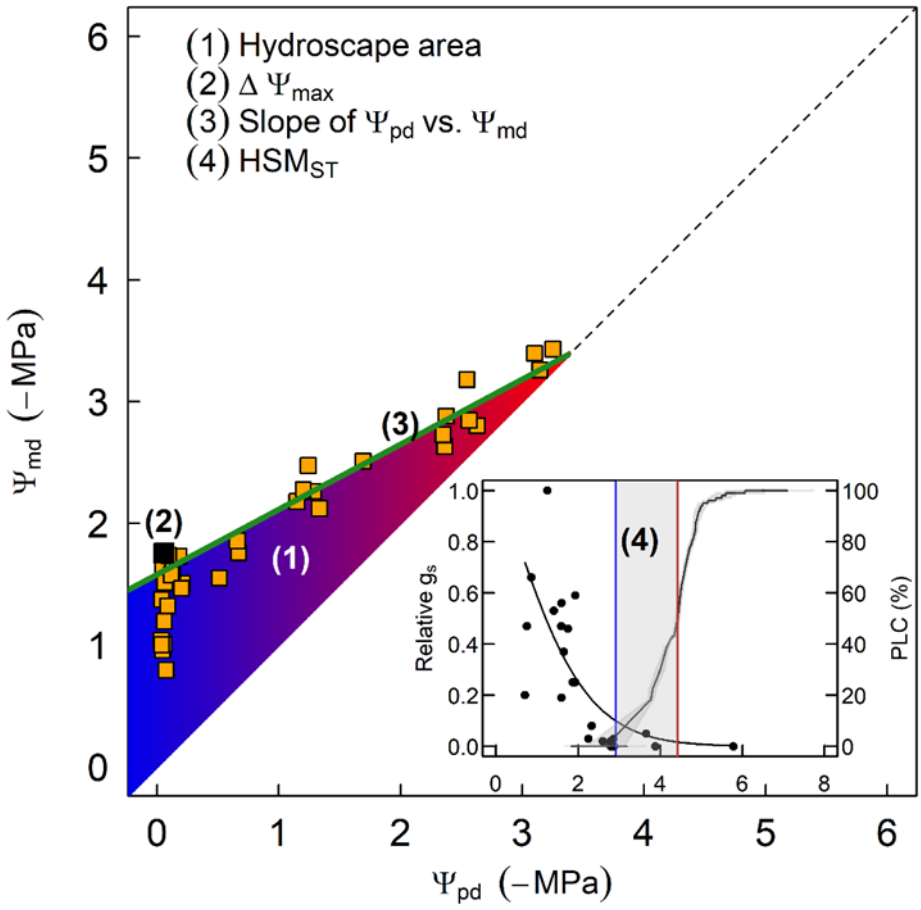

Figure 3-1 Illustrative figure showing different metrics for characterizing the degree of iso/anisohydricity of plant. Predawn (Ψ_{pd}) and midday leaf water potential (Ψ_{md}) measured during dehydration are plotted against each other (yellow square). A linear regression is made after excluding the water potential values affected by environmental factors other than water availability at the early phase of dry-down (Slope, green solid line). Degree of fluctuation in plant water potential is defined as the maximum different between Ψ_{pd} and Ψ_{md} ($\Delta\Psi_{max}$, black square) along the dehydration trajectory. Hydroscape is represented by the area bounded by the regression line and 1:1 line (area shaded by blue-red colour gradient). Furthermore,

relative stomatal conductance (g_s, filled circle) and percentage loss of conductivity (PLC) for leaf are plotted against water potential. The distance between stomatal closure point (P_{gs90}, blue vertical line) and xylem water potential inducing 50% loss of conductivity (P_{L50}, red vertical line) is defined as safety margin of stomata (HSM_{ST}, P_{gs90}-P_{L50}).

3.2 Material and methods

3.2.1 Plant material and experimental design

Ten eucalypt species representing four major woody vegetation ecosystems across NSW, Australia were chosen for the study (Table 3-1). Across this ecologically diverse group, species climate-of-origin (averaged across their native distributional range) varied tremendously, with the mean annual precipitation (MAP, mm) ranging from 250 to 1124 mm, and mean annual temperature (MAT, ^{o}C) ranging from 10 to 18 ^{o}C. The aridity index (AI), defined as the ratio of MAP and potential evaporation, ranged from 0.2 for *Eucalyptus largiflorens* (most arid) to 1.1 for *E. viminalis* (most mesic).

Seeds were obtained from Mount Annan Botanical Garden (Mount Annan, NSW, Australia) and were sown in forestry tubes in a sun-lit polytunnel provided by Greening Australia (Richmond, NSW, Australia) under ambient environmental conditions until seedlings were approximately 15 cm tall. On 21st Nov 2017, seedlings were moved to the polytunnel greenhouse facility of Western Sydney University (33^{o}33’S, 150^{o}44’E, Richmond, NSW, Australia) and transplanted into 25 litre woven planter bags filled with roughly 20 kg loamy sand soil (Menangle Sand & Soil, Menangle, NSW, Australia). Pots were placed onto palettes to prevent root growth outside the pots. Soil was manually watered to drainage immediately after transplanting and was watered for 10 min every other day using a computer controlled

irrigation system to keep the water content at field capacity. Commercial controlled-release fertilizer (Osmocote, All purpose) was applied to ensure plants were not nutrient limited during the experimental period. Environmental conditions in the polytunnel were recorded at 15-min intervals by a data-logger (CR300, Campdell Scientific Inc) connected to a light sensor (Decagon Devices Inc., Pullman, WA, USA) and temperature/relative humidity probe (HMP60-L, Campbell Scientific Inc., Logan, UT, USA) installed at 1.5 m above the ground. During the experimental period, mean daily photon flux density was 6.67 mol m^{-2} day^{-1}, mean daily temperature was 22.6 ^{o}C and mean daily relative humidity was 64.3%.

The polytunnel was divided into six replicate blocks to account for potential environmental variation. In addition, we had a single row of border trees with randomly selected species to minimise environmental perturbation from outside. Within each block, three or four plants of each species were randomly allocated. Species differed greatly in their rate of growth, so we separated the species into three sub-groups and applied the drought treatment to each group at different times once the plants had grown between 60 and 100 cm tall. Group 1 consisted of the species *Eucalyptus blakelyi*, *E. grandis* and *E. viminalis*; group 2 consisted of *Angophora costata, Corymbia gummifera*, *E. melliodora* and *E. sideroxylon*; and group 3 consisted of *E. lagiflorens*, *E. macrorhyncha* and *E. populnea*. All groups were subject to the drought treatment within a two-month period, from early to mid-Autumn. During a pre-treatment drought hardening cycle, plants were dried until leaves were visually wilting, which was usually achieved within 1-2 weeks depending on weather conditions and species drought sensitivity. Thereafter, soil was rewatered and maintained at field capacity for 4-6 days to achieve full leaf water content (i.e. $\Psi_{pd} \approx 0$). In the drought treatment, irrigation was discontinued and plants were allowed to use up available soil water and dehydrate. During the drought treatment, soil water potential was monitored regularly using predawn leaf water

potential (Ψ_{pd}) as a proxy. For leaf water potential measurement, one leaf per plant was excised and immediately sealed in humidified plastic zip-lock bags. The leaf samples were transported to the lab and leaf water potential measured using a Scholander-type pressure chamber (PMS Instruments, Corvalis, OR, USA).

Table 3-1 Summary of species and corresponding code, vegetation types, mean annual temperature (MAT, ^{o}C), mean annual precipitation (MAP, mm) and aridity index (AI) averaged within the species native distributional range. Lower AI indicates more arid site.

Species	Code	Vegetation type	MAT	MAP	AI
Eucalyptus grandis (W.Hill)	Egr	Wet sclerophyll	18.5	1436.3	1.1
Eucalyptus viminalis (Labill.)	Evi	forest	13.2	803.3	1.0
Angophora costata ((Gaertn.) Britten)	Aco	Dry sclerophyll	17.3	1119	0.8
Corymbia gummifera (K.D.Hill & L.A.S.Johnson)	Cgu	forest	16.8	1119	0.8
Eucalyptus sideroxylon (A.Cunn. ex Woolls)	Esi		16.3	641.9	0.5
Eucalyptus blakelyi (Maiden)	Ebl	Grassy woodland	14.9	717.6	0.6
Eucalyptus macrorhyncha (F.Muell. ex Benth)	Ema		13.7	736.3	0.8
Eucalyptus melliodora (A.Cunn. ex Schauer)	Eme		14.5	677.7	0.7
Eucalyptus largiflorens (F.Muell.)	Ela	Semiarid woodland	17.4	333.2	0.3
Eucalyptus populnea (F.Muell.)	Epo		18.8	498.1	0.3

3.2.2 Leaf vulnerability curves

Leaf vulnerability curves were generated using the newly-developed optical visualisation (OV) technique (Brodribb et al. 2016). Three well-watered individuals for each species were selected for leaf vulnerability determination, with the exception of *E. populnea*, which was

represented by two individuals. Plant material was collected in the early morning when xylem tension was minimal. Whole plants were excised within 5 cm of the soil surface and quickly transferred to a bucket filled with clean water. The cut end was immediately recut under water and the whole shoot portion placed inside an opaque plastic bag and transported to the lab.

Leaf images were captured using two custom-built leaf clamps (Version 1) equipped with a digital camera (Camera Module v2, Raspberry Pi Foundation, ENG, UK) and macro-lens (detailed description of the leaf clamp is available at www.opensourceov.org). For each individual, a recent, fully expanded leaf was mounted to the leaf clamp, with the adaxial side covered by a microscope slide to ensure a flat surface. The branch was dried under lab conditions (*ca.* 48 to 120 hr, depending on species) until the targeted leaf became crispy. Images of the leaf within the clamp were taken at 5 min intervals. Leaf water potential (Ψ_{leaf}) was monitored simultaneously using a psychrometer (ICT International, Armidale, NSW, Australia) installed on the stem and close to the targeted leaf. It is possible that small water potential gradients may exist due to leaf cuticular conductance or leaky stomata after stomatal closure, resulting in a gradient between Ψ_{leaf} and stem water potential (Ψ_{stem}). However, by measuring Ψ_{leaf} regularly using the pressure chamber, we found this difference was negligible (data not shown).

Leaf images were analysed using an image subtraction method with ImageJ (National Institutes of Health, Bethesda, MD, USA) following Skelton (2017a). Briefly, images were stacked and any difference between two consecutive images were revealed by the “Image Difference” function in OSOV toolbox (www. opensourceov.org). The image stack containing the differences was then thresholded and pixels representing embolism were

highlighted using “Analyse Particles” function. Noise was removed manually when necessary. The number of pixels on each image was calculated using the “Measure Stack” function. Then pixels were summed to give the total area symbolizing embolized veins during leaf dehydration. Percentage of embolism over time was calculated as the ratio of pixel area at each time point to the cumulative pixel area, and then plotted against Ψ_{leaf} to give the leaf vulnerability curve. Water potential inducing 50% loss of leaf conductivity (P_{L50}) was taken as the Ψ_{leaf} when 50% of the total pixels appeared.

3.2.3 Pressure-volume traits

Unlike our previous study in which leaf pressure-volume (PV) curves were conducted on well-watered plants (Li et al. 2018a), here three drought-hardened individuals per species were used. Given leaf hydraulics have been shown to be plastic (Johnson et al. 2018), it was expcted that pressure-volume traits can be altered by drought hardening. For each individual, one upper canopy leaf was sampled before sunrise and the cut end immediately placed in water. For species with reduced petioles, a terminal branchlet containing mature leaves was used. Samples were allowed to rehydrate in darkness for up to 3 hr. Leaf PV curves were generated following Tyree & Hammel (1972). Leaves or small shoots were slowly dehydrated under lab conditions, Ψl_{eaf} and leaf fresh mass (FW) were measured periodically with the pressure chamber and a digital balance (weighed to 0.1 mg), respectively. PV curve analysis was performed following Lenz et al. (2006). To facilitate calculation, the inverse of leaf water potential ($1/\Psi_{leaf}$) was plotted against leaf relative water content (RWC_{leaf}, %). Leaf turgor loss point (TLP, -MPa) was taken as the inverse of the inflection point.

3.2.4 Stem and stomatal traits

Additional stem and stomatal traits were sourced from previous work with the same species under similar conditions (Li et al. 2018a). These traits include water potential inducing 50%

loss of conductivity in stem (P_{x50}, -MPa) and stomatal closure (P_{gs90}, -MPa), maximum conductivity of stem (K_{max}, kg m^{-2} s^{-1} MPa^{-1}) and maximum stomatal conductance (g_{smax}, mol m^{-2} s^{-1}). Experimental protocols are detailed therein. Briefly, plants were subjected to progressive dry-down and percentage loss of conductivity (PLC, %) of stem and stomatal conductance (g_s) were measured periodically. Obtained PLC and g_s were plotted against Ψ_{stem} and Ψ_{leaf}, respectively, and then fitted using sigmoidal function to estimate P_{x50} and P_{gs90}. K_{max} was measured with a digital flowmeter on stem samples flushed using 2 mmol KCL solution under high pressure (2 kPa). g_{smax} was taken as the g_s measured on well-watered plants.

3.2.5 Morphological traits

For each species, 8-10 upper canopy leaves were collected from five individuals for measurement of specific leaf area (SLA, m^2 kg^{-1}). Leaf area was measured using a leaf area meter (Li-3100C, Licor, Lincoln, NE, USA). Samples were oven-dried at 70 ^oC for 48 hr until constant and then weighed. SLA was calculated as the ratio of leaf area to dry mass. The above-ground portion of the plants was harvested at the end of the experiment by cutting the stem from the base. Leaves were collected and oven-dried until constant mass. Total canopy leaf area was estimated using leaf dry weight and SLA. Basal sapwood diameter was measured using digital callipers. Huber value (HV, m^2 m^{-2}) was calculated as the ratio of basal sapwood area to total canopy leaf area.

3.2.6 Data analysis

As in the previous paper (Li et al. 2018a), the climate envelope of each species was sourced from Atlas of Living Australia using the Mapping & Analysis channel (http://spatial.ala.org.au/, accessed in May 2016).

Four metrics quantifying species water use strategy were calculated (see Figure 3-1). Metric 1: The slope of the relationship between Ψ_{pd} and Ψ_{md} (Slope; Martinez-Vilalta et al., 2014) was calculated by linear regression. To minimize the variation of leaf water potential related to other environmental factors (e.g. light, vapour pressure deficit or temperature), we took the data closest to the 1:1 line as the starting point. Data were progressively added until the R^2 of the linear regression reached its maximum (Meinzer et al. 2016). We excluded the water potential data beyond $\Psi_{pd}=\Psi_{md}$ because stomatal regulation plays no role in regulating plant water status after stomatal closure,.

Metric 2: The maximum range of daily leaf water potential variation ($\Delta\Psi_{max}$; Klein, 2014) was calculated as the maximum difference between Ψ_{pd} and Ψ_{md} over the course of the dry-down.

Metric 3: The Hydroscape area (hereafter Hydroscape) is the region bounded by the Ψ_{pd} vs. Ψ_{md} regression and 1:1 line, which was calculated as:

$$\text{Hydroscape}=\frac{a\times b}{2}$$

where a is the intercept of Ψ_{pd} vs. Ψ_{md} regression, which represents the most negative Ψ_{md} when $\Psi_{pd}=0$ (i.e. $\Delta\Psi_{max}$). b is the intersection of Ψ_{pd} vs. Ψ_{md} regression and 1:1 line, which is the water potential at $\Psi_{pd}=\Psi_{md}$.

Metric 4: The stomatal hydraulic safety margin (HSM_{ST}) was calculated as the difference in water potential at stomatal closure and xylem cavitation threshold of leaf (Skelton et al. 2015):

$$HSM_{ST} = P_{gs90}-P_{L50}$$

The P_{x50} and P_{gs90} across species were compared using bootstrap confidence intervals (CIs) and were considered statistically different if CIs do not overlap (Duursma and Choat 2017). For other traits, one-way ANOVA with a Tukey HSD *post-hoc* test was used to examine the difference across species. Principal component analysis (PCA) was used to test the multivariate associations among hydraulic traits and metrics of isohydricity with prcomp() function. Furthermore, each of the key hydraulic traits including P_{gs90}, P_{L50}, P_{x50}, g_{smax}, HV and hydraulic segmentation (HSM_{HS}, defined as P_{L50}-P_{gs90}) was regressed against four metrics with multivariate regression and a stepwise algorithm based on Akaike's information criterion (AIC) was used to choose the best model. The relative importance of each metric in explaining the variation of traits was assessed using lmg index estimated by calc.relimp() function. In addition, the bivariant relationship among traits and their correlation with climatic variables were examined using linear regression. All statistical analyses were performed using R (version 3.5.0, R Development Core Team, 2014).

3.3 Results

3.3.1 Species ranking using different metrics

Of the four metrics, the Hydroscape varied most strongly across species (co-efficient of variation [CV]=39.1%), ranging from 1.13 MPa^2 in *E. grandis* to 3.82 MPa^2 in *E. populnea* (Figure 3-2a, also see Figure A3 in Appendix). The stomatal hydraulic safety margin (HSM_{ST}) of leaves also varied considerably (CV=38.2%), ranging from 0.4 MPa in *E. largiflorens* to 1.63MPa in *E. macrorhyncha* (Figure 3-2d), while $\Delta\Psi_{max}$ (CV=21.7%) ranged from 1.85 MPa in *E. largiflorens* to 0.97 in *C. gummifera* (Figure 3-2c). Much lower variation (CV=14.3%) was observed among species in the slope of the relationship between Ψ_{md} and Ψ_{pd} during drought (Figure 3-2b). Species rankings were dependent on the metrics in

use. Furthermore, the Hydroscape was correlated with $\Delta\Psi_{max}$ (Figure 3-2e; R^2=0.72, $p<0.01$), but not with the slope of Ψ_{md} vs. Ψ_{pd} relationship nor HSM_{ST}. In addition, positive correlation was found between the rankings produced by Hydroscape and $\Delta\Psi_{max}$ (Spearman's ρ=0.67, $p<0.05$), whereas no significant correlation was found among the rankings given by other metrics (Table A-4).

Table 3-2 Values of key hydraulic traits of ten eucalyptus species. Species are ordered according to their Hydroscape area (low to high). Hydraulic traits are shown either in mean ± standard error of mean (SE, n=3~5) or values with lower and upper bounds of 95% confidence interval (CI, bracketed). Numbers differ in superscript are statistically significant at $p \leq 0.05$ level. TLP: leaf turgor point. P_{gs90}: leaf water potential causing 90% stomatal closure. P_{L50}/P_{x50}: leaf and stem water potential inducing 50% loss of hydraulic conductivity. HSM_{HS}: hydraulic safety margin of hydraulic segmentation defined as P_{L50}-P_{x50}. g_{smax}: maximum stomatal conductance. K_{max}: maximum stem hydraulic conductivity. HV: Huber value.

Species	TLP (-MPa)	[a]P_{gs90} (-MPa)	P_{L50} (-MPa)	[a]P_{x50} (-MPa)	HSM_{HS} (MPa)	[a]g_{smax} (mol m^{-2} s^{-1})	[a]K_{max} (kg m^{-2} s^{-1} MPa^{-1})	HV (m^2 m^{-2})
Egr	1.95 ± 0.04^{bcd}	2.27[1.95,]	3.43 ± 0.19^{bc}	2.85[2.36,3.34]	-0.58	0.22 ± 0.02^{bc}	2.31 ± 0.11^{a}	3.91 ± 0.26^{c}
Cgu	1.85 ± 0.16^{cd}	2.09[1.65,]	3.45 ± 0.27^{bc}	3.59[2.91,4.28]	0.14	0.21 ± 0.03^{bc}	1.75 ± 0.11^{abcde}	4.7 ± 0.4^{c}
Evi	1.64 ± 0.03^{d}	2.37[1.87,]	3.32 ± 0.19^{c}	3.15[2.7,4.32]	-0.17	0.26 ± 0.04^{bc}	2.17 ± 0.13^{ab}	4.63 ± 0.4^{c}
Aco	2.33 ± 0.15^{ab}	2.66[2.17,]	3.8 ± 0.27^{abc}	2.81[2.15,3.34]	-1	0.21 ± 0.02^{bc}	1.19 ± 0.16^{ef}	4.29 ± 0.31^{c}
Ema	1.97 ± 0.07^{bcd}	2.79[2.36,]	4.42 ± 0.05^{ab}	4.01[3.32,4.59]	-0.42	0.36 ± 0.06^{abc}	1.95 ± 0.2^{abc}	8.4 ± 0.68^{b}
Ebl	2.07 ± 0.1^{abcd}	3.11[2.39,]	3.64 ± 0.25^{bc}	4.51[4.11,5.01]	0.87	0.34 ± 0.04^{bc}	1.86 ± 0.15^{abcd}	6.43 ± 0.42^{bc}
Eme	2.31 ± 0.13^{abc}	3.26[2.31,]	4.17 ± 0.22^{abc}	5.02[4.23,5.52]	0.84	0.3 ± 0.03^{bc}	1.85 ± 0.08^{abcd}	5.38 ± 0.39^{bc}
Esi	2.21 ± 0.05^{abc}	2.72[1.76,]	4.15 ± 0.1^{abc}	4.12[3.5,4.66]	-0.03	0.31 ± 0.06^{bc}	1.62 ± 0.11^{bcde}	6.79 ± 0.36^{bc}
Ela	2.49 ± 0.04^{a}	4.26[3.12,]	4.67 ± 0.2^{a}	7.4[6.89,8.3]	2.73	0.58 ± 0.07^{a}	1.33 ± 0.14^{cdef}	15.78 ± 1.64^{a}
Epo	2.32 ± 0.06^{abc}	3.87[2.53,]	4.64 ± 0.25^{a}	5.64[4.99,6.06]	1	0.4 ± 0.08^{ab}	1.26 ± 0.16^{def}	15.51 ± 2.6^{a}

[a]: Data are sourced from Li et al. (2018a)

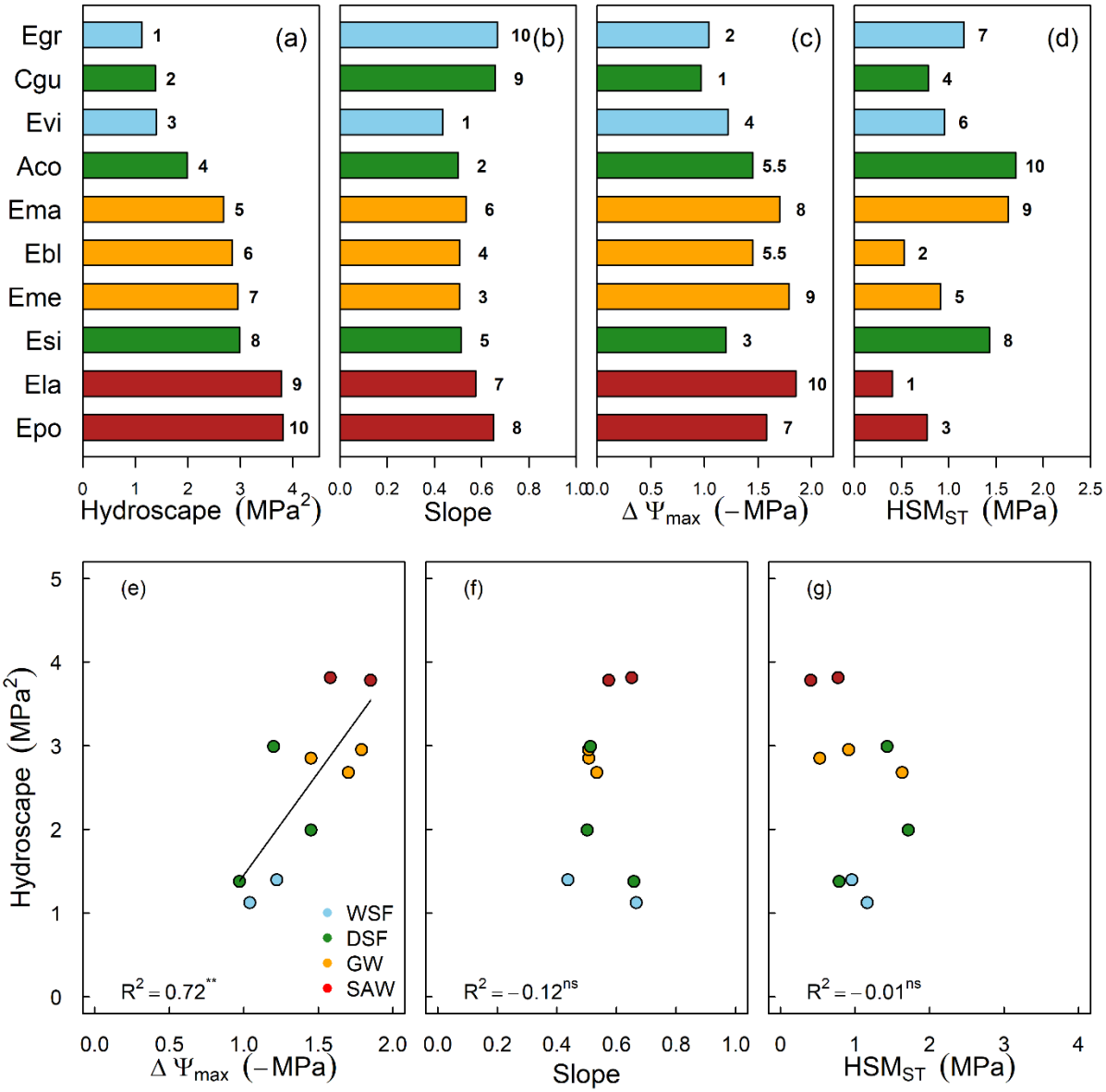

Figure 3-2 Values of four different metrics (panel a~d) and correlations between Hydroscape and other three metrics (panel e~g). Numbers in panel a~d indicate species ranking along the iso/anisohydry continuum according to each metric. To increase readability, species are ordered according to the ranking given by Hydroscape. Colours represent different vegetation types (WSF: Wet sclerophyll forest; DSF: Dry sclerophyll forest; GW: Grassy woodland; SAW: Semiarid woodland). Adjusted R^2 of linear regressions are shown. Asterisk indicates significant level (***, $p < 0.001$; **, $p < 0.01$; *, $p < 0.05$).

3.3.2 Defining water use strategies across species

Key hydraulic traits and morphological traits varied markedly across the ten species (Table 3-2, Figure 3-3a,b). Arid zone species generally showed more negative water potential threshold inducing 50% embolism in leaf (P_{L50}) and leaf turgor loss point (TLP) in the present study. Also, arid zone species exhibited higher Huber value (HV) and hydraulic safety margin of hydraulic segmentation (HSM_{HS}) than mesic zone species. A similar pattern along the aridity gradient was found for other traits including the water potential inducing stomatal closure (P_{gs90}) and 50% loss of stem conductivity (P_{x50}) and maximum stomatal conductance (g_{smax}), whereas an opposite pattern was detected for maximum stem conductivity (K_{max}), as shown in our previous study (Li et al. 2018a). In addition, P_{gs90}, P_{L50} and P_{x50} were highly co-ordinated across species (Table A-3).

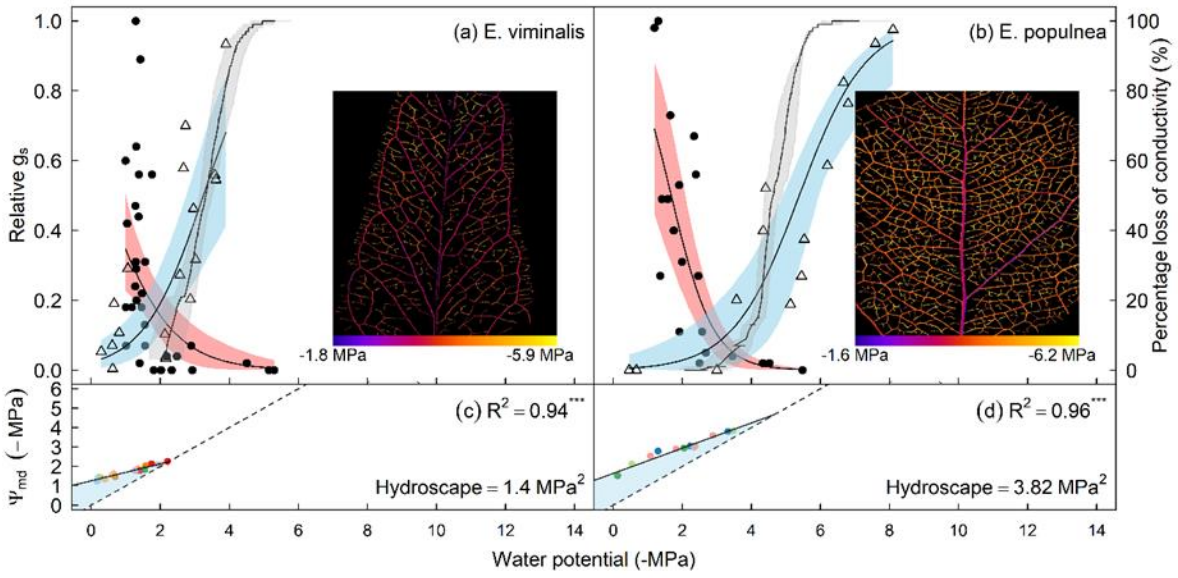

Figure 3-3 Percentage loss of xylem conductivity of leaf (solid line, light grey band), stem (open triangle, light blue band) and relative stomatal conductance (closed circle, pink band)

respond to water potential in two species (Figure 3-3a, b) with contrasting Hydroscape area (Figure 3-3c, d). Shaded bands represent confidence interval for stem and stomatal response to water potential and denote standard error for leaf response. Inset images show the propagation of embolism within leaf vein network during dehydration. Veins are coloured differently according to the water potential at which embolism occurs. Numbers below the scale bar indicate the water potential at which first and last embolism events were observed. Colours of datapoints in panel c and d represent different individuals. R^2 of linear regression is also shown . Asterisk indicates significant level (***, $p < 0.001$; **, $p < 0.01$; *, $p < 0.05$).

A principal component analysis of these traits identified two major axes, cumulatively explaining 79.2% of the variation across species (Figure 3-4). The first component (PC1), which accounted for 66.1% of total variation, was positively linked to drought tolerance traits (i.e. TLP, P_{gs90}, P_{x50}, P_{L50}, HSM_{HS}) as well as g_{smax} and HV. The second component (PC2) accounted for 13.1% of variation, and was negatively related to K_{max}. The ten species were primarily spread along the axis defined by PC1. Two of the four metrics, namely Hydroscape and $\Delta\Psi_{max}$, were loaded on the positive side of PC1, while the Slope and HSM_{ST} were heavily loaded on the positive and negative side of the second component (PC2), respectively. Moreover, a relative importance analysis showed that Hydroscape was ranked highest in explaining the variation of key hydraulic traits including P_{gs90}, P_{L50}, P_{x50}, g_{smax}, HSM_{HS} and HV across species (Table 3-3).

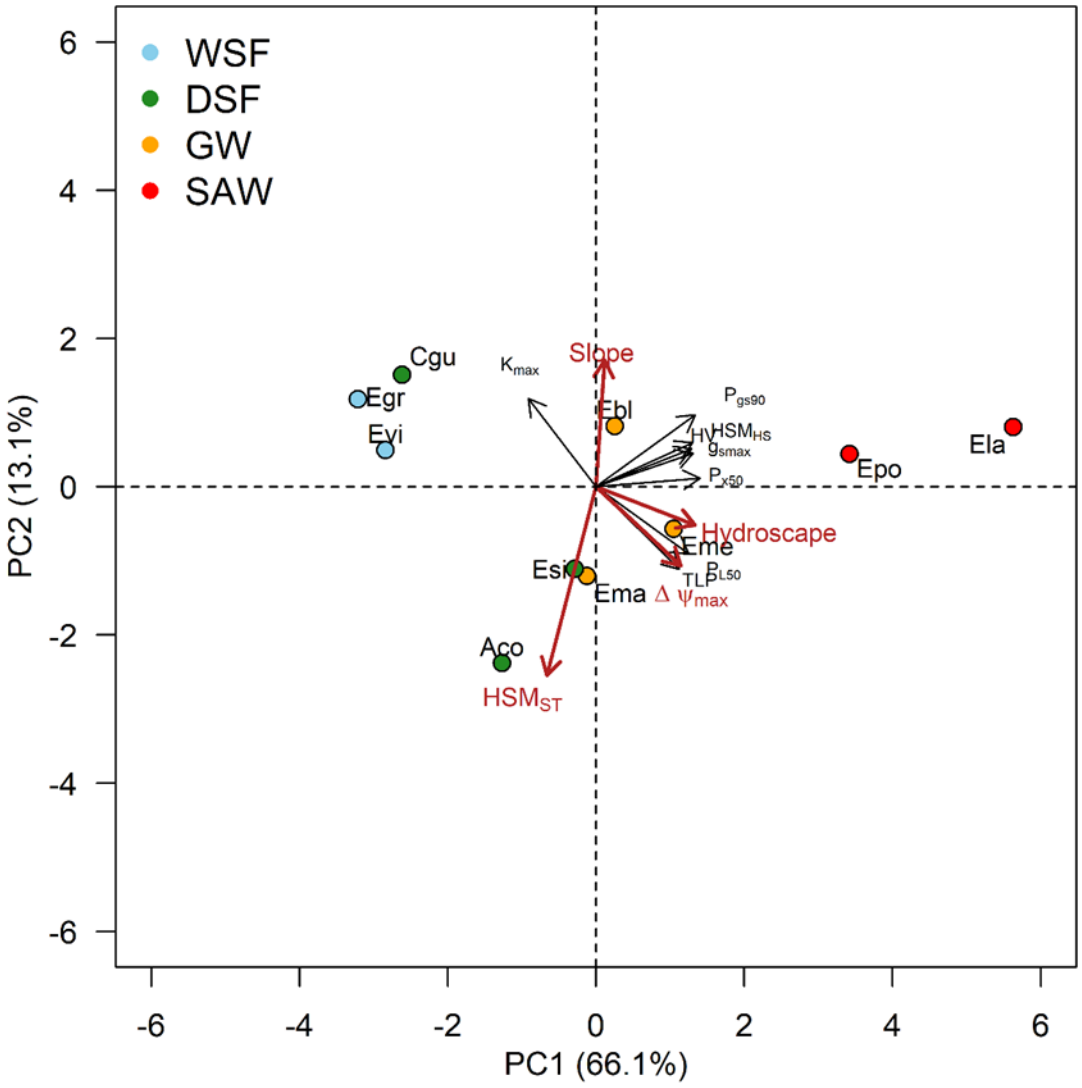

Figure 3-4 Bi-plot showing the results of principal component analysis (PCA) among metrics of isohydricity and plant traits. Traits used for PCA are turgor loss point (TLP), stomatal closure point (P_{gs90}), xylem water potential inducing 50% loss of conductivity in stem (P_{x50}) and leaf (P_{L50}), maximum stomatal conductance (g_{smax}), maximum stem conductivity (K_{max}) and Huber value (HV). Different vegetation types are abbreviated using initials and are coloured differently (WSF: Wet sclerophyll forest; DSF: Dry sclerophyll forest; GW: Grassy woodland; SAW: Semiarid woodland).

3.3.3 Correlations between metrics and key hydraulic traits

Species with contrasting Hydroscape exhibited distinct responses to drought in terms of stomatal conductance and xylem embolism (Figure 3-4, Figure A-3, A-4). Small Hydroscape (e.g. Figure 3-3a) species typically showed less negative water potential thresholds for stomatal closure and xylem embolism; while species with large Hydroscape (e.g. Figure 3-3b) exhibited an opposite pattern. Despite the difference in threshold, the propagation of embolism within leaves followed a similar pattern across species, with the initiation and progression of embolisms starting at higher water potentials in mid-ribs than secondary and tertiary veins (Figure 3-3a,b). Across species, strong positive correlations were found between Hydroscape and traits characterizing drought tolerance including TLP (Figure 3-5a; R^2=0.53, p<0.01), P_{gs90} (Figure 3-5b; R^2=0.83, p<0.001), P_{L50} (Figure 3-5c; R^2=0.79, p<0.001), P_{x50} (Figure 3-5d; R^2=0.79, p<0.001) and HSM_{HS} (Figure 3-5e; R^2 = 0.58, p<0.01). Furthermore, a positive correlation was found between Hydroscape and g_{smax} (Figure 3-5f; R^2=0.64, p<0.01). In addition, a positive correlation was found between g_{smax} and HV (Figure 3-6; R^2=0.83, p<0.001).

Table 3-3 lmg scores showing the relative importance of metrics in explaining traits variation across species in multivariant regression based on stepwise algorithm. Higher score means greater contribution to R^2. Blank cells indicate metrics are removed from model. Traits used for lmg analysis are stomatal closure point (P_{gs90}), water potential inducing 50% loss of conductivity in leaf (P_{L50}) and stem (P_{x50}), maximum stomatal conductance (g_{smax}), safety margin of hydraulic segmentation (HSM_{HS}, i.e. P_{L50}-P_{gs90}) and Huber value (HV).

	P_{gs90}	P_{L50}	P_{x50}	g_{smax}	HSM_{HS}	HV
Hydroscape	0.41	0.54	0.48	0.79	0.35	0.88
$\Delta\Psi_{max}$	0.24	0.37	0.36	-	0.29	0.12
Slope	0.06	0.05	-	-	-	-
HSM_{ST}	0.29	0.04	0.16	0.21	0.36	-

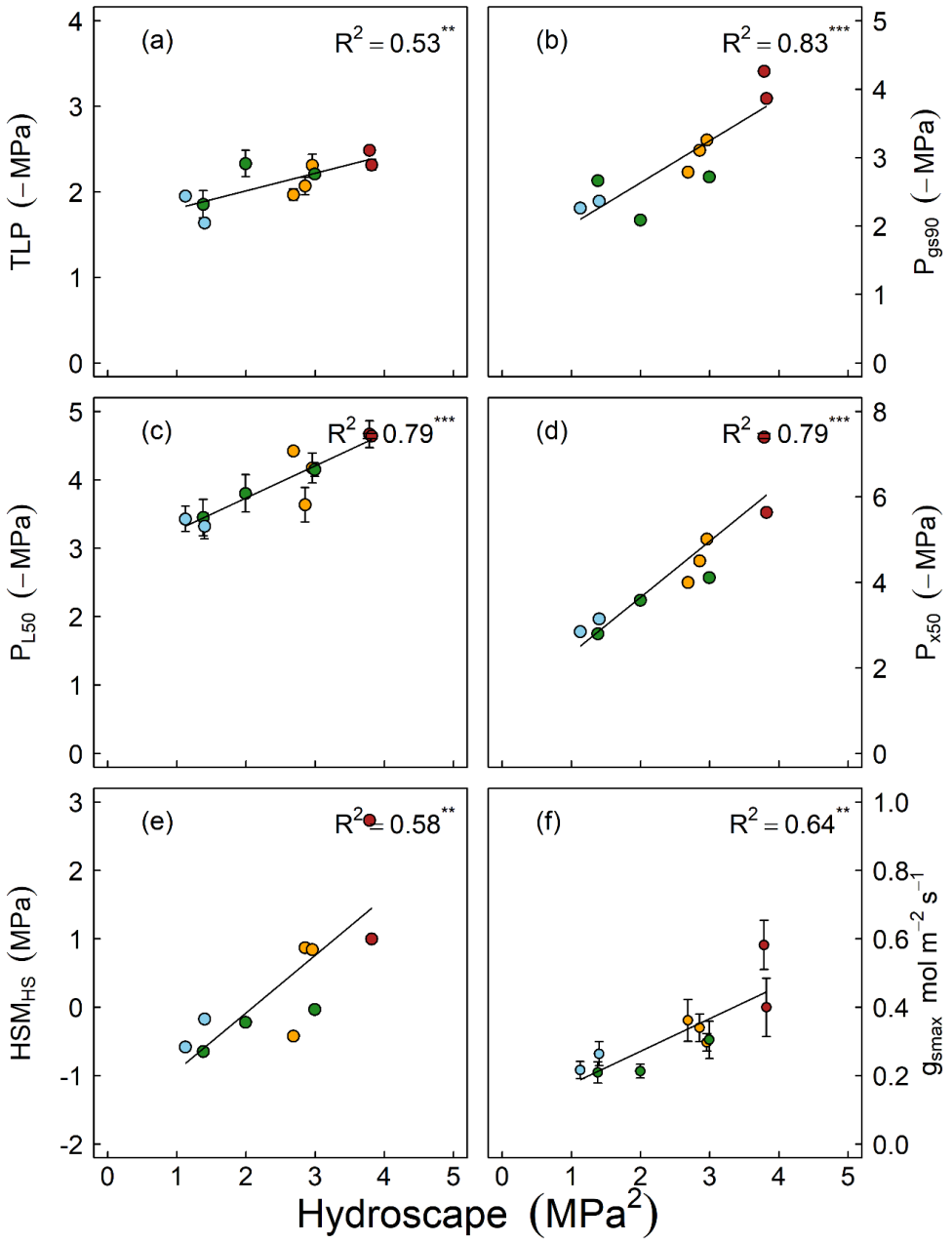

Figure 3-5 Relationships between Hydroscape and key hydraulic traits. Traits for linear regression include leaf turgor loss point (TLP, panel a), water potential inducing 90% loss of maximum stomatal conductance (P_{gs90}, panel b), 50% loss of conductivity in leaf (P_{L50}, panel c, in stem (P_{x50}, panel d), safety margin of hydraulic segmentation defined as P_{x50}-P_{L50} (HSM_{HS}, panel e) and maximum stomatal conductance (g_{smax}, panel f). Error bars indicate standard error. Adjusted R^2 of linear regressions are shown. Asterisk indicates significant level (***, $p < 0.001$; **, $p < 0.01$; *, $p < 0.05$).

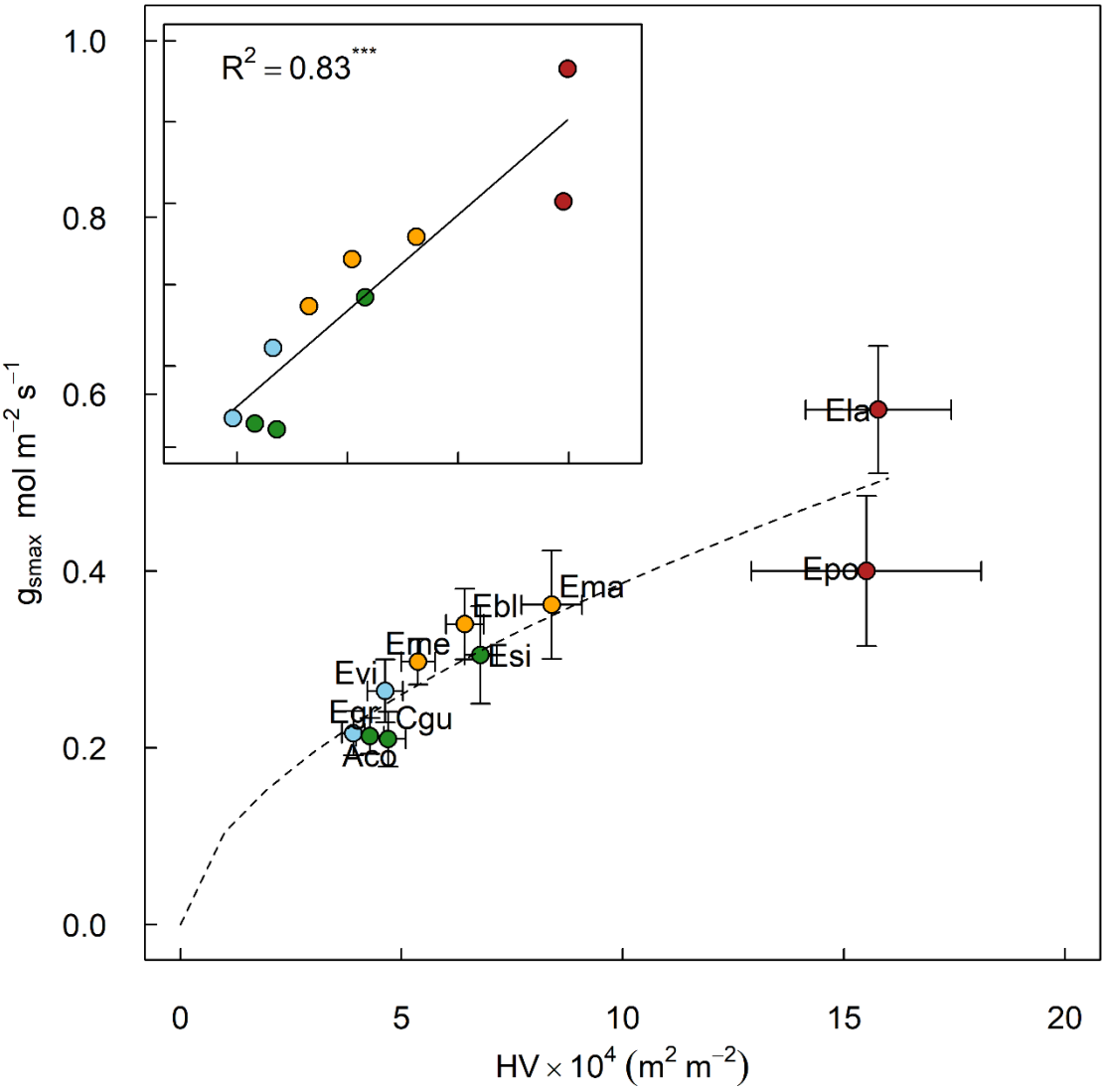

Figure 3-6 The correlations between maximum stomatal conductance (g_{smax}) and Huber value (HV). Inset figure shows the same relationship at log-log scale. Error bars indicate standard error. Adjusted R^2 of linear regressions are shown. Asterisk indicates significant level (***, $p < 0.001$; **, $p < 0.01$; *, $p < 0.05$).

3.3.4 Which metric is most strongly related to climate variables?

Among the four metrics, the Hydroscape was most strongly correlated with species home-site climatic variables including MAP (Figure 3-7b; R^2=0.76, p<0.001) and AI (Figure 3-7c; R^2=0.86, p<0.001). The slope of the Ψ_{pd} vs. Ψ_{md} relationship was positively correlated with MAT (Figure 3-7d; R^2=0.55, p<0.01). $\Delta\Psi_{max}$ was negatively linked to MAP (Figure 3-7h; R^2=0.46, p<0.05) but not AI. No significant correlation between HSM_{ST} and climatic variables was detected.

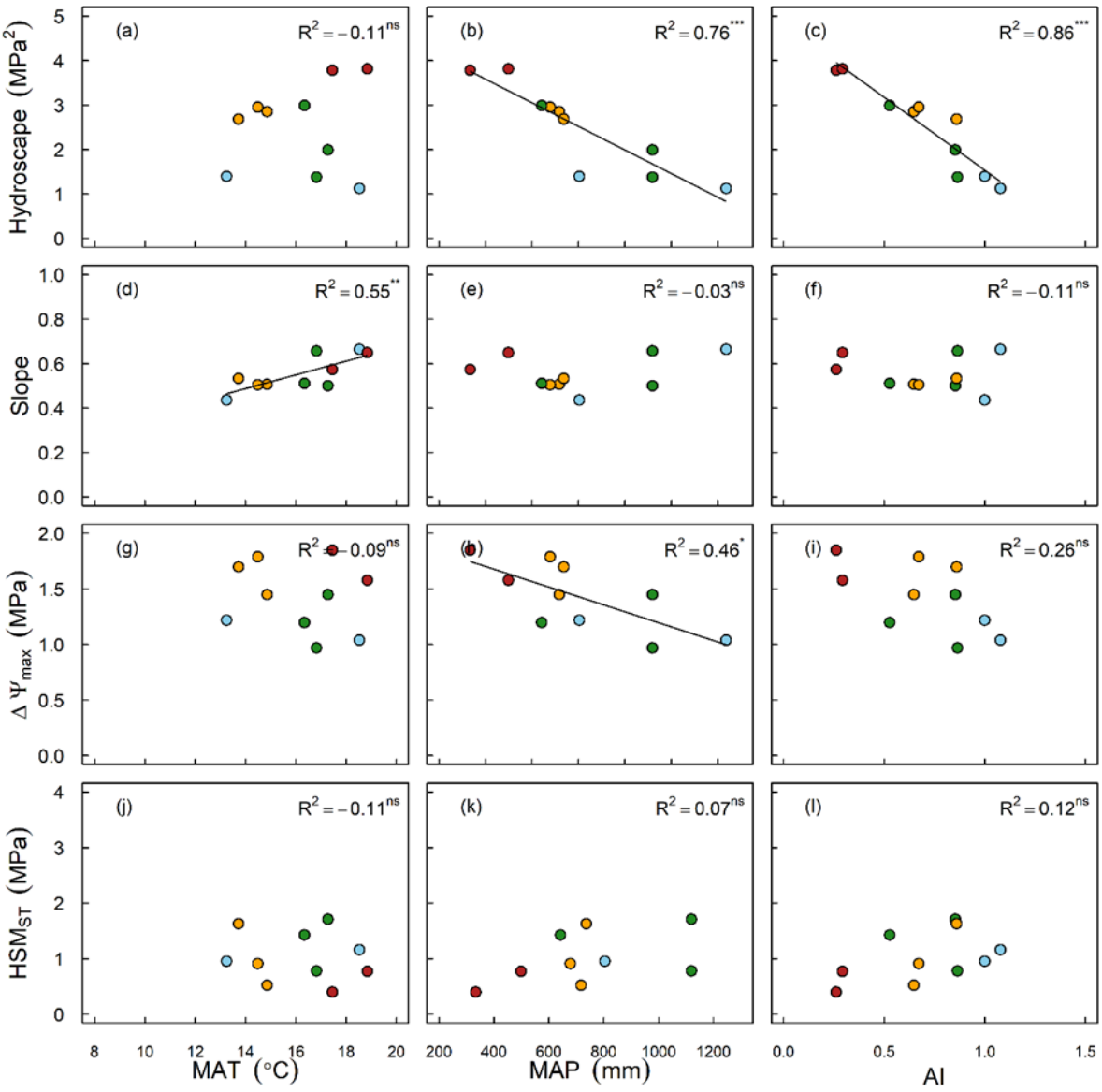

Figure 3-7 Relationships between metrics of isohydricity and home-climate averaged across species distributional range. Climatic variables include mean annual temperature (MAT, ^{o}C), mean annual precipitation (MAP, mm) and aridity index (AI). Colours indicate different vegetation types. Adjusted R^2 of significant linear regressions are shown. Asterisk indicates significant level (***, $p < 0.001$; **, $p < 0.01$; *, $p < 0.05$).

3.4 Discussion

We assessed the consistency of different metrics of plant drought response strategy as well as their links to stomatal and hydraulic traits related to plant water use and drought tolerance across ten woody species from contrasting climates. We found that the species ranking was highly dependent on the metric applied. Among these, the Hydroscape was most strongly correlated with key hydraulic traits characterizing drought tolerance, suggesting that the area defined by $\Delta\Psi_{max}$ and the operating range over which stomata control water potential is constrained by hydraulic safety thresholds. In addition, the linkage between Hydroscape and home-climate indicates that water regulation strategies are under genetic control. Species with stringent stomatal control (i.e. small Hydroscape area) tended to occupy mesic regions, were more vulnerable to embolism, and less likely to protect stem hydraulic integrity *via* hydraulic vulnerability segmentation. Contrary to expectations, they also had leaves with lower stomatal conductance. Hydroscape appears to be a good proxy of species performance and drought tolerance, and is indicative of more than just the degree of isohydry, summarising the species' water use strategy overall.

3.4.1 Comparison of metrics

Cross-species studies consistently show species ranking along the drought response spectrum differ markedly according to the metric in use, which represents the chief uncertainty

surrounding the assessment of species stomatal regulation strategy in response to drought (Martínez-Vilalta et al. 2017, Hochberg et al. 2018). Disagreement in species rankings may be due to differences in the environmental conditions under which the metric is measured (2018). Indeed, leaf water status at any given time is a function of stomatal regulation and site-specific growth conditions (Rogiers et al. 2011), suggesting that caution should be taken when assessing stomatal regulation based on single time point measurements. However, we found that inconsistency in species rankings still exists even when measured under relatively uniform growth conditions, indicating that the discrepancy was not solely caused by environment and may be a result of the uncertain in the metrics. Furthermore, all metrics showed some level of coordination with stomatal and hydraulic traits related to drought tolerance with the exception of the slope of the Ψ_{md} vs. Ψ_{pd} relationship.

The slope was relatively invariant across species, suggesting that this metric might not be able to differentiate species stomatal regulation strategy, at least for the set of species studied here. Indeed, species with similar slope may operate over distinct envelopes of water potential during dehydration, leading to false positive errors when assessing species isohydricity (Meinzer et al. 2016; Fu and Meinzer 2018). This result differs from previous cross-species analyses which showed that the slope was highly variable among species (Martínez-Vilalta et al. 2014, Meinzer et al. 2016), but is consistent with Martinez-Vilalta and Garcia-Forner (2017), who found that no clear pattern between this metric and stomatal sensitivity across 44 species.

According to Klein (2014), species with higher or lower $\Delta\Psi_{max}$ can be classified as more or less isohydric, and therefore the variation of $\Delta\Psi_{max}$ across species observed here indicates that species differ in the degree of isohydry. However, it is worth noting that in our experiment,

$\Delta\Psi_{max}$ occurs when soil water content is relatively high. Under such conditions, $VPD \times g_{smax} = HV \times K_{max} \times \Delta\Psi_{max}$, so $\Delta\Psi_{max} = VPD \times g_{smax}/(HV \times K_{max})$ (Zirnmermann 1983). Therefore, rather than defining the stomatal regulation strategy during drought, $\Delta\Psi_{max}$ instead reflects plant water use and transport under well-watered conditions, as shown here by the positive correlation between $\Delta\Psi_{max}$ and g_{smax} (Table A-3).

On the other hand, Skelton et al. (2015) defined species with positive and negative stomatal-hydraulic safety margins to be anisohydric and isohydric, respectively. In each of our ten species, stomata closed at water potentials prior to (or close to) the inception of xylem embolism in both leaves and stems, indicating that stomatal closure acts to protect the integrity of the xylem water transport throughout the plant (Li et al. 2018a). Consequently, all ten species would be classified as being isohydric according to this definition. Although anisohydric behaviour with negative HSM_{ST} has been reported in some species (Skelton et al. 2015, Pivovaroff et al. 2018), there is mounting evidence that stomatal closure occurs prior to the occurrence of embolism in many species (Martin-StPaul et al. 2017, Sperry et al. 2017, Choat et al. 2018a). Considering that embolism recovery in woody plants may be limited (Choat et al. 2018b, Creek et al. 2018, Li et al. 2018b), the occurrence of 'extreme' anisohydry, where stomata remain open beyond the point where significant cavitation occurs, may be rare. Furthermore, because this metric correlated poorly with hydraulic plant traits and home-climate, it does not inform on stomatal response to soil water limitation. We conclude that the Hydroscape best quantifies the species drought response strategy, given it clearly separated species along the home-climate continuum and was tightly correlated with various hydraulic traits, therefore encapsulating plant water regulation strategy under both well-watered and drought conditions (see below).

3.4.2 Hydroscape integrates drought tolerance traits

The strong correlation between Hydroscape and hydraulic traits related to drought tolerance suggests that the Hydroscape itself results from the integration of a wide range of water regulation and drought tolerance traits . Indeed, the landscape within which stomata are functional to prevent the decrease of water potential is partially determined by the point at which Ψ_{pd} and Ψ_{md} converges, which represents the theoretical stomatal closure point (i.e. P_{gs90}). This interpretation is in agreement with strong relationships reported between the Hydroscape area and the water potential at turgor loss (Meinzer et al. 2016) given TLP and P_{gs90} are often tightly coupled. In the current study, we also observed a significant correlation between Hydroscape area and TLP, highlighting the functional links between TLP, stomatal conductance, stomatal closure and embolism resistance, as well as its usefulness as a potential proxy for species stomatal regulation strategy (Bartlett et al. 2016). We found that the Hydroscape was positively related to both P_{x50} and P_{L50}, indicating that xylem of species with more stringent stomatal control was more vulnerable to drought-induced embolism. In support of our finding, Skelton et al. (2015) reported that species with stringent stomatal control tended to have less negative P_{x50}. Such correlation underpins the functional convergence between stomatal regulation and embolism resistance. Species with larger Hydroscapes maintain open stomata during drought, and thus experience more negative xylem pressure. To minimize the risk of hydraulic dysfunction at these more negative water potentials, it is necessary to build more embolism resistant xylem.

Our results suggest that species with smaller Hydroscapes are less likely to protect the integrity of stem xylem during drought via hydraulic segmentation in leaves and stems, reported here as HSM_{HS}. The relationship between hydraulic segmentation and the degree of isohydricity has been rarely examined. In the study of Pivovaroff et al. (2014), no clear pattern between daily range of leaf water potential and HSM_{HS} was observed, but Zhang et al.

(2017) reported positive safety margins in more isohydric species. In the current study, hydraulic vulnerability was less variable in leaves than stems, which may be due to the notion that leaf hydraulic traits, including embolism resistance, may be responsive to growth conditions (Blackman et al. 2014, Johnson et al. 2018a). Nevertheless, our results suggest that vulnerability segmentation may be prevalent in species from arid environments where strategic leaf shedding is important in delaying the onset of catastrophic hydraulic failure during extreme drought events.

3.4.3 Trade-off between stomatal conductance and sensitivity

The positive correlation between g_{smax} and Hydroscape suggests that species which have lower stomatal sensitivity to leaf water potential also have higher leaf conductance under well-watered conditions. This finding contrasts with an earlier study suggesting that species with high stomatal sensitivity to vapor pressure deficit generally display higher g_{smax} (Oren et al. 1999), but is consistent with Meinzer et al. (2017), who showed that more anioshydric species generally exhibit higher g_{smax} and carbon assimilation rate under well-watered conditions. It also appears to contrast with an overarching paradigm that species with low hydraulic safety have high maximum rates of photosynthesis, in accordance with the fast-slow leaf economic spectrum (Reich 2014). However, we acknowledge that this positive relationship between drought tolerance and leaf level conductance is likely mediated by variation in hydraulic architecture (Meinzer et al. 2010) and the relationship between hydraulic supply (stem xylem area) and demand (leaf transpiration area) - that is, the Huber-value, which was shown to be strongly correlated with g_{smax} across species in line with increasing site aridity. Thus, at the whole-plant scale, we might expect total canopy conductance to be inversely related to Hydoscape, although higher canopy conductance was observed in a more anisohydric *Populus* genotype when soil water content was not limiting

(Attia et al. 2015). Nevertheless, in the current study, species with larger Hydroscape areas tended to occupy more xeric habitats where rainfall is extremely stochastic, which is in line with the finding of a recent global meta-analysis (Fu and Meinzer 2018). The positive correlation between Hydroscape area and leaf-level stomatal conductance, suggests that drought tolerant species from more arid environments require traits that both maximize photosynthesis when soil water is available, while also being able to sustain longer periods of carbon gain during drought via embolism resistant xylem.

3.4.4 Climate drives the diversification of plant water use

We found that species Hydroscape area was the metric most strongly correlated with species climate-of-origin, providing evidence that climate is a major determinant shaping adaptive plant hydraulic strategy across species (Fu and Meinzer et al. 2018). It has been shown in many studies that isohydric and anisohydric species can co-exist (Quero et al. 2011, Pivovaroff et al. 2014, Konings and Gentine 2017) because species-specific features, such as rooting depth or leafing phenology, may enable species to occupy different hydraulic niches within the same site (Jacobsen et al. 2008). However, the positive correlation between Hydroscape, embolism resistance and aridity observed in our common garden study is in agreement with *in situ* studies showing that aridity strongly determines species hydraulic traits within *Eucalyptus* (Pfautsch et al. 2016), suggesting the adaption to aridity comprises various traits.

3.5 Conclusion

Recent forest dieback worldwide has renewed research focusing on plant iso/anisohydry, but the confounding definitions and limitations of characterizing plant water use based solely on stomatal regulation suggest a more sophisticated and comprehensive definition is required for this classification. Hydroscape appears to be a good metric for characterising plant water use

strategy because it integrates plant drought tolerance and performance under well-watered conditions, thus providing more information than the isohydricity of stomatal regulation. Compared to small-Hydroscape species, large-Hydroscape species are less vulnerable to water deficit given their high embolism resistance and slightly higher safety margin for hydraulic segmentation. Nevertheless, given that large-Hydroscape species tend to occur in more arid sites, the lower sensitivity to water deficit (i.e. greater safety margins) is compensated for by the higher exposure to severe drought. As a consequence, the risk of mortality in different species due to climate change drought may be spread relatively evenly across environments (Choat et al. 2012).

Chapter 4

Drought tolerance traits do not vary across sites differing in water availability in *Banksia serrata* (Proteaceae)

4.1 Introduction

Drought is among the most common abiotic stresses worldwide, and will likely be exacerbated by rapid global climate change (Dai 2013, Choat et al. 2018a). Variation in the structure and function of the plant water transport pathway (xylem) is a key determinant of survival, reproduction and productivity of terrestrial plants, and thus strongly influences species distribution (Pockman et al. 2000, Maherali et al. 2004, Choat et al. 2012a). It has been well established that the hydraulic architecture of plants is strongly influenced by water availability, as evidenced by the systematic change of key hydraulic characteristics along rainfall gradients at regional scales (Brodribb et al. 1999, Trueba et al. 2017). The vast majority of studies documenting inter-specific variation of plant hydraulic traits typically find that arid-zone species have traits that confer greater drought tolerance than plants from mesic environments (Choat et al. 2012b, Gleason et al. 2013, Pfautsch et al. 2016, Trueba et al. 2017, Li et al. 2018a). On the other hand, the level of intra-specific variation (that is, variation within species) of hydraulic traits along gradients of moisture availability is inconsistent among different species and studies (Choat et al. 2007, López et al. 2016, Larter et al. 2017). Evidence of intraspecific variation in hydraulic traits potentially has important implications for the survival of plants under global climate change because it suggests there may be adaptive capacity within the species, either linked to genetic differentiation among

populations and/or phenotypic plasticity, that may provide greater resilience under future drying climates.

Drought tolerance is a highly integrative feature, incorporating multiple hydraulic traits of different organs along the water transport pathway. Given the difficulty in completely mapping the hydraulics of plants, several key traits have been identified. The capacity to withstand xylem embolism, among others, has emerged as an important characteristic in contributing drought resistance because drought-induced hydraulic impairment primarily occurs via embolism resulting from the blockage of conduits by air bubbles, which compromises water transport and carbon assimilation (Charrier et al. 2016, Martin‐StPaul et al. 2017). Embolism resistance is often assessed as the water potential corresponding to 50% or 88% loss of xylem hydraulic conductivity (P_{50} and P_{88}, respectively) and these parameters have been quantitatively linked to drought mortality thresholds (Brodribb et al. 2009, Urli et al. 2013).

Similarly, the leaf resistance to embolism can be quantified. Leaves that are more vulnerable to embolism than stems may allow plants to constrain stem water potential within the safe zone through reductions in leaf area via leaf loss or shedding (Zhu et al. 2016), known as hydraulic vulnerability segmentation (Zimmermann 1983). The hydraulic segmentation safety margin is defined as the difference between leaf P_{50} and stem P_{50} (Pivovaroff et al. 2014, Zhu et al. 2016). Leaf turgor loss point (TLP) has also long been recognized as an indicator of drought tolerance because it determines the minimal water potential for net carbon assimilation given that stomatal closure is primarily regulated by leaf turgor (Bartlett et al. 2012, Blackman 2018). The variation of these traits among species is commonly shown

to strongly correlate with water availability, while the intraspecific variation of these traits along environmental gradients is less well characterised.

It has been proposed that selective pressures tend to drive the efficiency of water transport and vulnerability to embolism of vessels in opposite directions, such that species with higher embolism resistance also have lower maximum hydraulic conductivities (Santiago et al. 2018). Given the tight linkage between water transport and photosynthesis, this efficiency-safety trade-off connects the plant carbon economy and water relations, and potentially explains why some species may out-compete other species under different environmental conditions. In support of this hypothesis, a negative correlation between xylem P_{50} and maximum conductivity per sapwood cross-section area (K_s) has been observed in many studies (Markesteijn et al. 2011, Santiago et al. 2018). However, the distinct structural basis of water transport and embolism resistance, taken together with compensatory hydraulic strategies, may lead to a weak correlation at the global scale (Gleason et al. 2016). Whether this trade-off exists within species remains largely unknown.

Apart from physiological characteristics, plant morphology plays an important role in regulating plant drought tolerance. A correlation between sapwood density (WD) and cavitation resistance in stems has been reported, although the mechanistic basis for this correlation is confounded because sapwood density integrates multiple wood properties (Markesteijn et al. 2011). Furthermore, WD is closely associated with hydraulic capacitance, which may act to buffer the fluctuation of water potential on a daily basis, and subsequently contributes to prolonged time to reach water potentials that trigger critical xylem embolism levels after stomatal closure (Gleason et al. 2014). In addition, greater drought tolerance can be achieved by increasing the ratio of sapwood cross-section area (i.e. water supply) to the

distal leaf area (i.e. water demand) (HV; Huber value), which reduces the water potential gradient required between leaf and stem for a given transpiration rate (Liu et al. 2018). The response of HV to water availability has been observed across species grown along aridity gradients, and within species subjected to different levels of water deficit (Schultz and Matthews 1993, Mencuccini and Grace 1995, Maherali and DeLucia 2000).

Species that occur across rainfall gradients provide the opportunity to explore adaptive variation of hydraulic traits, at the same time as assessing the possible susceptibility of populations to climate change. *Banksia serrata*, commonly known as old man banksia, is a tall woody shrub or small tree native to the central east coast region of Australia. Belonging to the Proteaceae, it is evergreen and sclerophyllous. It typically occurs on well-drained sandy soils that are low in nutrients, and is accompanied by other native tree species such as *Eucalyptus piperita* and *Corymbia gummifera*. Given its adaptation to bushfire with the ability to re-sprout from epicormic buds under the bark of the main trunk, the fire ecology of this species has been well documented (Bradstock and Myerscough 1988, Freestone et al. 2015) . Much less is known, however, about its hydraulic traits. Here, we measured a range of key hydraulic and morphological traits related to plant water use and drought tolerance in three populations of *B. serrata* from sites varying in mean annual precipitation and temperature within the Greater Sydney Region. We hypothesised that plants from the warmer and drier site would exhibit traits that confer greater drought tolerance than plants from cooler wetter sites. Assuming that a trade-off exists between hydraulic safety and efficiency, we also expected plants from the cooler wetter site to exhibit higher hydraulic conductivity.

4.2 Material and methods

4.2.1 Site description and plant material

Field sampling was conducted from December 2017 to March 2018 at three sites. The Patonga site (Warm-Wet) is located at the south end of the Central Coast region of New South Wales (33.53 ºS, 151.28 ºE, 104 m a.s.l.). The Agnes Banks site (Warm-Dry) is located at the centre of the Western Sydney region (33.64 ºS, 150.69 ºE, 22 m a.s.l.). The Mount Banks site (Cool-Wet) is located in the Blue Mountains region west of Sydney (33.58 ºS, 150.36 ºE, 1049 m a.s.l.). The three sites differ considerably in local climate, primarily in mean annual precipitation and mean maximum temperature (Figure 4-1; www.bom.gov.au). The soil profiles are similar among sites with deep sandy soils (http://espade.environment.nsw.gov.au/).

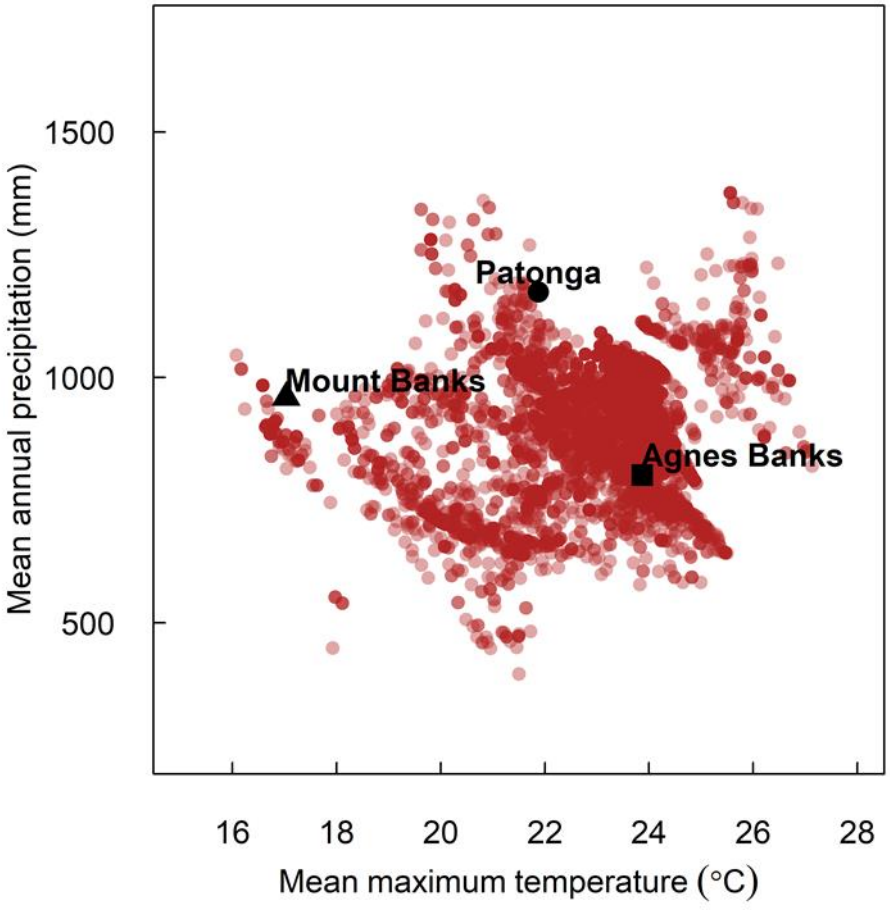

Figure 4-1 Mean annual precipitation (mm) and mean maximum temperature (ºC) within the natural distributional range (red) and the sampling sites (black) for *B. serrata*. Climatic data

are sourced from Atlas of Living Australia (www.ala.org.au) and Bureau of Meteorology of Australia government (www.bom.gov.au; Station number: 63292 [Mount Banks]; 67021 [Agnes Banks]; 61425 [Patonga]).

Within each site, 6-10 healthy individuals of approx. 5 m height were randomly selected and one secondary branch per tree, approximately 1.5 m long and 2 cm in diameter, was removed from the north-facing, fully sunlit section of the upper canopy (ca. 4 m height) using a pole saw. The length of the sampled branches was adequate to avoid potential artefacts arising from open vessels, as confirmed by the maximum vessel length measured using the air injection method (*ca.* 7.5 cm). Branches were immediately sealed in opaque plastic bags, humidified by moist paper towels, and transported back to the laboratory of the Hawkesbury Institute for the Environment, Western Sydney University, Richmond, NSW, within 2 hrs. Branches were transferred into 75 litre bins filled with clean water and an approximately 20 cm segment was recut underwater from the base of the branch. Samples were allowed to rehydrate in darkness overnight. Leaf water potential (Ψ_{leaf}) was measured using a Scholander-type pressure chamber (PMS Instruments, Corvallis, OR, USA) on the next day. Samples were considered adequately rehydrated when $\Psi_{leaf} \geq -0.5$ MPa, and subsequently used for hydraulic measurements.

4.2.2 Stem vulnerability curves

Stem vulnerability curves (VC_S) were generated using the bench dehydration method (Sperry et al. 1988, Choat et al. 2010). Branch samples were allowed to slowly desiccate under lab conditions and stem water potential (Ψ_{stem}) was measured periodically using Ψ_{leaf} as a surrogate. Once the desired water potential was achieved, the branch was placed into an opaque plastic bag for up to 1 h to maximize hydraulic equilibrium between leaves and stems.

Ψ_{leaf} was remeasured on at least two leaves of the equilibrated sample and the average value was taken as the Ψ_{stem}. The targeted branchlet was cut off under water and left for 20 min to relax tension (Torres-Ruiz et al. 2015). Then, the branchlet was trimmed alternately from the upstream and downstream ends at 2-min intervals until a desired length was acquired. The segment was connected to a pressure head (0.002 MPa) and the initial flow rate ($K_{initial}$) was measured with a digital liquid flow meter (Liqui-FlowL10, Bronkhorst High-Tech BV, Ruurlo, Gelderland, The Netherlands) using flow analysis programs. Thereafter, the stem segment was flushed under high pressure (200 kPa) using 2 mmol KCL solution for at least 25 min to remove any possible embolism and the final flow rate (K_{final}) was measured. Thereafter, bark was carefully removed. Outer and pith diameters of the sample were measured using digital callipers and sapwood area was calculated as the difference between cross-sectional area and pith area. K_{final} was normalized by the pressure gradient, sapwood area, and stem length to obtain initial and final xylem-specific hydraulic conductivity (K_s, kg m^{-1} s^{-1} MPa^{-1}). Percentage loss of conductivity (PLC, %) was calculated as (1-$K_{initial}/K_{final}$)×100. VC_s was established by plotting PLC against the corresponding Ψ_{stem}. Following VC_s measurements, leaves above the targeted segment were collected and oven-dried. Dried leaves were weighed, and distal leaf area was estimated using dry mass and SLA. Huber value was calculated as the ratio of sapwood area to corresponding distal leaf area. Leaf specific conductivity (K_L, kg m^{-1} s^{-1} MPa^{-1}) was calculated as the product of K_s and HV.

4.2.3 Leaf vulnerability curve

Leaf vulnerability curves (VC_L) were assessed using the rehydration kinetics method following Brodribb and Holbrook (2003b). Briefly, branch samples were allowed to slowly dehydrate under lab conditions for up to 72 hrs. At different stages during desiccation, sample

leaves were excised under water and allowed to rehydrate for different amounts of time depending on the water status. A neighbouring leaf was used to estimate the water potential of the target leaf at the time of excision. The rehydrated leaf was quickly blotted dry and Ψ_{leaf} was measured after equilibrating in bags for several minutes to obtain the Ψ_{leaf} after rehydration. Leaf conductivity (K_{leaf}, mmol m^{-2} s^{-1} MPa^{-1}) was calculated as:

$$K_{leaf} = C \ln\left[\frac{\Psi_0}{\Psi_f}\right] t^{-1}$$

where C (mmol m^{-2} MPa^{-1}) is leaf capacitance; Ψ_0 and Ψ_f (-MPa) are leaf water potential before and after rehydration, respectively; and t (s) is duration of rehydration. The value of K_{leaf} was then plotted against corresponding Ψ_{leaf} to construct VC_L.

4.2.4 Pressure-volume traits

For each site, one leaf per branch was collected from five fully rehydrated samples for leaf pressure-volume (PV) analysis. Leaf PV curves were generated following Tyree & Hammel (1972). In short, leaves were slowly dehydrated under lab conditions, Ψ_{leaf} and leaf fresh mass (FW) were measured periodically with pressure chamber and a digital balance (weighed to 0.1 mg), respectively. PV curves were analysed following Lenz et al. (2006). To facilitate calculation, the inverse of leaf water potential ($1/\Psi_{leaf}$) was plotted against leaf relative water content (RWC_{leaf}, %). Leaf turgor loss point (TLP, -MPa) was taken as the inverse of the inflection point. Modulus of elasticity (ε, MPa) was estimated as the slope of leaf pressure potential (Ψ_p) vs. 100-total relative water content relationship using water potential data that were higher (i.e. less negative) than TLP. Similarly, leaf specific capacitance (C^*_{FT}, mmol m^{-1} MPa^{-1}) was calculated as the slope of pre-turgor loss relative water content vs. leaf water potential relationship multiplied by the saturated mass of water in the leaf and divided by leaf area.

4.2.5 Morphological traits

For each site, 8 to 10 leaves were collected per branch from five sample branches. Leaf area was measured using a leaf area meter (LI-3100A, Li-Cor Inc., USA). In addition, an approximately 5 cm long segment was excised from the base of the tertiary branch. Bark was carefully removed, and the volume of sapwood was estimated using the water displacement method (Markesteijn et al. 2011). All samples were oven-dried at 70 ^{o}C until constant mass, and then weighed for dry mass. Specific leaf area (SLA, m^2 kg^{-1}) and sapwood density (g cm^3) were calculated as the ratio of leaf area to leaf dry mass and stem volume to sapwood dry mass, respectively.

4.2.6 Statistical analysis

Leaf and stem vulnerability curves were fitted with a sigmoidal function using '*fitplc*' package in R to obtain water potentials thresholds inducing 50% and 88% loss of conductivity in leaf and stem (i.e. P_{50} and P_{88}) (Duursma et al. 2017b). Maximum K_{leaf} was considered as the highest K_{leaf} value across leaf samples within each site. Differences in these traits among sites were compared using bootstrap confidence intervals. Statistical differences of other hydraulic traits among sites were tested by one-way ANOVA, and if significant, subsequently assessed using Turkey HSD *post hoc* using '*ez*' package. Statistical significance was reported at $p \leq 0.05$ level.

4.3 Results

Water potentials inducing 50% and 88% loss of leaf hydraulic conductivity (P_{L50} and P_{L88}, respectively) did not significantly differ across sites, given their overlapping 95% confidence intervals (Table 4-1; Figure 4-2). Similarly, no difference was found for stem water potential at 50% and 88% loss of conductivity (P_{x50} and P_{x88}, respectively) across sites (Table 4-1).

The safety margin (MPa) between P_{L50} and P_{x50} was positive for all sites, indicating leaves were generally more sensitive to drought-induced hydraulic dysfunction than stems, although the difference was small (Table 4-1).

Table 4-1 Water potential triggering 50% and 88% loss of xylem conductivity in leaves (P_{L50} and P_{L88}) and stems (P_{x50} and P_{x88}), and hydraulic safety margin of hydraulic segmentation (HSM) defined by P_{L50}-P_{x50} of *B. serrata* in three sites (Patonga [Warm-Wet], Mount Banks [Cool-Wet], Agnes Banks [Warm-Dry]). Numbers in brackets are the lower and upper 95% confidence interval.

Site	P_{L50} (-MPa)	P_{L88} (-MPa)	P_{x50} (-MPa)	P_{x88} (-MPa)	HSM_{HS} (MPa)
Patonga	2.78	4.13	3.57	3.97	0.79
	[2.61,2.92]	[3.84,4.55]	[3.07,3.67]	[3.76,4.17]	
Mount Banks	2.92	4.85	3.57	4.49	0.65
	[2.67,3.28]	[4.36,]	[3.27,3.74]	[4.14,4.7]	
Agnes Banks	2.81[	4.16	3.4	4.58	0.59
	2.39,3.19]	[3.62,5.3]	[3.08,3.96]	[4.07,]	

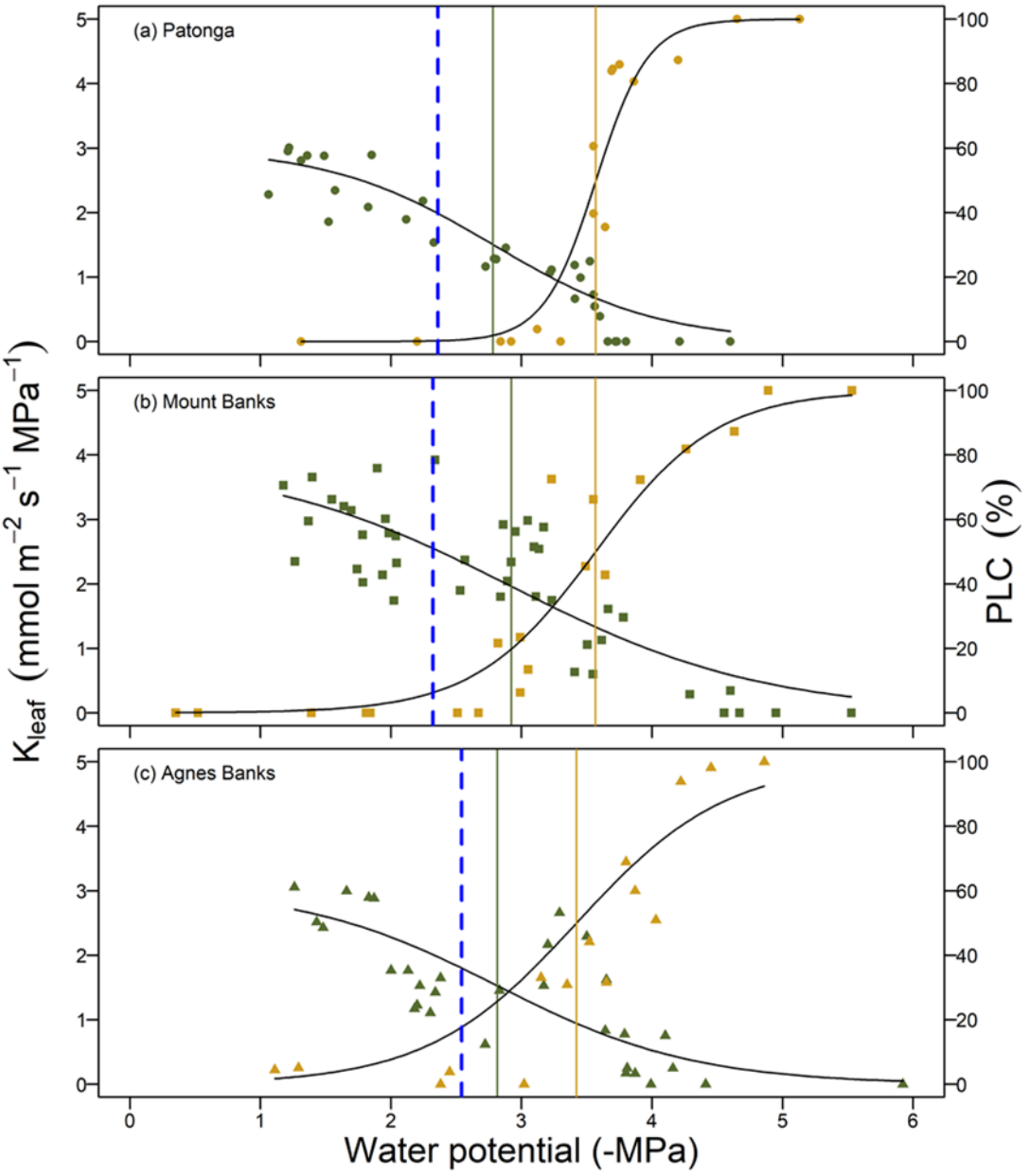

Figure 4-2 Response of leaf hydraulic conductivity (K_{leaf}, green) and percentage loss of conductivity in stem (PLC, yellow) to water potential of B. serrata in three different sites (panel a: Patonga [Warm-Wet]; panel b: Mount Banks [Cool-Wet]; panel c: Agnes Banks [Warm-Dry]). Green and yellow solid lines indicate water potential inducing 50% decline or increase for Kleaf and PLC, respectively. Blue dashed lines indicate the turgor loss point (TLP).

Leaf turgor loss point (TLP) did not vary significantly across sites ($F=3.57$, $p=0.06$; Figure 4-2). Notably, for all sites, complete turgor loss occurred at leaf water potentials corresponding to *ca.* 30% loss of leaf hydraulic conductivity, and always preceded the onset of embolism in the stem (Figures 4-2 and 4-3a). Leaf capacitance (C^*_{FT}) was significantly higher for plants from Patonga (Warm-Wet) and Mount Banks (Cool-Wet) compared to Agnes Banks (Warm-Dry) ($F=9.41$, $p<0.01$; Figure 4-3b). On the other hand, leaf modulus of elasticity of Agnes Banks (Warm-Dry) was significantly higher than at the other two sites ($F=19.14$, $p<0.01$; Figure 4-3c).

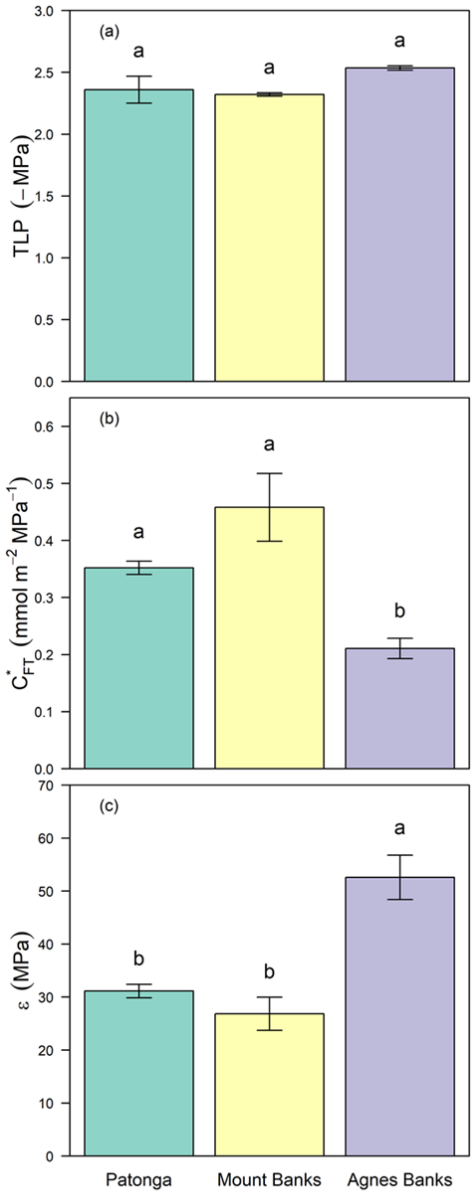

Figure 4-3 Variation of leaf turgor point (TLP, panel a), leaf hydraulic capacitance (C^*_{FT}, panel b) and modulus of elasticity (ε, panel c) of B. serrata across sites (Patonga [Warm-Wet], Mount Banks [Cool-Wet], Agnes Banks [Warm-Dry]). Error bars represent stand error of mean (n=5). Letters above each bar indicate statistical significance at $p \leqslant 0.05$ level.

Plants from the Warm-Dry and Warm-Wet sites showed higher sapwood cross-section area based maximum stem conductivity (K_s) than the Cool-Wet site ($F=7.11$, $p<0.05$; Figure 4a). When normalized by the total distal leaf area (K_L), plants in all sites were similar ($F=0.69$, $p=0.53$; Figure 4b).

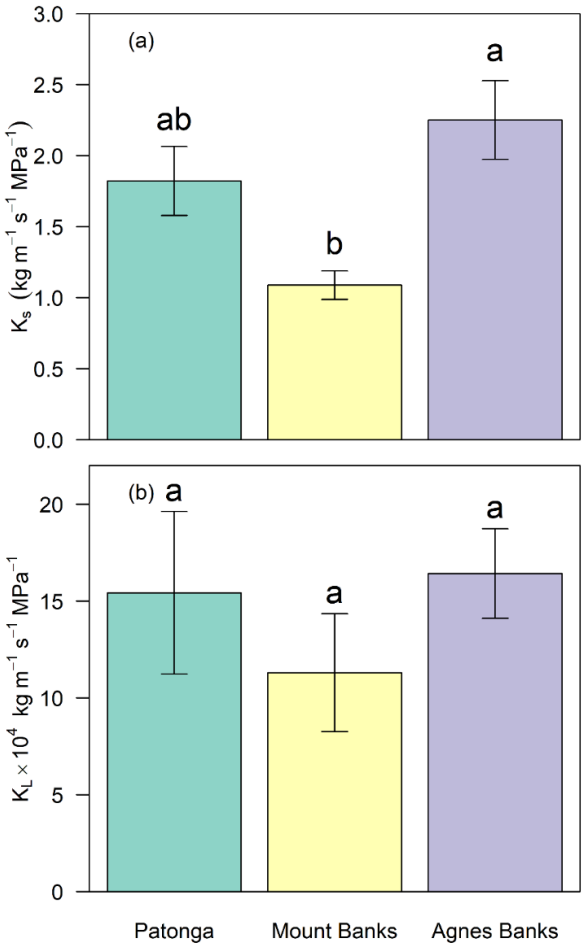

Figure 4-4 Variation of stem specific conductivity (K_s, panel a) and leaf specific conductivity (K_L, panel b) of *B. serrata* across sites (Patonga [Warm-Wet], Mount Banks [Cool-Wet], Agnes Banks [Warm-Dry]). Error bars represent stand error of mean (n=4). Letters above each bar indicate statistical significance at $p \leq 0.05$ level.

Branch Huber values (HV) were similar between sites ($F=0.80$, $p=0.49$; Figure 4-5a). Specific leaf area (SLA) was significantly lower at the Cool-Wet site ($F=13.78$, $p<0.01$) than the other two sites (Figure 4-5b) and sapwood density (WD) was significantly lower in the Warm-Dry site ($F=6.76$, $p<0.05$) than the other two sites (Figure 4-5c).

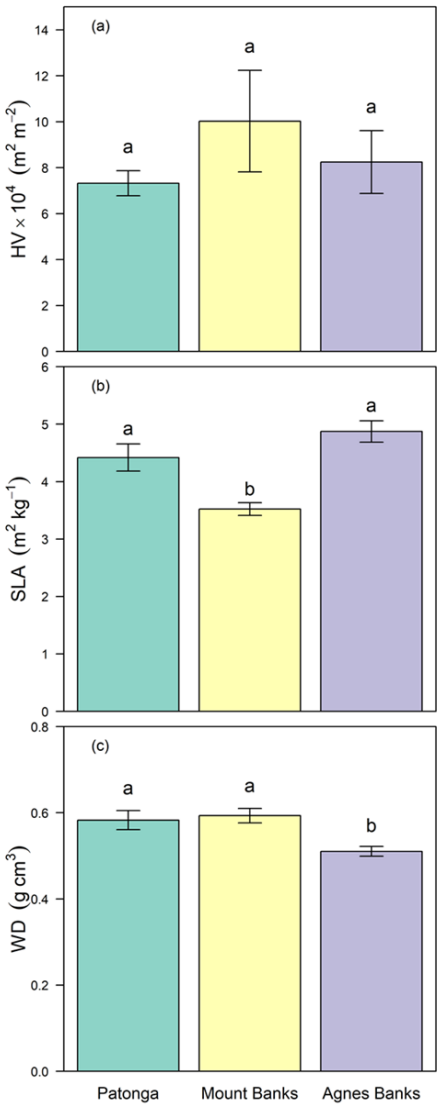

Figure 4-5 Variation of branch Huber value (HV, panel a), specific leaf area (SLA, panel b) and sapwood density (WD, panel c) of *B. serrata* across three sampling sites (Patonga [Warm-Wet], Mount Banks [Cool-Wet], Agnes Banks [Warm-Dry]). Error bars denote stand error of mean (n=5). Letters above each bar indicate statistical significance at $p \leq 0.05$ level.

4.4 Discussion

4.4.1 Intraspecific variation in hydraulic traits

In contrast to our hypothesis, xylem vulnerability to drought-induced embolism (i.e. P_{x50} and P_{x88}) did not differ among the three populations despite differences in site rainfall and temperature. A number of studies have examined within species variability of xylem vulnerability, but the results to date are variable. For example, Lamy *et al.* (2014) reported a lack of intraspecific variation in P_{x50} across *Pinus pinaster* (Pinaceae) populations, suggesting that vulnerability to embolism in this species is highly canalized. Low variability in P_{x50} has also been observed among populations of widespread angiosperms *Quercus petraea* (Fagaceae) (Lobo et al. 2018), and *Betula pendula* (Betulaceae) and the conifers *Picea abies* and *Pinus sylvestris* (Pinaceae) (Martínez-Vilalta et al. 2009, González-Muñoz et al. 2018). However, shifts towards lower stem hydraulic vulnerability in populations from drier sites have been found in two Pinaceae species (*Pseudotsuga menziesii* (Kavanagh et al. 1999) and *Pinus ponderosa* (Maherali et al. 2000)), as well as the tropical tree species *Cordia alliodora* (Boraginaceae) (Choat et al. 2007) and the shrub species *Artemisia tridentata* (Asteracea) from semi-arid environments (Kolb and Sperry 1999). In some species, adjustments in vulnerability to embolism only occur at the very dry edge of their distributional range (Wortemann et al. 2011; López *et al.* 2016; Stojnić et al. 2017). In our study, low intraspecific variability in embolism resistance may be attributable to the fact that our sites did not include the driest and wettest edges of our species' distribution. The MAP across the natural distribution of *B. serrata* ranges from *ca*. 400 mm to *ca*. 1400 mm, whereas the MAP across our sample sites ranged from *ca.* 800 mm at the driest site (Agnes Banks) to *ca.* 1200 mm at the wettest site (Patonga). Nevertheless, our results do not indicate a trend of increasing embolism resistance with increasing aridity, suggesting that hydraulic vulnerability in *B. serrata* may be similar between populations even at the extremes of site water availability across its distribution.

Few studies have assessed the variation of leaf hydraulic traits within species. It has been suggested that hydraulic characteristics of leaves are more plastic than those of stems (Meinzer et al. 2014). Indeed, adjustments in leaf TLP has been observed in response to changes in water availability at both temporal and spatial scales (Mitchell and O'Grady 2015, Farrell et al. 2017, Johnson et al. 2018a). Meanwhile, plasticity in leaf hydraulic vulnerability has been observed in response to soil water deficit in species with less conservative stomatal regulation (Johnson et al. 2018a), and in response to warmer growth temperatures (Blackman et al. 2017). In the current study, both leaf vulnerability to drought (i.e. P_{L50} and P_{L88}) and TLP were invariable among sites. However, we observed difference in other leaf traits, including higher leaf ε and lower C^*_{FT} in the Warm-Dry site. It is hypothesized that more rigid leaves (i.e. higher ε) may have less negative TLP (Lenz et al. 2006). However, the variation of ε across our sites implies a decoupling between leaf stiffness and TLP, which would agree with some studies showing that ε plays no direct role in regulating TLP (Bartlett et al. 2012). Nonetheless, higher ε can prevent cell deformation due to leaf shrinkage during desiccation (Scoffoni et al. 2013, Nadal et al. 2018). Furthermore, higher ε permits greater change in the water potential gradient between leaf and soil for a given amount of water loss, which may help plants at the Warm-Dry site to maintain soil water uptake during drought (Niinemets 2001).

4.4.2 Safety-efficiency trade-off

The safety-efficiency trade-off has been documented at the interspecific level, especially within clades (Choat et al. 2007, Markesteijn et al. 2011, Larter et al. 2017, Santiago et al. 2018). Globally, a weak but significant correlation has been identified between these two variables (Gleason et al. 2016). A number of studies examining this trade-off at the intraspecific level have yielded inconclusive results. For instance, K_s and P_{50} were negatively

correlated among populations of *Pinus pinaster* (Corcuera et al. 2011), whereas Choat et al. (2007) reported that K_s of *C. alliodora* varied independently with P_{50} across sites with contrasting MAP; similar results have been found for other species distributed along natural aridity gradients (Kavanagh et al. 1999, Maherali et al. 2000). Our findings are supportive of studies showing no correlation between K_s and P_{50}, indicating the absence of the safety-efficiency trade-off within this species. Interestingly, we found that plants grown in the drier site displayed higher K_s. Higher K_s can reduce the water potential gradient between soil and terminal organs, thus minimizing the risk of reaching tension-induced embolism thresholds during soil drying (Maherali et al. 2000).

4.4.3 Cross-site variation of morphological traits

Plants in dry environments tend to have higher HV (Maherali et al. 2000, Liu et al. 2018). A main benefit of this adjustment is that the tension in xylem can be alleviated during water stress due to the increased ratio of water transport area to transpiration surface area. However, this pattern was not observed in the current study, suggesting that differences in site water availability did not trigger alteration in branch allometry. Indeed, adjustment in HV has limited capacity to alter plant drought tolerance, as evidenced by the lack of correlation between HV and site water availability in some cases (Choat et al. 2007). Variation in HV may be mediated by SLA, as higher SLA permits larger leaf area for a given biomass. Lower SLA in response to lower water availability is frequently observed. However, in our study, the lowest SLA was observed at the Coolest site (Mount Banks), not the driest, suggesting that the difference in SLA could have been driven by lower temperatures inhibiting cell expansion, resulting in denser and thicker leaves (Poorter et al. 2009), and in turn, lower leaf area per unit sapwood area.

A negative correlation between WD and P_x has been frequently observed, suggesting that WD can be used as a good proxy of embolism resistance (Lens et al. 2011, Markesteijn et al. 2011). Contrary to these findings, we found that WD was not related to P_{x50}. Our finding is consistent with some studies showing no correlation between these two traits (Lamy et al. 2012, Schuldt et al. 2016, Santiago et al. 2018). It has been proposed that plants grown under dry environments generally have small vessels with thick cell walls that contribute to higher embolism resistance and WD (Pfautsch et al. 2016). However, vessel dimensions and embolism resistance are not mechanistically linked, and cell wall collapse has rarely been observed in stems. In addition to vessel characteristics, WD integrates other sapwood features that may not affect plant water relations, thus allowing variation in WD without changes in plant hydraulics (Russo et al. 2010).

4.4.4 Ecological implications

Within species variability in stem xylem embolism resistance has also been examined within other *Banksia* species. Canham *et al*. (2009) studied four *Banksia* species from Western Australia occurring along an ecohydrological gradient of varying water table depth. Among the four species, the two facultative phreatophyte species (*B. attenuata* and *B. menziesii*) showed significant variation in P_{x50}, whereas the obligate phreatophyte species (*B. ilicifolia*) did not. These findings suggest that species of *Banksia*, which are not strictly limited to sites with reliable access to ground water, are able to adjust hydraulic traits *via* phenotypic plasticity to suit local conditions. However, this contrasts with the results of the current study, where leaf and stem vulnerability did not vary among populations of *B. serrata* despite site differences in rainfall and perhaps other hydrological attributes related to water table depth (e.g. rooting depth). Furthermore, compared to species from other genera of Proteacea, such as *Hakea* and *Grevillea* that are much more resistant to embolism and that occupy more arid

sites (<400 mm rainfall p.a.), *Banksia* species frequently occupy sites characterised by low nutrients and relatively reliable access to water. Despite having relatively tough leaves associated with nutrient-deficient sites and low SLA, the genus does not contain species with the structural attributes linked to strong embolism resistance (e.g. high xylem wall reinforcement (Jordan et al. 2013, Blackman 2018) that enable plants to survive in water limited environments.

The low levels of intraspecific variability in P_{x50} that we observed may indicate that embolism resistance is relatively fixed within *B. serrata*. This low capacity to adjust key hydraulic traits related to drought tolerance suggests the species may be susceptible to possible future increases in drought severity and frequency. Indeed, recent drought conditions within the Sydney Basin and much of NSW during 2017 and 2018 (BOM; http://www.bom.gov.au/climate/drought/) have coincided with widespread reports of mortality of *B. serrata* plants (personal observations). At Mount Banks, these drought conditions have also been attributed to significant canopy dieback in a co-occurring tree species *Eucalyptus piperita*, which is known to have a similar level of embolism resistance to *B. serrata* (Li et al. 2018b). Widespread mortality of another species of *Banksia* (e.g. *B. grandis*) was also reported following severe drought in south-west Western Australia in 2013 (Matusick et al. 2013). Taken together, these findings suggest species of *Banksia* are not well suited to a future drying climate and may not be able to survive without management intervention, including assisted migration into regions that are projected to be similar climatically to the current species distribution.

4.5 Conclusion

Plant hydraulic traits govern plant growth and productivity, and constrain plant distributional ranges, but intra-species variation of plant hydraulic traits is less well-documented than inter-species variation. We found that water transport efficiency varied substantially across sites in *B. serrata*, while traits conferring drought tolerance were generally invariant. Although we acknowledge that the precipitation regime was not fully covered in this study, our findings suggest that key hydraulic traits are primarily conserved in this species. Therefore, *B. serrata* populations currently growing at the drier edge of the distribution may be more vulnerable to drought stress related to climate change. Further research is required to more fully elucidate the genetic and environmental contributions to trait variation, and subsequent potential for adaptive capacity through genetic adaptation and/or phenotypic plasticity in response to more extreme drought events in the future.

Chapter 5

Xylem embolism measured retrospectively is linked to canopy dieback in natural populations of *Eucalyptus piperita* following drought

5.1 Introduction

The world's forests have experienced massive diebacks due to drought, and these events are expected to become more frequent and severe in the future (Allen et al. 2010, Dai 2013, Allen et al. 2015). Of the proposed physiological mechanisms leading to canopy dieback during drought, the "hydraulic-failure hypothesis" suggests that drought-induced xylem cavitation and the formation of embolisms (the entry and spread of air bubbles in xylem conduits) reduces the ability of plants to transport water, and eventually results in tree mortality due to cellular desiccation (Tyree and Sperry 1988). Findings from controlled environment experiments generally support this hypothesis on the basis that dead trees commonly show substantial xylem embolism (Adams et al. 2017). However, evidence from field studies under natural drought conditions is rare (Davis et al. 2002, Hoffmann et al. 2011, Nardini et al. 2013, Venturas et al. 2016).

Trees minimise the risk of catastrophic hydraulic failure during severe drought via various mechanisms. Among these, the "hydraulic vulnerability segmentation hypothesis" (HVSH) states that lower carbon-investment organs such as leaves may act as "safety valves", such

that the loss of these organs during drought reduces rates of plant desiccation and minimises the risk of hydraulic failure in more carbon-expensive stems (Zirnmermann 1983, Tyree and Ewers 1991). While our understanding of these processes, as well as the drought mortality thresholds of species (Brodribb et al. 2009, Urli et al. 2013, Choat et al. 2015a, Li et al. 2016) is improving, the mechanisms by which trees survive and recover from severe drought in the field is much less well known (O'Brien et al. 2017, Skelton et al. 2017b). Given the importance of hydraulic conductance to photosynthesis and growth (Brodribb et al. 2000), a major uncertainty surrounding the ability of plants to recover from drought is whether drought-induced xylem embolisms can be refilled. It has been proposed that embolism refilling occurs once water stress is alleviated and plant water status is restored, and that for some plant species a cycle of xylem embolism-refilling occurs on a daily basis (Meinzer and McCulloh 2013, Ogasa et al. 2013, Brodersen et al. 2018). However, the refilling hypothesis is not supported by other studies examining xylem embolism during drought and recovery cycles (e.g. Choat et al. 2015b), suggesting that embolism refilling may not be a universal strategy, especially in trees, and that restoring post-drought hydraulic function may primarily depend on new xylem growth (Brodribb et al. 2010).

Assessing the negative impacts of severe drought on plant function under natural conditions usually depends on our ability to identify plants that are responding *in situ* to extreme drought (Leuzinger et al. 2005, Nardini et al. 2013). However, this task can be difficult due to the lack of certainty surrounding when and where trees are being negatively impacted by drought events. Within the Blue Mountains region, 50-100 km west of Sydney, Australia, the winter-spring of 2017 was characterised by an extended period without substantive rain (Figure 5-1a). At our study site, only 46 mm of rain fell between 10 June and 16 October, well below the ~50 year average rainfall of *ca.* 162 mm recorded from a nearby Bureau of Meteorology

weather station (Station number: 063246; http://www.bom.gov.au/climate/data/index.shtml) for the same period (Figure A-5). The period was also characterised by higher than normal maximum temperatures, with the mean maximum of 13.3 ^{o}C being 1.2 ^{o}C higher than the long term average (Figure 5-1b). These winter-spring drought conditions coincided with substantial branchlet and leaf dieback in several woody species, including the co-dominant tree *Eucalyptus piperita* (Sydney peppermint). Responding to this dieback event retrospectively, we conducted measurements on the level of native embolism (i.e. the steady state embolism level *in situ*)and characterised the allometry of branches from co-occurring *E. piperita* trees that were either visibly affected or unaffected by leaf dieback one month after the drought had ended, during which time the site had received rainfall (83.6 mm, Figure 5-1). We also measured leaf and stem hydraulic vulnerability in trees that were visibly unaffected by dieback. We hypothesised that the leaf and branchlet dieback that we observed in *E. piperita* was caused by drought-induced hydraulic failure. As such, branchlets from dieback affected trees were predicted to exhibit higher levels of native embolism than those from unaffected trees.

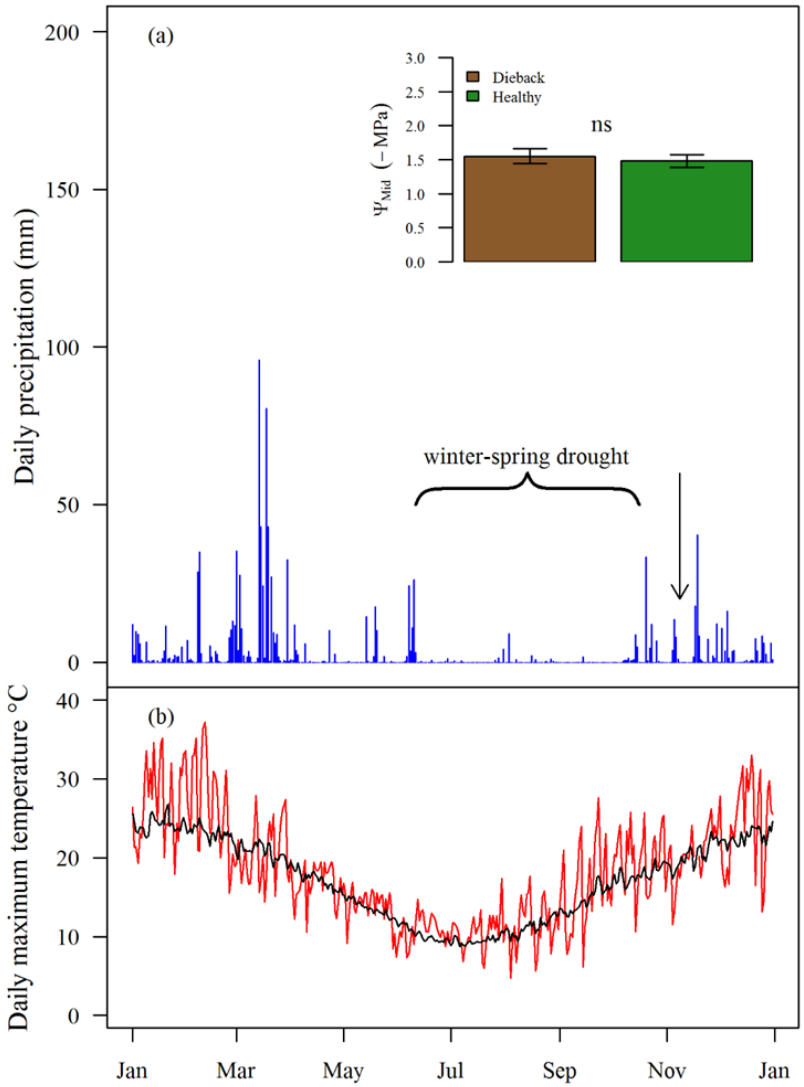

Figure 5-1 Daily precipitation (mm; panel a) at the sampling site and daily maximum temperature (°C; panel b, red solid line) in 2017 as well as long term mean maximum temperature (°C; panel b, black solid line) recorded by a nearby weather station (www.bom.gov.au; Station number: 063292). Brackets indicate the duration of the winter-spring drought. Inset figure shows midday leaf water potential (Ψ_{mid}) of dieback (brown bar) and healthy (green bar) *E. piperita* trees recorded on Nov 8th 2017 (arrow). Error bars indicate standard error (dieback trees n=4, healthy trees n=3). Differences between dieback and healthy trees were not significant (p=0.71). Note that the relatively high leaf water

potentials suggest that drought stress had been alleviated due to the resumption of rainfall during mid-October.

5.2 Materials and methods

5.2.1 Site description and plant material

The sampling site was located on an exposed north facing ridge below Mount Banks (33°35'S, 150°22'E; 1049 m a.s.l) within the Blue Mountains National Park. Monthly mean maximum temperature within this region spans from 24.1 °C in summer (January) to 9.5 °C (July) in winter. Mean annual precipitation is 1255 mm (http://www.bom.gov.au; Station number: 063246), with more than 65% rainfall typically occurring in summer and autumn (i.e. between Dec and May). Rainfall at the foot of Mount Banks was recorded hourly using a tipping-bucket rain collector (7852M, Davis, Goulburn, NSW, AU) connected to an Arduino-based data logger. Details regarding data logger calibration and error-rate are available on Github (https://github.com/DesiQuintans/sneesl-rain-logger). The soil at the site is mainly characterized as sandstone, with low moisture-holding capacity (http://espade.environment.nsw.gov.au/), while the vegetation is characterised as open dry sclerophyll forest dominated by two species of *Eucalyptus* and an understorey of woody shrubs dominated by Proteaceous species (TERN Australian Transect Network, Biodiversity and Adaptation Transect Sydney (BATS)-Vegetation and trait data (2011-2015); http://aekos.org.au/collection/adelaide.edu.au/TAB). The study species, *Eucalyptus piperita* Sm., has a distribution largely confined to the Sydney basin where it occurs as a component of dry sclerophyll forest across a range of elevations from near sea level to ~1100 m.a.s.l. in the Blue Mountains (https://www.ala.org.au/).

Plant material was collected on 8th November 2017, approximately one month after the drought event had been alleviated by rainfall in mid-October (see Figure 5-1), but before new growth had occurred. Four 6-8 m tall mature trees with clear signs of partial dieback, as represented by substantial leaf death and shedding on tertiary-order branches (herein referred to as *branchlets*), especially those positioned further from the growing tip of each secondary branch (Figure A-8), and three co-occurring healthy trees with no sign of dieback were chosen. For each individual tree, one or two second-order branches *ca.* 3.5 m in length were removed from the trunk *ca.* 3.5 m above ground level using a pole saw. These branch lengths were sufficient to avoid open vessels during hydraulic measurements (i.e. the maximum vessel length recorded was 73 cm). Furthermore, one leaf per tree was collected and sealed in a zip-lock bag for measurement of mid-day leaf water potential (Ψ_{mid}, MPa) using a Scholander-type pressure chamber (PMS Instruments, Corvallis, OR, USA). Branches were placed in large opaque plastic humidified bags and transported back to the laboratory where they were recut under water and allowed to rehydrate overnight.

5.2.2 Native embolism

Native embolism (%) was determined in the basal section of smaller tertiary branchlets (diameter *ca.* 3-5 mm) positioned at three-four different distances from the tip of each secondary branch (at 0.5-1.0, 1.0-1.5, 1.5-2.0, and 2.0-2.5 m; see Figure A-8). Note that the maximum distance from the tip that measurements were made in dieback affected branches was 1.5-2.0 m, beyond which all branchlets were dead. Stem water potential (Ψ_{stem}, MPa) of equilibrated branches was estimated using leaf water potential (Ψ_{leaf}, -MPa) as a proxy (Choat et al. 2010), which was measured immediately prior to stem sample preparation to ensure xylem tension was sufficiently relaxed to avoid potential cutting artefacts (Wheeler et al. 2013, Torres-Ruiz et al. 2015). The level of native embolism in each stem sample was

determined by calculating the ratio of the flow rate measured prior to ($K_{initial}$) and after the removal of any embolisms by flushing the sample with 2 mmol KCL under 200 kPa (K_{final}), and was expressed as PLC (%). Further details about sample preparation and measurement protocol are provided in the Supporting Information of Li et al. (2018b).

5.2.3 Vulnerability curves

Stem hydraulic vulnerability (VC_{stem}) was determined from three branches, each from a separate tree unaffected by dieback using the bench-top dehydration method, as described elsewhere (Nolf et al. 2015). From these same branches, we also measured leaf hydraulic vulnerability using the timed rehydration kinetics method (Brodribb et al. 2003b). The rehydration kinetics method requires leaf hydraulic capacitance (C_{leaf}) to be known, which can be obtained from leaf pressure-volume (PV) curves. Leaf PV was measured following Maréchaux et al. (2015). C_{leaf} was calculated before and after leaf turgor was lost, and then normalized by leaf mass per area and saturated water content following Brodribb and Holbrook (2003b). Detailed protocols for stem and leaf vulnerability curves, and leaf PV curves, have described in previous chapters.

5.2.4 Branch allometry and degree of leaf dieback

Following native embolism measurements, the basal stem diameter of each branchlet was measured using a digital calliper, and all green leaves above the cut section were collected. It was evident that shedding of dead leaves had occurred prior to field sampling; thus, any dead leaves still attached to the branchlet were ignored. Green leaves were oven-dried (70 °C for 72 hrs) and weighed. The total green leaf area of each branchlet was estimated from leaf dry mass (LDM) and specific leaf area (SLA, $m^2\ kg^{-1}$), which had been determined from ten representative leaves collected from each secondary branch. The extent of leaf death in individual branchlets positioned along the stem of secondary branches was estimated by the

ratio of remaining green leaf area (cm^2) to stem cross-sectional area (mm^2) measured at the base of each branchlet ($LA_{green}:X_s$).

5.2.5 Statistical analysis

Vulnerability curves were fitted using a sigmoidal model and key traits (Table A-5) were statistically tested by comparing bootstrap confidence intervals (CI) using the *fitplc* package in R (Duursma and Choat 2017). The difference in native embolism between healthy and dieback trees as well as the relationship between native embolism and $LA_{green}:X_s$ were tested using a linear mixed-effect model (*lme4()* package in R) with different individual trees treated as a random effect. Statistical significance was considered when $p \leq 0.05$. Native embolism and $LA_{green}:X_s$ data were $\log_{10}$ transformed to stabilize variance in the linear regression models.

5.3 Results

On average, the level of native embolism was significantly higher in dieback affected trees (26.2 ±5.1 %) than in healthy trees (11.1 ±1.9 %; p=0.04, Figure 5-2). In dieback trees, branchlets with higher native embolism had lower remaining green leaf area relative to stem cross-sectional area ($LA_{green}:X_s$, Figure 5-3), indicating higher leaf dieback in branchlets experiencing greater embolism (r^2=0.51, P<0.001). Leaf specific conductivity (K_L, mmol m^{-1} s^{-1} MPa^{-1}) in branchlets of healthy trees was higher than those of dieback trees, but the difference was only marginally significant (p=0.05, Figure A-6). Furthermore, branchlet $LA_{green}:X_s$ in dieback trees increased with increasing distance from the tip of the second-order branch to which they were attached, whereas the level of leaf dieback in branchlets from healthy trees was unrelated to branchlet position (Figure 5-4).

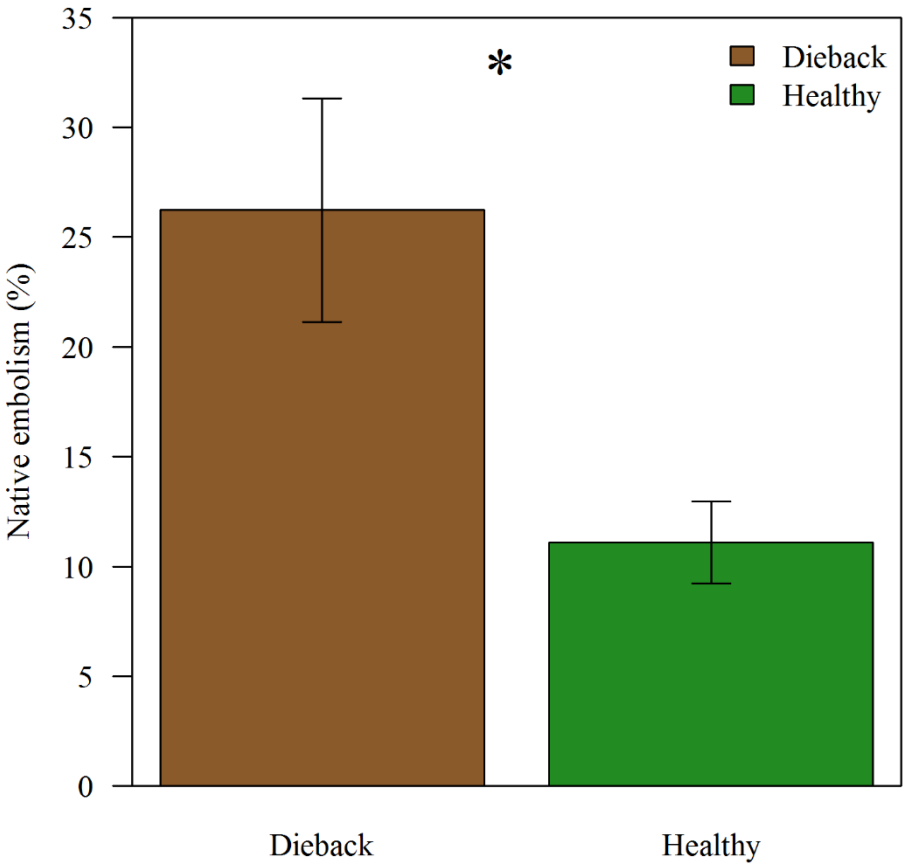

Figure 5-2 Branch native embolism (%) of trees showing canopy dieback (red bar) and healthy trees (blue bar) of *E. piperita*. Error bars indicate standard error (n=4 and 3 for dieback and healthy trees, respectively). Levels of native embolism were compared using linear mixed-effect model. Asterisk represents statistical significance at $p \leq 0.05$ level.

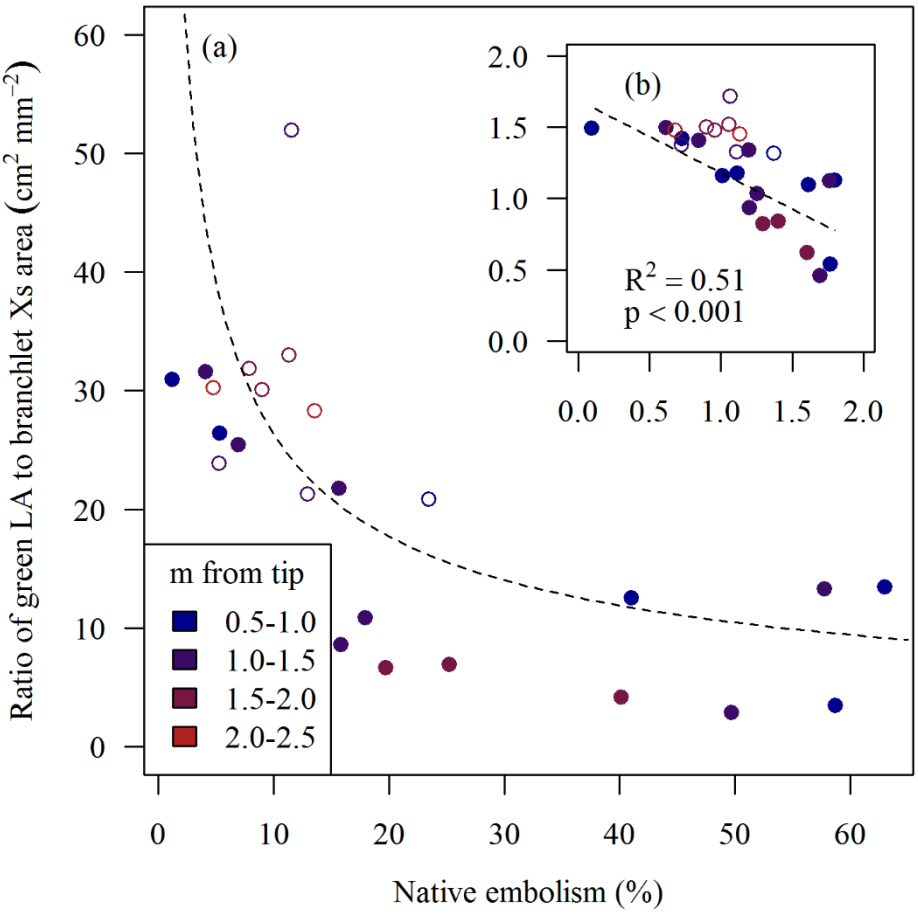

Figure 5-3 The relationship between the level of leaf dieback and native stem embolism (panel a). The degree of leaf dieback was estimated from the ratio of green leaf area (LA_{green}, cm^2) to basal xylem cross sectional area (X_s, mm^2) of individual branchlets. Filled circles represent dieback trees and open circles represent healthy trees. Different colours denote the distance between each branchlet and the tip of the main branch. Inset figure (panel b) shows the same relationship on a log-log scale after data were log_{10} transformed.

On the day of field sampling (approximately one month after the drought event), midday leaf water potentials were similar between dieback (-1.55 ±0.11 MPa) and healthy (-1.48 ±0.09 MPa) trees (Figure 5-1a). These water potentials would not have been sufficient to cause hydraulic dysfunction in either leaves or stems (Figure 5-5), indicating that the native

embolism we observed most likely formed as a consequence of the winter-spring drought event. In terms of hydraulic vulnerability, the water potential causing 50% loss of conductivity (P_{50}) was found to be -2.65 MPa (95% CI: 2.44,2.85) in leaves and -3.25 MPa (95% CI: 2.96,3.60) in stems (Figure 5-5, Table A-5).

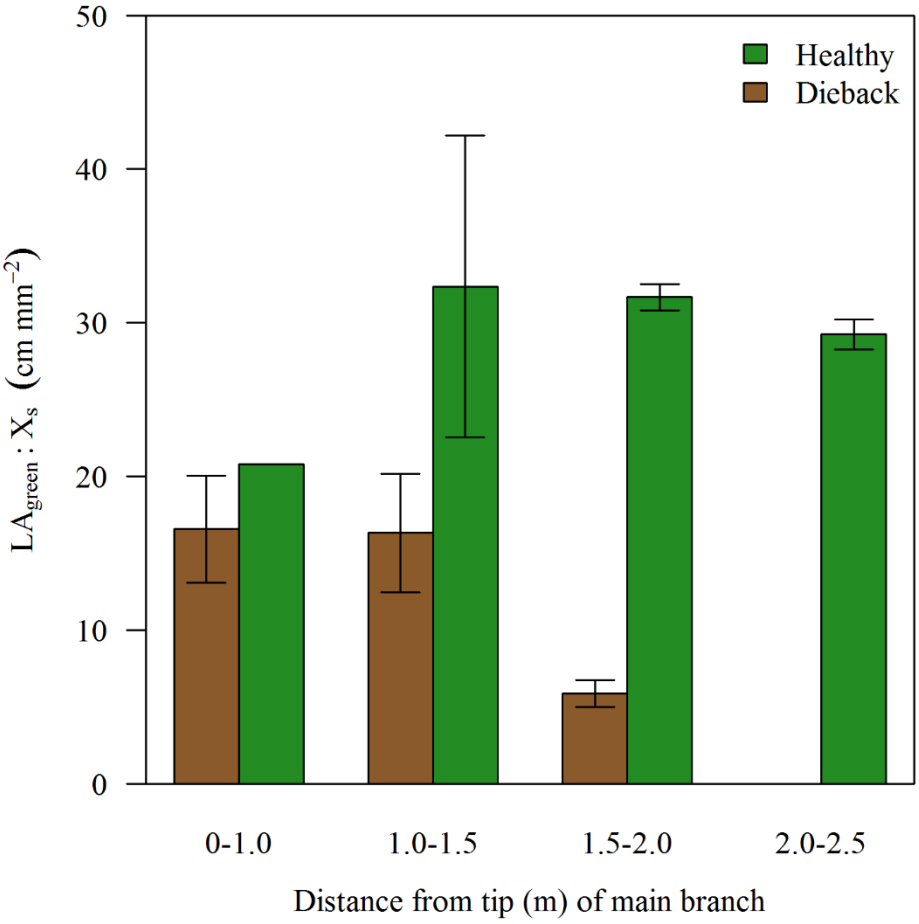

Figure 5-4 Plot showing that the level of branchlet dieback increased with increasing distance from the tip of the main branch in dieback trees only. Error bars indicate standard error.

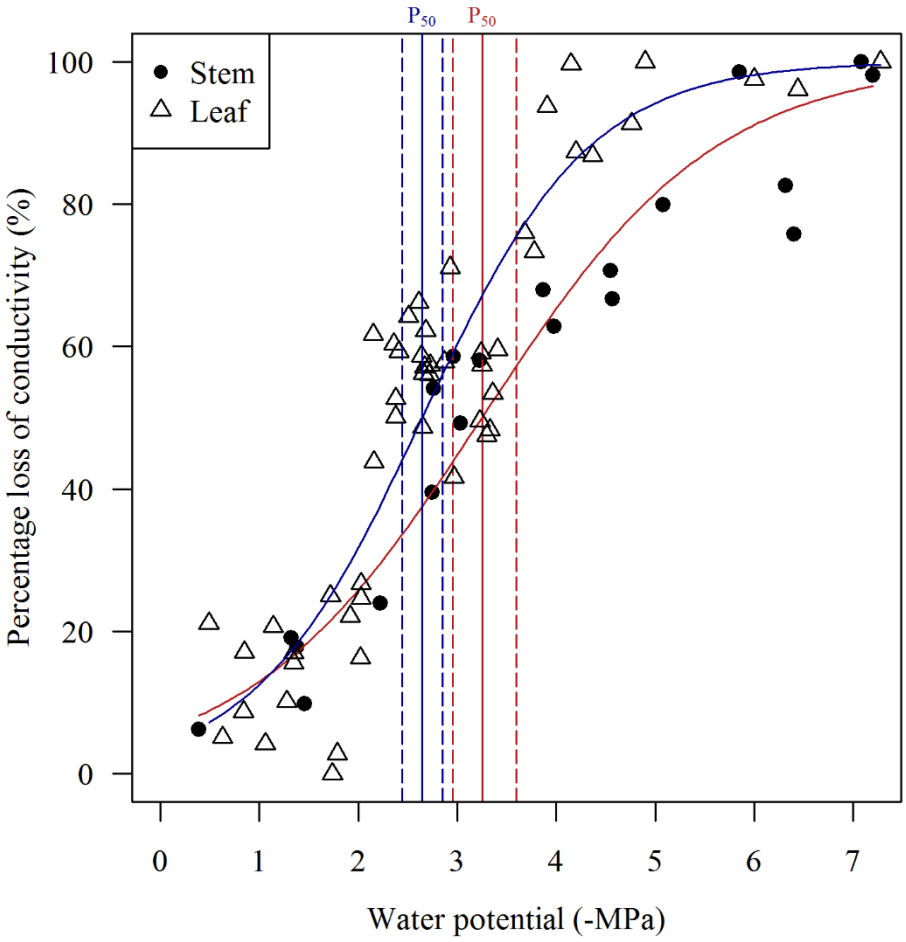

Figure 5-5 Leaf (open triangle, blue solid line) and stem (closed circle, red solid line) vulnerability curves of *E. piperita*. Blue and red solid vertical lines indicate the water potential corresponding to 50% loss of xylem conductivity (P_{50}, -MPa) in leaves and stems, respectively. Corresponding dashed lines represent the upper and lower confidence interval.

5.4 Discussion

Natural drought events occur stochastically. Therefore, measuring tree physiological status leading up to and during peak drought is often difficult. In this study, we took hydraulic and branch allometry measurements retrospectively in a small number of branches, one month after drought stress had been alleviated, yet were still able to detect strong legacy effects of the drought event. Similar to observations from previous natural droughts where xylem

embolism was reported to be higher in dieback affected trees than in healthy trees (Nardini et al. 2013), our findings provide indirect evidence that supports the notion that leaf and branch dieback was caused by drought-induced embolism, although we acknowledge that our findings were based on a small number of replicates, which increases the risk of observing false positive results. Nevertheless, given that significant levels of native embolism were observed in dieback affected branchlets one month after the drought had ended, these trees were apparently unable to completely refill xylem embolisms, despite restoring favourable plant water status (Delzon et al. 2014). Our findings provide no evidence for rapid or substantial embolism refilling and instead suggest that the recovery of full hydraulic function in embolised branchlets is either slow or dependent on new xylem growth, as has been observed in manipulative experiments (Brodribb et al. 2010).

After a period of high rainfall in March and April (Austral Autumn), our study site received significantly below-average rainfall during the 5 months from June to October, which was the lowest recorded rainfall in the area over this period within the last 50 years. This exceptional dry period most likely generated severe soil water deficit at our study site, with trees growing in higher sun-exposed positions more susceptible to drought (personal observation). Higher-than-average temperatures during the same period most likely increased rates of evapotranspiration. However, daily maximum temperatures did not exceed 25 °C (mean maximum was 13.3 °C), so it is very unlikely that leaf death was directly linked to heat stress, although the ongoing drought would have decreased the capacity for transpirational leaf cooling (Drake et al. 2018). Thus, we suggest that the primary mechanism of leaf and branch dieback observed in these trees is linked directly to the drought event. Furthermore, the observed canopy dieback response is supported by a recently developed eco-climatic

framework that associates canopy collapse in forest trees with a 1-in-20 year water deficit event (Mitchell et al. 2016).

In our study species, leaves were more hydraulically vulnerable than stems (Figure 5-5), which is consistent with a number of recent studies in support of hydraulic vulnerability segmentation (Nolf et al. 2015; Pivovaroff et al. 2014; Zhang et al. 2017; but see Villagra et al. 2013; Zhu et al. 2016). Although we did not measure leaf water potentials *in situ*, at the peak of water stress during the 2017 winter-spring drought, we speculate that dieback affected trees of *E. piperita* most likely reached minimum water potentials between -2 and -4 MPa, which corresponds to the levels of embolism observed across individual branchlets, in association with stem vulnerability (Figure 5-5). Also, if we assume that leaf death in woody angiosperms begins to occur at water potentials that exceed 88% loss in leaf hydraulic conductance, as shown in previous studies (Blackman et al. 2009), it is possible that dieback affected trees reached water potentials more negative than -4.3 MPa (i.e., the water potential at leaf P_{88}; Figure 5; Table S1). The possible reasons why some co-occurring trees were apparently unaffected by dieback include small differences in hydraulic vulnerability (Salmon et al. 2015), although this is unlikely considering the strong potential for gene flow and that significant intraspecific variation in hydraulic vulnerability has so far only been observed between populations from contrasting climates (López et al. 2016, Blackman et al. 2017). It is more likely that unaffected healthy trees had greater access to soil water, possibly as a function of heterogeneity in the soil depth profile.

Our finding that branchlet leaf dieback increased with distance from the growing tip of secondary branches suggests that the minimum water potential was lower in branchlets further from the growing tip. However, this is contrary to the notion that water potentials

should decrease with increasing distance along the hydraulic pathway (Sack and Holbrook 2006). Alternatively, leaf senescence and abscission of leaves in dieback affected trees may have resulted from hormonal signalling in an effort to reduce evaporative surface area in response to increasing levels of soil water deficit during the drought (Munné-Bosch and Alegre 2004). Either way, our findings suggest that dieback affected trees may be operating to preserve either younger or more productive leaves in the upper canopy at the expense of older or more shaded leaves. Furthermore, the lack of a strong difference in leaf specific conductivity between healthy and dieback affected branchlets suggests some degree of coordination between hydraulic supply (stem conductivity) and demand (leaf surface area) was maintained by dieback affected trees in response to the drought, although we note that greater replication is needed to provide a stronger statistical test. Interestingly, stems tended to maintain a minimum level (*ca.* 40%) of hydraulic conductivity even in branchlets that exhibited near-complete leaf death, providing further evidence that the hydraulic integrity of stems was prioritised during drought. Residual hydraulic conductivity in stems may also be important to post-drought recovery of gas exchange, as well as the resumption of new growth.

Our data, measured retrospectively, suggest that leaf and branch dieback in field populations of *E. piperita* following a strong winter-spring drought was linked to xylem embolism. Branchlet stem xylem did not recover hydraulic functionality, therefore these trees may suffer short- to medium-term legacy effects of the drought event, including reduced canopy transpiration and productivity (Skelton et al. 2017b) and increased susceptibility to future drought (Hacke et al. 2001b).

Chapter 6

Synthesis

This PhD research was aimed at identifying traits determining the risk of drought related mortality for some of the dominant tree species across NSW, Australia using an eco-physiological approach. To this end, variation of key hydraulic traits that are theoretically linked to tree death were investigated for 12 species native to five different vegetation types (Rainforest, Wet sclerophyll forest, Dry sclerophyll forest, grassy woodland and semiarid woodland) in a common garden experiment (Chapter 2). In addition, metrics of water regulation strategy were compared and contrasted under the same experimental conditions using a subset of species to identify the best metrics to quantitatively describe how plants behave under well-watered conditions and respond to drought (Chapter 3). Furthermore, within-species variation of key hydraulic traits was examined for *Banksia serrata* grown in three climatically contrasting sites (Chapter 4). Finally, the relationship between hydraulic failure and canopy dieback was studied on field grown *Eucalyptus piperita* by taking advantage of a natural drought event (Chapter 5). Through this work, I sought to answer the following questions:

1. How are hydraulic traits coordinated across species, and how do they relate to species climate-of-origin?
2. To what degree do key hydraulic traits vary within a species?
3. Is hydraulic failure responsible for canopy dieback of field grown trees?

6.1 Synthesis

6.1.1 Hydraulic traits co-vary across species and are linked to climate-of-origin

Hydraulic traits are often strongly correlated with species natural distributional ranges. In particular, traits conferring drought tolerance have been identified as key factors that determine the response and fate of plants when exposed to drought stress (Anderegg et al. 2016, Blackman et al. 2016a, Choat et al. 2018a). The interspecific variation of hydraulic traits has been documented in many studies, and results typically show that traits vary systematically across species along moisture gradients (Engelbrecht et al. 2007, Trueba et al. 2017, Oliveira et al. 2019). However, these results often incorporate limited set of functional traits, therefore does not allow the hydraulic regulation of plants to be mapped completely. Global database comprising multiple traits, on the other hand, is sourced from different studies, therefore may suffer the error arise from differences in plant material (e.g. genotype, age), drought treatment (e.g. duration, severity) and experimental protocol (Choat et al. 2012a, Klein 2014). A precise and comprehensive understanding on trait-trait coordination and trait relationships to climate is still lacking, which represent one of the major knowledge gaps hampering the projection of forest fate under climate change scenario.

In the present study, key hydraulic traits of both stem (e.g. P_{x50}, K_s) and leaf (e.g. P_{L50}, TLP) varied considerably across species. Moreover, significant interspecific variation in different types of hydraulic safety margin (i.e. HSM_{SM}, HSM_{ST}) was also observed. It was found that plant hydraulic traits were highly coordinated. Water potential thresholds inducing xylem embolism in stems (Chapter 2) and leaves (Chapter 3) were correlated with P_{gs90}, indicating the functional convergence of these traits. Importantly, P_{gs90} was consistently higher (less negative) than P_{x50} and P_{L50} across species. This finding contradicts the notion that stomatal

closure is signaled by xylem embolism (Nardini and Salleo 2000), and providing evidence that stomatal closure protects the integrity of xylem water transport. These results suggest that the overall drought tolerance of plants is multi-dimensional, in which diverse traits within the water transport pathway function in cooperation, exerting control over the supply-demand relationship of the hydraulics. Such presumption is well validated in Chapter 3, in which the overall operating range of water potential was manipulated by multiple hydraulic traits, including stomatal regulation and xylem embolism resistance, as evidenced by their relationships between the Hydroscape. In addition, several trade-offs were identified among traits. P_{x50} was negatively correlated with K_s, supporting the efficiency-safety trade-off between the capacity of xylem water transport and resisting embolism. While A negative correlation was also found between WD and C_{branch}, indicating that water storage capacity and mechanical strength of sapwood cannot be maximized simultaneously. Moreover, key hydraulic traits including P_{gs90}, P_{x50}, P_{L50}, HSM_{ST} and HSM_{SM} were linked to climatic variables representing water availability of species climate origin (Chapter 2, 3).

Overall, hydraulic traits associated with drought induced tree mortality showed remarkable variation among these ecologically important tree species across NSW. Hydraulic traits were also highly coordinated and linked to aridity of species' climate of origin, thus providing strong evidence for the significant role of hydraulic traits in adapting dry environment, as has been suggested previously (Engelbrecht et al. 2007, Brodribb et al. 2017). Moreover, species native to arid regions typically showed negative thresholds of stomatal closure and xylem embolism. Also, stomata of these species will shut down at less negative water potentials relative to the inception of xylem embolism, and leaves may shed to constrain the xylem water potential within a safe range if drought persists. Such results indicate that adaption to low rainfall environment incorporate multiple features other than embolism resistance, thus

adding to the body of knowledge regarding plant growth strategy. Furthermore, the close associations between traits and species climate-of-origin substantiate the genetic bases for the trait variation across species.

6.1.2 Key hydraulic traits are highly conserved within species

Despite variation of hydraulic traits across species has been well-documented, far less attention has been given to how traits vary within species. In the few studies in which intraspecific variation of hydraulic traits are investigated either *in situ* or using provenance trials, highly variable results have been generated, with adjustments in hydraulics being reported in some species but not in others (López et al. 2016, Schuldt et al. 2016, Larter et al. 2017), which poses a barrier to the prediction of plant response to drought at regional or global scales.

In this study, the intraspecific variation of hydraulic traits was examined using two approaches. Firstly, I investigated the relationships among hydraulic traits and species climate-of-origin in a common garden experiment, which allows the variation caused by phenotypic plasticity to be minimized (Chapter 2 and 3). I found that several key hydraulic traits including P_{gs90}, P_{x50}, P_{L50}, HSM_{ST} and HSM_{SM} were linked to climatic variables representing water availability of species climate of origin, indicating that these traits were controlled genetically and thus may not be able to rapidly acclimate to local climate. Secondly, I compared the hydraulic traits of *Banksia serrata* from three sites that are characterized by contrasting climates (Chapter 4). The results showed that hydraulic traits such as P_{x50}, P_{L50} or TLP did not differ significantly across sites. However, some physiological or morphological traits including C_{leaf}, ε, K_s or HV did exhibit adjustments in response to the local climate.

Collectively, results of this study do not support the notion that hydraulic traits are highly plastic, at least for the species examined here (Jacobsen et al. 2007). Instead, these results are in line with a number of studies showing that hydraulic traits are conserved within species, probably because plant hydraulics traits are largely canalized, making them robust to environmental perturbation.

6.1.3 Hydraulic failure underpins canopy dieback under natural conditions

Since the emergence of "carbon-hydraulic framework" for explaining the underlying mechanisms related to drought induced tree mortality (McDowell et al. 2008), numerous studies have attempted to test the role of carbon starvation and hydraulic failure in tree death (Anderegg et al. 2016, Adams et al. 2017). Hydraulic failure is currently the most well supported mechanism, with a theoretical framework underpinned by several lines of evidence. Firstly, plant death due to desiccation is quantitively linked to the water potential thresholds causing massive embolism, such that patterns of tree death can be explained by this trait (Anderegg et al. 2016). Secondly, studies examining the dynamics of carbohydrate and hydraulics have generally found dead trees show minimal xylem hydraulic conductivity with variable carbohydrate contents (reviewed by Adams et al. 2017). However, this evidence is often derived from controlled experiments with potted seedlings; observations from field-grown adult trees are still limited.

In this study, the correlation between hydraulic dysfunction and canopy dieback was examined using natural population of *E. piperita* by taking advantage of a severe Winter-Spring drought spell that occurred in NSW in 2017 (Chapter 5). Results of this study indicate that the level of canopy dieback, represented by the ratio of green leaf area to xylem cross-

section area, was tightly correlated with corresponding levels of branch native embolism. Notably, the level of canopy dieback appeared more pronounced for branchlets that were close to the main branch. Overall, compared with trees that were unaffected by drought stress, trees exhibiting symbols of crown dieback showed significantly higher levels of native embolism (26% vs. 11%). In addition, it was found that leaves and stems had similar P_{50}, therefore leaf death as drought progressed may have had limited ability to protect the water transport in xylem.

Results of this study support previous findings that canopy dieback in field grown trees is accompanied with increased level of xylem embolism, therefore providing strong evidence for the crucial role of hydraulic failure in tree death. Critically, xylem embolism was still able to be detected one month after the drought stress had been alleviated, indicating that embolized xylem cannot be fully repaired during a short period of time.

6.2 Implications and future directions

Most tree species in NSW are considered to be well-adapted to drought because of the high interannual variation in precipitation (Nicholls et al. 1997). However, mortality resulting from severe drought stress is likely to occur with increased probability and frequency as the climate becomes warmer, largely because water transport in many tree species operates close to their physiological threshold, as evidenced by the narrow hydraulic safety margin of a wide range of tree species across the globe (Choat et al. 2012a). Indeed, mortality events triggered by drought stress have been documented for some tree species distributed across NSW recently (Mitchell et al. 2014, Li et al. 2018b). Given that drought related to tree mortality is primarily underpinned by hydraulic dysfunction, knowledge of the variation of plant functional traits that are involved in regulation of plant water stress should be

incorporated into process-based models therefore greatly advance the predictability of the pattern of tree mortality under the scenario of global climate change.

Hydraulic traits of tree species studies in the current research showed marked variation. In general, species originating from the arid regions exhibited more negative thresholds for xylem cavitation and stomatal closure, as well as turgor loss point. Importantly, these species possessed wide hydraulic safety margins for stomatal closure and hydraulic segmentation, suggesting that these species would delay the formation and spread of xylem embolism by resisting water loss from leaves. Therefore, species with these characteristics are under lower mortality risk during severe drought if all else being equal. Furthermore, the drought resistant xylem enables these species operate over a wider range of water potential, which will facilitate CO_2 assimilation, especially under stress conditions. However, given the habitats of these species are characterized by reduced and stochastic rainfall, which results to a higher chance of being exposed to intense drought, species native to arid region are likely to be equally risky compare to mesic zone species in terms of drought induced mortality upon global climate change. Furthermore, the lack of intraspecific variation for most hydraulic traits suggests a limited ability to acclimate to rapidly changing environmental conditions. Collectively, these results illustrate that tree species may be equally vulnerable to global change type drought. Therefore, conservation should be planned and applied for all tree species regardless of their provenances.

Results presented in this research will also facilitate the modelling of tree dynamics in response to environmental perturbations with a trait-based approach. Two key hydraulic traits, the xylem embolism threshold and the stomatal closure point, were tightly correlated, suggesting that they can be predicted from each other if relevant data are otherwise

unavailable. Furthermore, the correlation between WD and P_{X50} indicates that WD is a robust predictor of xylem cavitation thresholds, at least for many NSW tree species, despite a weak correlation being reported between these two traits at global scale (Choat et al. 2012a, Klein 2014). Contrary to the conclusion that TLP is a good proxy for stomatal closure (Bartlett et al. 2016, Zhu et al. 2018), TLP was only weakly correlated with P_{gs90} for the species studied here, suggesting that this trait should be used with caution. Furthermore, key hydraulic traits are highly adaptive and therefore can be predicted from species climate of origin. Although values of key hydraulic traits have been accumulating, only a few species are currently available in global database. If findings of this research hold more widely, global trait database will be greatly expanded.

Although results presented in this study represent a significant advance towards a better understanding and parameterization of drought related tree mortality, many other gaps exist and thus hamper a precise forecasting of the risk and process of mortality events during drought stress. Functional traits investigated here comprise most characteristics that would influence the progression of mortality during drought stress. However, some traits that are unstudied in the present work can be of equal or more importance in determining the mortality risk. For example, cuticular conductance can exert a strong control over the water loss from plants after stomatal closure, which in turn determines the timing when critical water potential is reached. This trait, however, has been largely overlooked in early literature and its importance in drought adaption is not fully comprehended until recently (Duursma et al. 2019). Furthermore, this work has primarily focused on aboveground traits, while it has been shown that mortality events in some species are well underpinned by belowground process (Johnson et al. 2018b). Indeed, it has long been known that hydraulic failure can occur in the rhizosphere. Compare with the well-documented hydraulic processes for leaves

and stems, less attention has been devoted to the hydraulic traits of roots, despite its pivotal role in bridging the soil and plants. Therefore, knowledge about the inter- and intraspecific variation of these traits, together with their biological and environmental control will help to gain a comprehensive view of plants water regulation strategies. On the other hand, dynamics of drought response is also in paucity. For instance, leaf area adjustments will strongly alter the water balance and consequently affect the risk and timing of mortality resulted from drought stress, but this response is rarely quantified. Integrating such response into process-based models will greatly improve their predictive power. Finally, results of this study are chiefly obtained from phylogenetically monotonic species, further studies should examine if general pattern of traits correlation and trade-offs can be observed from diverse species, especially for different clades.

Appendix

Supplementary tables and figures

Chapter 2 Table A-1 Correlation matrix showing the relationship among climatic factors and plant functional traits. Definitions are given in Table 1. P-values of correlation are indicated by different symbols. ***, p<0.001; **, p<0.01; *, p<0.05.

	MAT	AI	MAP	P_{12}	P_{50}	P_{88}	K_s	P_{gs50}	P_{gs90}	HSM	TLP	C_{branch}	A	g_{smax}	SLA	WD
MAT	1															
AI	-0.66*	1														
MAP	-0.24	0.87***	1													
P_{12}	0.38	-0.78**	-0.82**	1												
P_{50}	0.49	-0.86***	-0.87***	0.95***	1											
P_{88}	0.55	-0.87***	-0.84***	0.86***	0.98***	1										
Ks	-0.45	0.47	0.38	-0.64*	-0.58*	-0.52	1									
P_{gs50}	0.12	-0.56	-0.68*	0.75**	0.76**	0.71**	-0.17	1								
P_{gs90}	0.49	-0.85***	-0.85***	0.94***	0.96***	0.91***	-0.55	0.81**	1							
HSM	0.46	-0.82**	-0.83***	0.90***	0.97***	0.97***	-0.56	0.66*	0.86***	1						
TLP	0.38	-0.5	-0.42	0.53	0.48	0.42	-0.43	0.57	0.61*	0.35	1					
C_{branch}	-0.29	0.56	0.56	-0.68*	-0.61*	-0.53	0.83***	-0.37	-0.67*	-0.51	-0.69*	1				
A	0.55	-0.79**	-0.74**	0.60*	0.75**	0.80**	-0.21	0.41	0.67*	0.77**	0.25	-0.26	1			
g_{smax}	0.43	-0.84***	-0.87***	0.75**	0.89***	0.93***	-0.24	0.73**	0.84***	0.87***	0.38	-0.36	0.90***	1		
SLA	-0.64*	0.57	0.32	-0.44	-0.46	-0.46	0.77**	-0.02	-0.41	-0.46	-0.3	0.64*	-0.23	-0.23	1	
WD	0.44	-0.80**	-0.76**	0.86***	0.80**	0.71*	-0.66*	0.60*	0.83***	0.72**	0.75**	-0.82***	0.43	0.58	-0.60*	1
VIGR	-0.41	0.65*	0.59*	-0.70*	-0.64*	-0.57	0.82**	-0.39	-0.70*	-0.54	-0.64*	0.93***	-0.24	-0.39	0.80**	-0.86***

Chapter 2 Table A-2 Summary of seed source information for 12 species from five vegetation types (rainforest (RF), wet sclerophyll forest (WSF), dry sclerophyll forest (DSF), grass woodland (GW), and semi-arid woodland (SAW)).

Family	Species	Abbreviation	Vegetation type	Description
Myrtaceae	*Acmena smithii*	Asm	RF	AUSTRALIA, NSW, Brogers Creek, Kangaroo Valley (34.73S, 150 .42E)
Myrtaceae	*Eucalyptus grandis*	Egr	WSF	AUSTRALIA, NSW, North Coast, Edge of Myall River, Bulahdelah (south side of river, west side of Pacific Highway (32.24S, 152.12E)
Myrtaceae	*Eucalyptus viminalis*	Evi	WSF	AUSTRALIA, NSW, Central Coast, Belgenny Reserve, Belgenny Reserve, Camden. Near bicycle track (34.41S, 150.42E)
Myrtaceae	*Angophora costata*	Aco	DSF	AUSTRALIA, NSW, Central Coast, Rear of property number 16 Park Road, Woodford (33.45S, 150.29E)
Myrtaceae	*Corymbia gummifera*	Cgu	DSF	AUSTRALIA, NSW, North Coast, Fortis Creek National Park, 1.2 km north of Chapman's Creek crossing on Grafton to Coaldale road (29.28S, 152.52E)
Myrtaceae	*Eucalyptus sideroxylon*	Esi	DSF	AUSTRALIA, NSW, Central Tablelands, 23.3 km from Rylstone towards Glen Davis at entrance to property no. 2334 (32.57S, 150.55E)
Myrtaceae	*Eucalyptus blakelyi*	Ebl	GW	AUSTRALIA, NSW, Central Tablelands, 13.5 km E along Glen Davis road from Capertee (33.81S, 150.45E)
Myrtaceae	*Eucalyptus macrorhyncha*	Ema	GW	AUSTRALIA, NSW, South Western Slopes, 3.8 km E of Talmalmo on road towards Jingellic (35.37S, 147.32E)
Myrtaceae	*Eucalyptus melliodora*	Eme	GW	AUSTRALIA, NSW, Central Coast, 800 m towards Glen Alice from intersection of Capertee to Glen Davis road (33.54S, 150.13E)
Fabaceae	*Acacia aneura*	Aan	SAW	AUSTRALIA, NSW, North Western Plains, Gundabooka National Park, Near Belah Homestead (30.34S, 145.35E)
Myrtaceae	*Eucalyptus largiflorens*	Ela	SAW	AUSTRALIA, NSW, North Western Plains, 10.9 km W of Walgett on Kamilaroi Highway (30.01S, 148.12E)
Myrtaceae	*Eucalyptus populnea*	Epo	SAW	AUSTRALIA, NSW, North Western Slopes, ca. 1 km N of "centre" of Terry Hie Hie (29.46S, 150.86E)

Chapter 3 Table A-3 Matrix showing the r values of Pearson correlation among climatic variables, hydraulic traits and metrics of isohydricity. Asterisk indicates significant level: ***, $p < 0.001$; **, $p < 0.01$; *, $p < 0.05$. MAT: mean annual temperature. MAP: mean annual precipitation. AI: aridity index. TLP: leaf turgor point. P_{gs90}: leaf water potential causing 90% stomatal closure. P_{L50}/P_{x50}: leaf and stem water potential inducing 50% loss of hydraulic conductivity. HSM_{HS}: hydraulic safety margin of hydraulic segmentation defined as P_{L50}-P_{x50}. g_{smax}: maximum stomatal conductance. K_{max}: maximum stem conductivity. HV: Huber value.

	MAT	MAP	AI	TLP	P_{gs90}	P_{L50}	P_{x50}	HSM_{HS}	g_{smax}	K_{max}	HV	Hydroscape	Slope	$\Delta\Psi_{max}$	HSM_{ST}
MAT	1														
MAP	0.02	1													
AI	-0.53	0.82**	1												
TLP	0.6	-0.57	-0.83**	1											
P_{gs90}	0.27	-0.85**	-0.85**	0.61	1										
P_{L50}	0.32	-0.83**	-0.85**	0.74*	0.77**	1									
P_{x50}	0.25	-0.87**	-0.85**	0.77**	0.93***	0.83**	1								
HSM_{HS}	0.19	-0.78**	-0.75*	0.69*	0.90***	0.64*	0.96***	1							
g_{smax}	0.13	-0.85**	-0.75*	0.56	0.89***	0.79**	0.93***	0.89***	1						
K_{max}	-0.5	0.51	0.70*	-0.78**	-0.46	-0.61	-0.58	-0.49	-0.42	1					
HV	0.36	-0.79**	-0.80**	0.58	0.90***	0.84**	0.87**	0.77**	0.90***	-0.58	1				
Hydroscape	0.25	-0.94***	-0.93***	0.77**	0.86**	0.90***	0.90***	0.79**	0.82**	-0.62	0.83**	1			
Slope	0.78**	0.2	-0.24	0.1	0.23	0.11	0.02	-0.03	0.03	-0.08	0.29	-0.03	1		
$\Delta\Psi_{max}$	-0.04	-0.74*	-0.6	0.66*	0.68*	0.79**	0.81**	0.72*	0.73*	-0.42	0.61	0.78**	-0.27	1	
HSM_{ST}	-0.07	0.38	0.36	-0.1	-0.69*	-0.06	-0.52	-0.67*	-0.5	0.03	-0.44	-0.31	-0.24	-0.15	1

Chapter 3 Table A-4 Spearman's rank correlation coefficient (ρ) among the species raking given by different metrics. Asterisk indicates correlation is statistically significant at $p \leq 0.05$ level.

	Hydroscape	$\Delta\Psi_{max}$	Slope	HSM_{ST}
Hydroscape	1			
$\Delta\Psi_{max}$	0.67*	1		
Slope	-0.07	-0.25	1	
HSM_{ST}	-0.42	-0.27	-0.27	1

Chapter 5 Table A-5 Summary of key traits for leaf and stem vulnerability to water stress. P_{12}, P_{50} and P_{88} represent water potential (-MPa) inducing 12%, 50% and 88% loss of hydraulic conductivity, respectively. Values in brackets following each number are the lower and upper bounds of 95% confidence intervals.

Organ	P_{12}	P_{50}	P_{88}
Leaf	0.96 [0.61,1.31]	2.64 [2.44,2.85]	4.33 [3.85,4.73]
Stem	0.90 [,1.28]	3.25 [2.96,3.60]	5.60 [4.88,6.60]

Chapter 2 Figure A-1 Natural distributional range of 12 woody species across Australia (panel a-e) and seed source location (panel f). Species coordination data were obtained from Atlas of Living Australia using *ALA4R* package in R. Vegetation types are coloured differently and are abbreviated using initials in panel f.

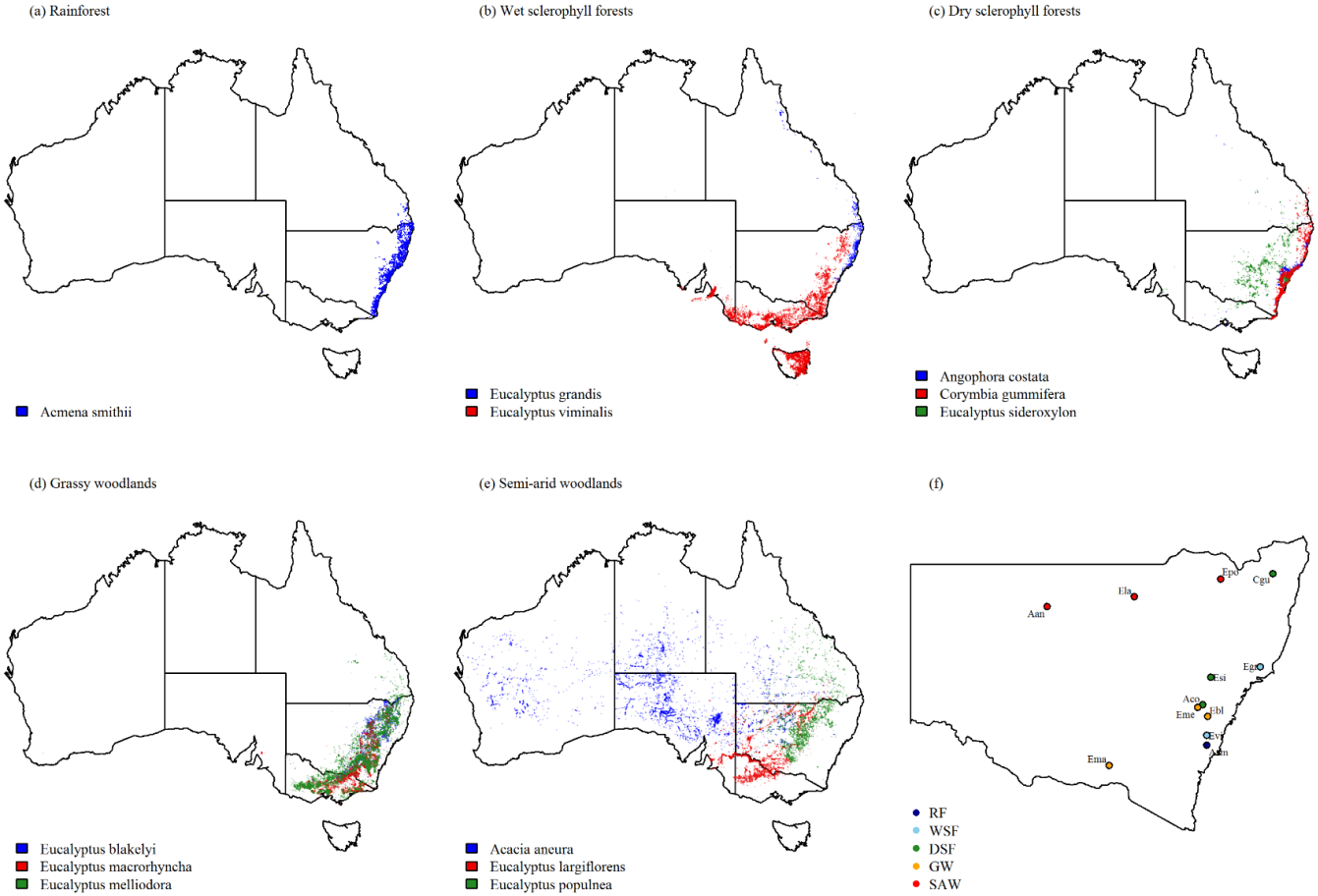

Chapter 2 Figure A-2 Relationship between species maximum photosynthetic rate (A_{max}, μmol m^{-2} s^{-1}) and hydraulic safety margin (HSM, -MPa). Regression lines and corresponding adjusted R^2 are given. Asterisk stands for P<0.01.

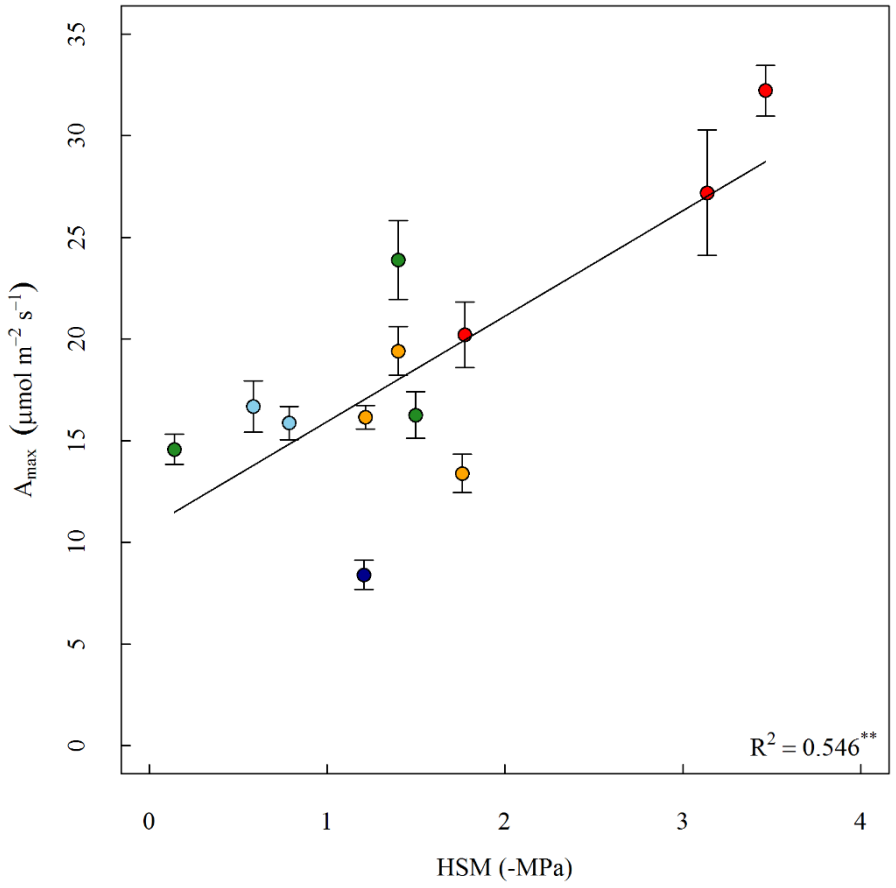

Chapter 3 Figure A-3 Trajectory of predawn (Ψ_{pd}) and corresponding midday leaf water potential (Ψ_{md}) of eight species during dehydration. Ψ_{md} is regressed against Ψ_{pd} after removing the fluctuation of water potential at the initial phase of dehydration caused by environmental factors other than soil water deficit. Hydroscape (shaded region) is the triangle bound by the regression line (solid) and 1:1 line (dashed). Also shown are the R^2 and p value of linear regression. Colours represent different individual.

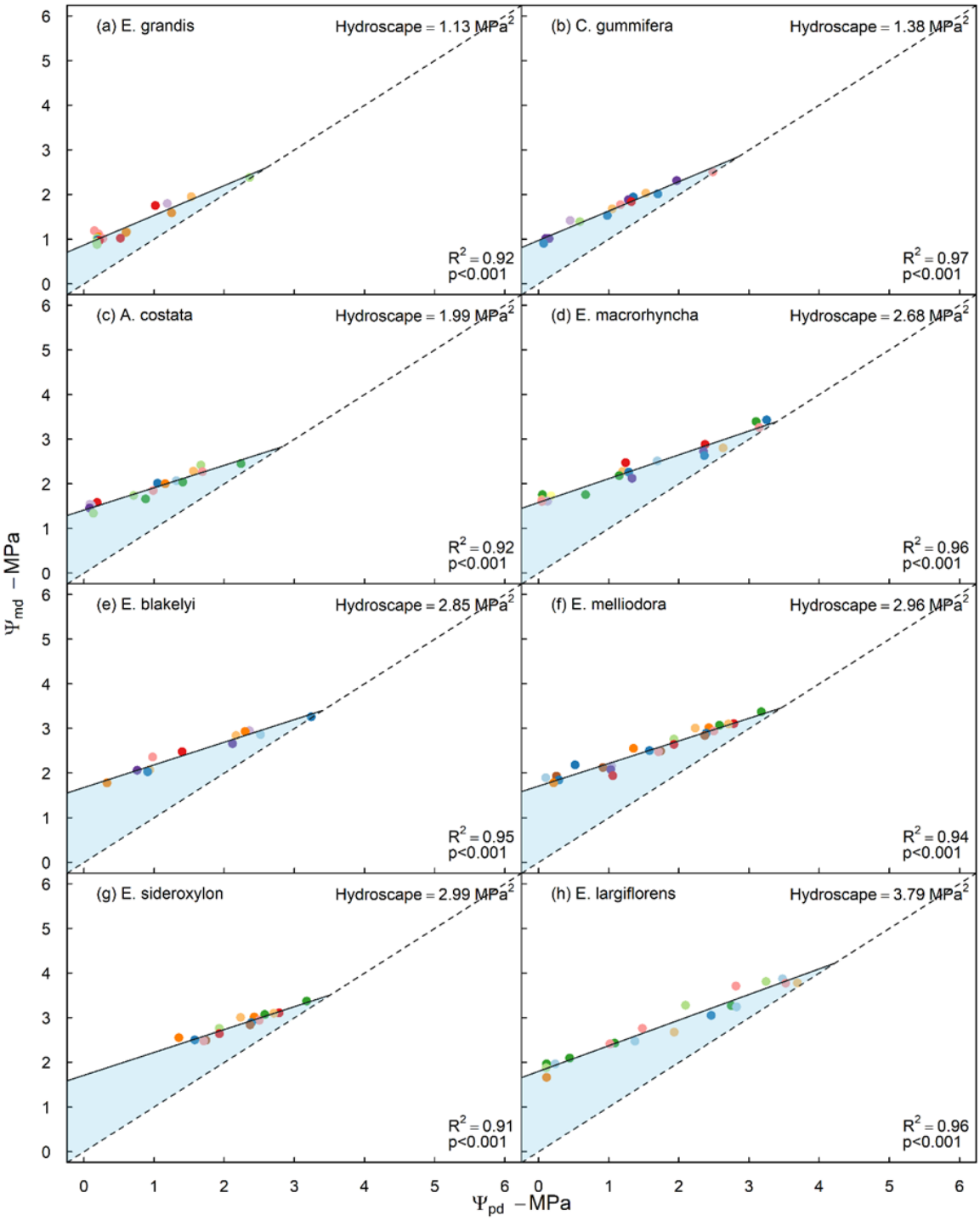

Chapter 3 Figure A-4 Stomatal conductance (close circle, pink bank), leaf (grey band) and stem (open triangle) xylem embolism response to water potential. Stomatal conductance is shown in relative values. Inset figures show the spatio-temporal development of xylem embolism following desiccation in leaves.

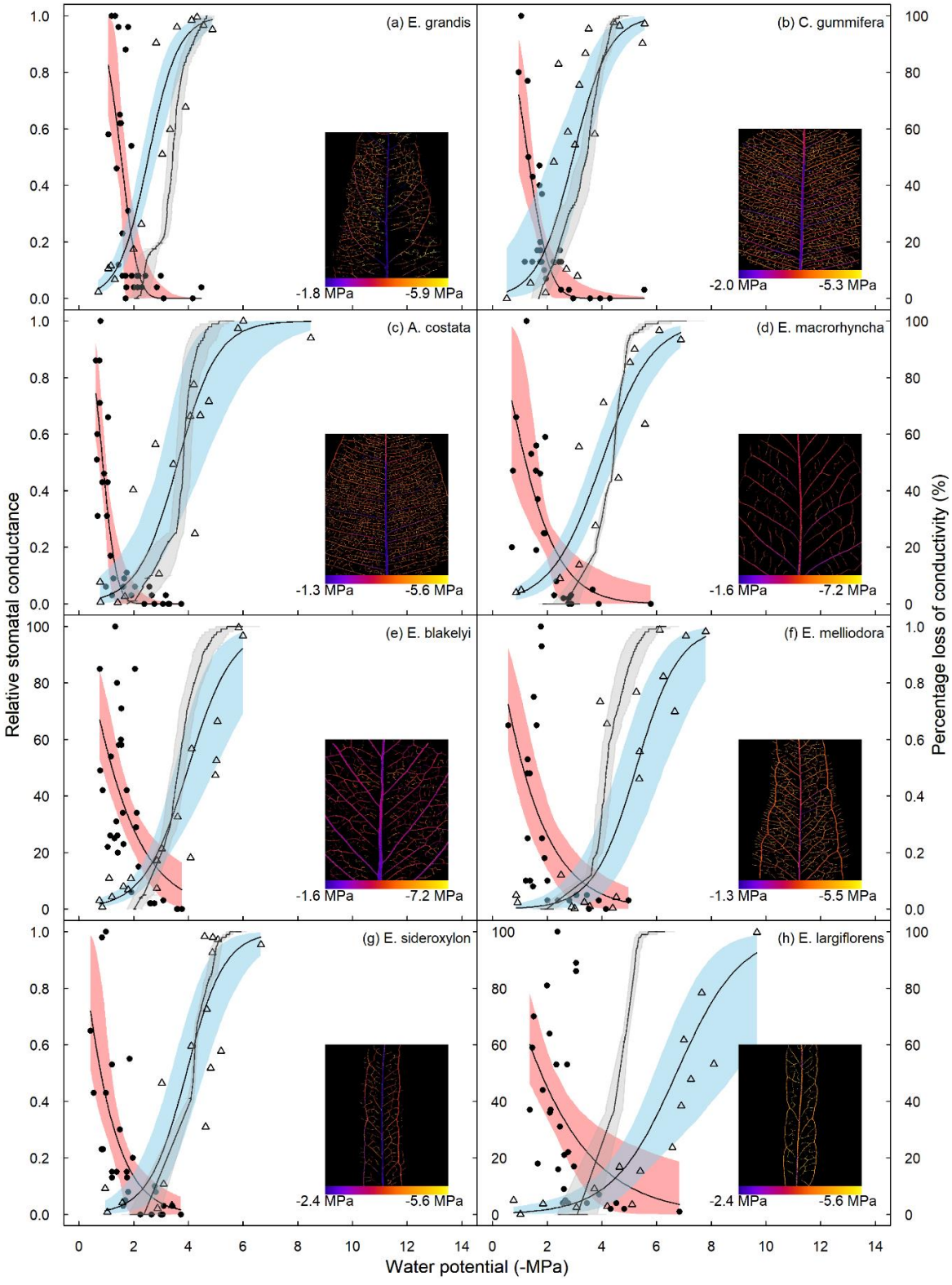

Chapter 5 Figure A-5 Historical rainfall amount (1970-2015) during the same seasonal period (i.e. 10 Jul to 15 Oct) logged by the weather station near our sampling site (www.bom.gov.au, Station number: 063246). Mean precipitation during this period is *ca*. 160 mm. Only rainfall years with complete datasets during this period were presented. Climate data were obtained from Australian Bureau of Meteorology.

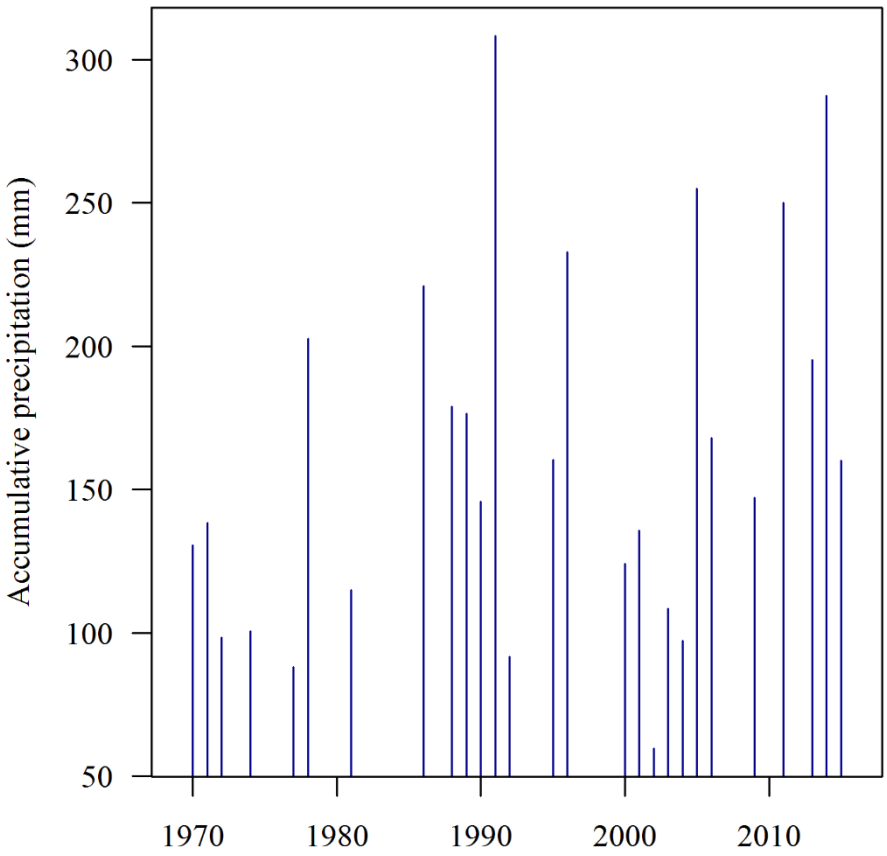

Chapter 5 Figure A-6 Leaf specific conductivity (K_L, kg m^{-1} s^{-1} MPa^{-1}) of dieback and healthy trees. Error bars indicate standard error (n=4 for dieback trees and n=3 for healthy trees). Difference in K_L was tested using linear mixed-effect model and was marginally significant (p=0.05).

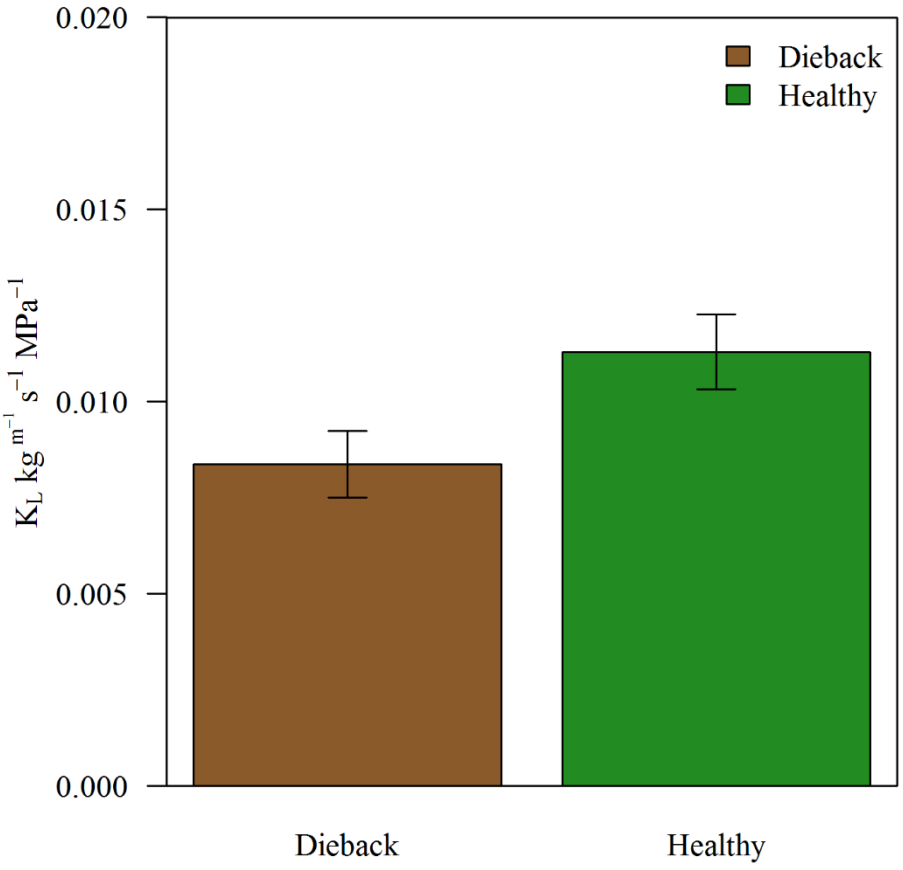

Chapter 5 Figure A-7 Leaf capacitance (C, mmol m^{-2} MPa^{-1}) of E. *piperita* before (C_{pre}) and after (C_{post}) leaf turgor loss. Error bars indicate standard error of mean (n=6). Both C_{pre} and C_{post} showed small variation among individual leaves.

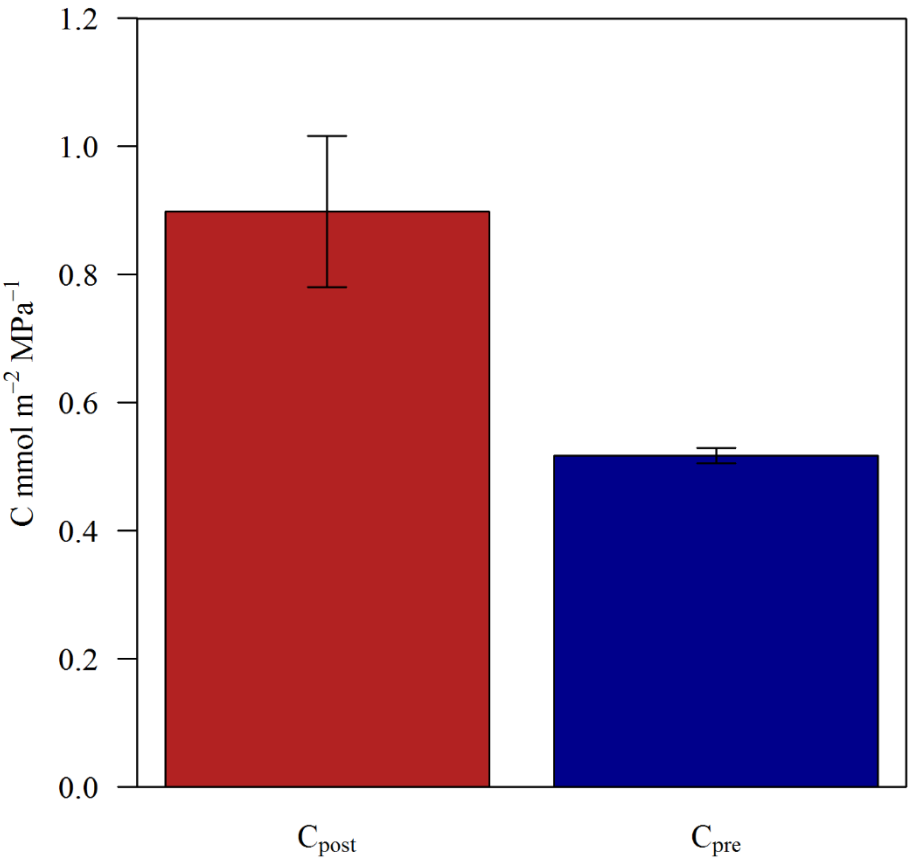

Chapter 5 Figure A-8 A basic diagram of the branching architecture of *E. piperita* trees. Importantly, we measured native embolism in tertiary branchlets (coloured) at a range of distances from the tip of the lower order secondary branch to which they were attached.

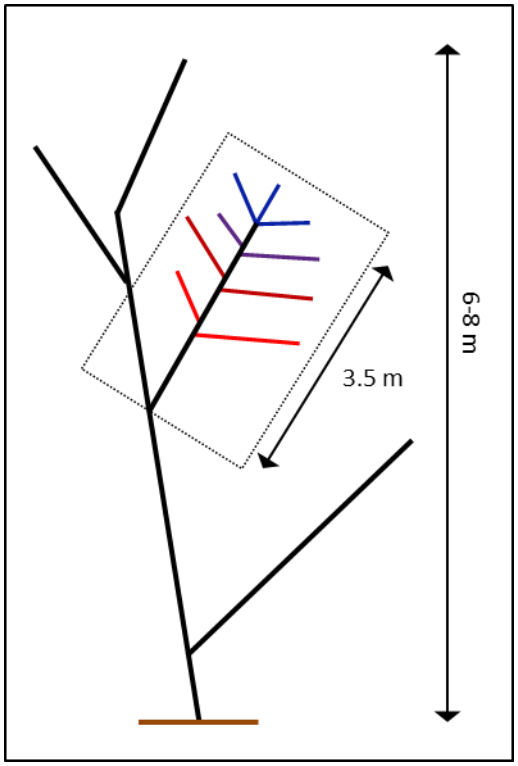

References

Adams HD, Guardiola-Claramonte M, Barron-Gafford GA, Villegas JC, Breshears DD, Zou CB, et al. (2009). Temperature sensitivity of drought-induced tree mortality portends increased regional die-off under global-change-type drought. Proceedings of the National Academy of Sciences 106: 7063-7066.

Adams HD, Williams AP, Xu C, Rauscher SA, Jiang X,McDowell NG (2013). Empirical and process-based approaches to climate-induced forest mortality models. Frontiers in plant science 4: 438.

Adams HD, Zeppel MJ, Anderegg WR, Hartmann H, Landhäusser SM, Tissue DT, et al. (2017). A multi-species synthesis of physiological mechanisms in drought-induced tree mortality. Nature ecology & evolution 1: 1285–1291.

Allen CD, Breshears DD,McDowell NG (2015). On underestimation of global vulnerability to tree mortality and forest die-off from hotter drought in the Anthropocene. Ecosphere 6: 1-55.

Allen CD, Macalady AK, Chenchouni H, Bachelet D, McDowell N, Vennetier M, et al. (2010). A global overview of drought and heat-induced tree mortality reveals emerging climate change risks for forests. Forest ecology and management 259: 660-684.

Anderegg WR (2015). Spatial and temporal variation in plant hydraulic traits and their relevance for climate change impacts on vegetation. New phytologist 205: 1008-1014.

Anderegg WR,Anderegg LD (2013a). Hydraulic and carbohydrate changes in experimental drought-induced mortality of saplings in two conifer species. Tree Physiol 33: 252-260.

Anderegg WR, Berry JA,Field CB (2012a). Linking definitions, mechanisms, and modeling of drought-induced tree death. Trends in plant science 17: 693-700.

Anderegg WR, Berry JA, Smith DD, Sperry JS, Anderegg LD,Field CB (2012b). The roles of hydraulic and carbon stress in a widespread climate-induced forest die-off. Proceedings of the National Academy of Sciences 109: 233-237.

Anderegg WR, Hicke JA, Fisher RA, Allen CD, Aukema J, Bentz B, et al. (2015). Tree mortality from drought, insects, and their interactions in a changing climate. New phytologist 208: 674-683.

Anderegg WR, Kane JM,Anderegg LD (2013b). Consequences of widespread tree mortality triggered by drought and temperature stress. Nature Climate Change 3: 30-36.

Anderegg WR, Klein T, Bartlett M, Sack L, Pellegrini AF, Choat B, et al. (2016). Meta-analysis reveals that hydraulic traits explain cross-species patterns of drought-induced tree mortality across the globe. Proceedings of the National Academy of Sciences 113: 5024-5029.

Attia Z, Domec J-C, Oren R, Way DA,Moshelion M (2015). Growth and physiological responses of isohydric and anisohydric poplars to drought. Journal of Experimental Botany 66: 4373-4381.

Bartlett MK, Klein T, Jansen S, Choat B,Sack L (2016). The correlations and sequence of plant stomatal, hydraulic, and wilting responses to drought. Proceedings of the National Academy of Sciences 113: 13098-13103.

Bartlett MK, Scoffoni C,Sack L (2012). The determinants of leaf turgor loss point and prediction of drought tolerance of species and biomes: a global meta-analysis. Ecology letters 15: 393-405.

Berger-Landefeldt U (1936). Der Wasserhaushalt der Alpenpflanzen. Bibliotheca Botanica 115.

Binkley D, Stape JL, Bauerle WL,Ryan MG (2010). Explaining growth of individual trees: light interception and efficiency of light use by Eucalyptus at four sites in Brazil. Forest ecology and management 259: 1704-1713.

Blackman CJ (2018). Leaf turgor loss as a predictor of plant drought response strategies. Tree physiology 38: 655-657.

Blackman CJ, Aspinwall MJ, Resco de Dios V, Smith RA,Tissue DT (2016a). Leaf photosynthetic, economics and hydraulic traits are decoupled among genotypes of a

widespread species of eucalypt grown under ambient and elevated CO_2. Functional Ecology 30: 1491-1500.

Blackman CJ, Aspinwall MJ, Tissue DT,Rymer PD (2017). Genetic adaptation and phenotypic plasticity contribute to greater leaf hydraulic tolerance in response to drought in warmer climates. Tree physiology 37: 583-592.

Blackman CJ, Brodribb TJ,Jordan GJ (2009). Leaf hydraulics and drought stress: response, recovery and survivorship in four woody temperate plant species. Plant, cell & environment 32: 1584-1595.

Blackman CJ, Brodribb TJ,Jordan GJ (2010). Leaf hydraulic vulnerability is related to conduit dimensions and drought resistance across a diverse range of woody angiosperms. New phytologist 188: 1113-1123.

Blackman CJ, Gleason SM, Chang Y, Cook AM, Laws C,Westoby M (2014). Leaf hydraulic vulnerability to drought is linked to site water availability across a broad range of species and climates. Annals of botany 114: 435-440.

Blackman CJ, Pfautsch S, Choat B, Delzon S, Gleason SM,Duursma RA (2016b). Toward an index of desiccation time to tree mortality under drought. Plant, cell & environment 39: 2342-2345.

Bonan GB (2008). Forests and climate change: forcings, feedbacks, and the climate benefits of forests. science 320: 1444-1449.

Bourne AE, Creek D, Peters JM, Ellsworth DS,Choat B (2017). Species climate range influences hydraulic and stomatal traits in *Eucalyptus* species. Annals of botany 120: 123-133.

Bradstock RA,Myerscough PJ (1988). The survival and population response to frequent fires of two woody resprouters Banksia serrata and Isopogon anemonifolius. Australian Journal of Botany 36: 415-431.

Breshears DD, Myers OB, Meyer CW, Barnes FJ, Zou CB, Allen CD, et al. (2009). Tree die-off in response to global change-type drought: Mortality insights from a decade of plant water potential measurements. Frontiers in Ecology and the Environment 7: 185-189.

Brodersen CR, Knipfer T,McElrone AJ (2018). In vivo visualization of the final stages of xylem vessel refilling in grapevine (*Vitis vinifera*) stems. New phytologist 217: 117-126.

Brodersen CR, McElrone AJ, Choat B, Lee EF, Shackel KA,Matthews MA (2013). *In vivo* visualizations of drought-induced embolism spread in Vitis vinifera. Plant physiology 161: 1820-1829.

Brodersen CR, McElrone AJ, Choat B, Matthews MA,Shackel KA (2010). The dynamics of embolism repair in xylem: In vivo visualizations using high-resolution computed tomography. Plant physiology 154: 1088-1095.

Brodribb T,Feild T (2000). Stem hydraulic supply is linked to leaf photosynthetic capacity: evidence from New Caledonian and Tasmanian rainforests. Plant, cell & environment 23: 1381-1388.

Brodribb T,Hill RS (1999). The importance of xylem constraints in the distribution of conifer species. New phytologist 143: 365-372.

Brodribb T, Holbrook N, Edwards E,Gutierrez M (2003a). Relations between stomatal closure, leaf turgor and xylem vulnerability in eight tropical dry forest trees. Plant, cell & environment 26: 443-450.

Brodribb TJ, Bowman DJ, Nichols S, Delzon S,Burlett R (2010). Xylem function and growth rate interact to determine recovery rates after exposure to extreme water deficit. New phytologist 188: 533-542.

Brodribb TJ,Cochard H (2009). Hydraulic failure defines the recovery and point of death in water-stressed conifers. Plant physiology 149: 575-584.

Brodribb TJ,Holbrook NM (2003b). Stomatal closure during leaf dehydration, correlation with other leaf physiological traits. Plant physiology 132: 2166-2173.

Brodribb TJ,McAdam SA (2011). Passive origins of stomatal control in vascular plants. science 331: 582-585.

Brodribb TJ, McAdam SA,Carins Murphy MR (2017). Xylem and stomata, coordinated through time and space. Plant, cell & environment 40: 872-880.

Brodribb TJ, Skelton RP, McAdam SA, Bienaimé D, Lucani CJ,Marmottant P (2016). Visual quantification of embolism reveals leaf vulnerability to hydraulic failure. New phytologist 209: 1403-1409.

Canham CA, Froend RH,Stock WD (2009). Water stress vulnerability of four *Banksia* species in contrasting ecohydrological habitats on the Gnangara Mound, Western Australia. Plant, cell & environment 32: 64-72.

Chapotin SM, Razanameharizaka JH,Holbrook NM (2006). Water relations of baobab trees (*Adansonia spp*. L.) during the rainy season: does stem water buffer daily water deficits? Plant, cell & environment 29: 1021-1032.

Charrier G, Torres-Ruiz JM, Badel E, Burlett R, Choat B, Cochard H, et al. (2016). Evidence for hydraulic vulnerability segmentation and lack of xylem refilling under tension. Plant physiology 172: 1657-1668.

Choat B (2013). Predicting thresholds of drought-induced mortality in woody plant species. Tree physiology 33: 669-671.

Choat B, Badel E, Burlett R, Delzon S, Cochard H,Jansen S (2015a). Non-invasive measurement of vulnerability to drought induced embolism by X-ray microtomography. Plant physiology 170: 273-282.

Choat B, Brodersen CR,McElrone AJ (2015b). Synchrotron X-ray microtomography of xylem embolism in *Sequoia sempervirens* saplings during cycles of drought and recovery. New phytologist 205: 1095-1105.

Choat B, Brodie TW, Cobb AR, Zwieniecki MA,Holbrook NM (2006). Direct measurements of intervessel pit membrane hydraulic resistance in two angiosperm tree species. American journal of botany 93: 993-1000.

Choat B, Brodribb TJ, Brodersen CR, Duursma RA, López R,Medlyn BE (2018a). Triggers of tree mortality under drought. Nature 558: 531-539.

Choat B, Cobb AR,Jansen S (2008). Structure and function of bordered pits: new discoveries and impacts on whole-plant hydraulic function. New phytologist 177: 608-625.

Choat B, Drayton WM, Brodersen C, Matthews MA, Shackel KA, Wada H, et al. (2010). Measurement of vulnerability to water stress-induced cavitation in grapevine: a comparison of four techniques applied to a long-vesseled species. Plant Cell and Environment 33: 1502-1512.

Choat B, Jansen S, Brodribb TJ, Cochard H, Delzon S, Bhaskar R, et al. (2012). Global convergence in the vulnerability of forests to drought. Nature 491: 752-755.

Choat B, Medek DE, Stuart SA, Pasquet-Kok J, Egerton JJ, Salari H, et al. (2011). Xylem traits mediate a trade-off between resistance to freeze-thaw-induced embolism and photosynthetic capacity in overwintering evergreens. New phytologist 191: 996-1005.

Choat B, Nolf M, Lopez R, Peters JM, Carins-Murphy MR, Creek D, et al. (2018b). Non-invasive imaging shows no evidence of embolism repair after drought in tree species of two genera. Tree physiology 39: 113-121.

Choat B, Sack L,Holbrook NM (2007). Diversity of hydraulic traits in nine Cordia species growing in tropical forests with contrasting precipitation. New Phytologist 175: 686-698.

Christoffersen BO, Gloor M, Fauset S, Fyllas NM, Galbraith DR, Baker TR, et al. (2016). Linking hydraulic traits to tropical forest function in a size-structured and trait-driven model (TFS v. 1-Hydro). Geoscientific Model Development 9: 4227-4255.

Cochard H, Casella E,Mencuccini M (2007). Xylem vulnerability to cavitation varies among poplar and willow clones and correlates with yield. Tree physiology 27: 1761-1767.

Cochard H, Froux F, Mayr S,Coutand C (2004). Xylem wall collapse in water-stressed pine needles. Plant physiology 134: 401-408.

Corcuera L, Cochard H, Gil-Pelegrin E,Notivol E (2011). Phenotypic plasticity in mesic populations of Pinus pinaster improves resistance to xylem embolism (P_{50}) under severe drought. Trees 25: 1033-1042.

Creek D, Blackman CJ, Brodribb TJ, Choat B,Tissue DT (2018). Coordination between leaf, stem, and root hydraulics and gas exchange in three arid-zone angiosperms during severe drought and recovery. Plant, cell & environment 41: 2869-2881.

Dai A (2013). Increasing drought under global warming in observations and models. Nature Climate Change 3: 52-58.

Davis SD, Ewers FW, Sperry JS, Portwood KA, Crocker MC,Adams GC (2002). Shoot dieback during prolonged drought in *Ceanothus* (*Rhamnaceae*) chaparral of California: a possible case of hydraulic failure. American journal of botany 89: 820-828.

de Villemereuil P, Gaggiotti OE, Mouterde M,Till-Bottraud I (2016). Common garden experiments in the genomic era: new perspectives and opportunities. Heredity 116: 249-254.

Delzon S,Cochard H (2014). Recent advances in tree hydraulics highlight the ecological significance of the hydraulic safety margin. New phytologist 203: 355-358.

Drake JE, Tjoelker MG, Vårhammar A, Medlyn BE, Reich PB, Leigh A, et al. (2018). Trees tolerate an extreme heatwave via sustained transpirational cooling and increased leaf thermal tolerance. Global Change Biology 24: 2390-2402.

Duan H, Duursma RA, Huang G, Smith RA, Choat B, O'Grady AP, et al. (2014). Elevated [CO_2] does not ameliorate the negative effects of elevated temperature on drought-induced mortality in Eucalyptus radiata seedlings. Plant, cell & environment 37: 1598-1613.

Duursma R,Choat B (2017). fitplc-an R package to fit hydraulic vulnerability curves. Journal of Plant Hydraulics 4: 002.

Duursma RA, Blackman CJ, Lopéz R, Martin-StPaul NK, Cochard H,Medlyn BE (2019). On the minimum leaf conductance: its role in models of plant water use, and ecological and environmental controls. New phytologist 221: 693-705.

Engelbrecht BM, Comita LS, Condit R, Kursar TA, Tyree MT, Turner BL, et al. (2007). Drought sensitivity shapes species distribution patterns in tropical forests. Nature 447: 80-82.

Fan Y, Miguez-Macho G, Jobbágy EG, Jackson RB,Otero-Casal C (2017). Hydrologic regulation of plant rooting depth. Proceedings of the National Academy of Sciences 114: 10572-10577.

Farrell C, Szota C,Arndt SK (2017). Does the turgor loss point characterize drought response in dryland plants? Plant, cell & environment 40: 1500–1511.

Fisher JB, Huntzinger DN, Schwalm CR,Sitch S (2014). Modeling the terrestrial biosphere. Annual Review of Environment and Resources 39: 91-123.

Freestone M, Wills TJ,Read J (2015). Post-fire succession during the long-term absence of fire in coastal heathland and a test of the chronosequence survey method. Australian Journal of Botany 63: 572-580.

Fu X,Meinzer FC (2018). Metrics and proxies for stringency of regulation of plant water status (iso/anisohydry): a global data set reveals coordination and trade-offs among water transport traits. Tree physiology 39: 122-134.

Garcia-Forner N, Sala A, Biel C, Savé R,Martínez-Vilalta J (2016). Individual traits as determinants of time to death under extreme drought in *Pinus sylvestris* L. Tree physiology 36: 1196-1209.

Garcia-Forner N, Adams HD, Sevanto S, Collins AD, Dickman LT, Hudson PJ, et al. (2016). Responses of two semiarid conifer tree species to reduced precipitation and warming reveal new perspectives for stomatal regulation. Plant, cell & environment 39: 38-49.

Gleason SM, Blackman CJ, Cook AM, Laws CA,Westoby M (2014). Whole-plant capacitance, embolism resistance and slow transpiration rates all contribute to longer desiccation times in woody angiosperms from arid and wet habitats. Tree physiology 34: 275-284.

Gleason SM, Butler DW,Waryszak P (2013). Shifts in leaf and stem hydraulic traits across aridity gradients in eastern Australia. International Journal of Plant Sciences 174: 1292-1301.

Gleason SM, Westoby M, Jansen S, Choat B, Hacke UG, Pratt RB, et al. (2016). Weak tradeoff between xylem safety and xylem-specific hydraulic efficiency across the world's woody plant species. New phytologist 209: 123-136.

González-Muñoz N, Sterck F, Torres-Ruiz J, Petit G, Cochard H, von Arx G, et al. (2018). Quantifying in situ phenotypic variability in the hydraulic properties of four tree species across their distribution range in Europe. PloS one 13: e0196075.

Hacke UG, Sperry JS, Pockman WT, Davis SD,McCulloh KA (2001a). Trends in wood density and structure are linked to prevention of xylem implosion by negative pressure. Oecologia 126: 457-461.

Hacke UG, Stiller V, Sperry JS, Pittermann J,McCulloh KA (2001b). Cavitation fatigue. Embolism and refilling cycles can weaken the cavitation resistance of xylem. Plant physiology 125: 779-786.

Hajek P, Leuschner C, Hertel D, Delzon S,Schuldt B (2014). Trade-offs between xylem hydraulic properties, wood anatomy and yield in Populus. Tree physiology 34: 744-756.

Hochberg U, Rockwell FE, Holbrook NM,Cochard H (2018). Iso/Anisohydry: A Plant-Environment Interaction Rather Than a Simple Hydraulic Trait. Trends in plant science 23: 112-120.

Hochberg U, Windt CW, Ponomarenko A, Zhang YJ, Gersony J, Rockwell FE, et al. (2017). Stomatal closure, basal leaf embolism and shedding protect the hydraulic integrity of grape stems. Plant physiology 175: 764-775.

Hoffmann WA, Marchin RM, Abit P,Lau OL (2011). Hydraulic failure and tree dieback are associated with high wood density in a temperate forest under extreme drought. Global Change Biology 17: 2731-2742.

Jacobsen AL, Ewers FW, Pratt RB, Paddock WA,Davis SD (2005). Do xylem fibers affect vessel cavitation resistance? Plant physiology 139: 546-556.

Jacobsen AL, Pratt RB, Davis SD,Ewers FW (2007). Cavitation resistance and seasonal hydraulics differ among three arid Californian plant communities. Plant, cell & environment 30: 1599-1609.

Jacobsen AL, Pratt RB, Davis SD,Ewers FW (2008). Comparative community physiology: Nonconvergence in water relations among three semi-arid shrub communities. New phytologist 180: 100-113.

Johnson DM, Berry ZC, Baker KV, Smith DD, McCulloh KA,Domec JC (2018a). Leaf hydraulic parameters are more plastic in species that experience a wider range of leaf water potentials. Functional Ecology 32: 894-903.

Johnson DM, Domec JC, Carter Berry Z, Schwantes AM, McCulloh KA, Woodruff DR, et al. (2018b). Co-occurring woody species have diverse hydraulic strategies and mortality rates during an extreme drought. Plant, cell & environment 41: 576-588.

Jordan GJ, Brodribb TJ, Blackman CJ,Weston PH (2013). Climate drives vein anatomy in Proteaceae. American journal of botany 100: 1483-1493.

Kavanagh K, Bond B, Aitken S, Gartner B,Knowe S (1999). Shoot and root vulnerability to xylem cavitation in four populations of Douglas-fir seedlings. Tree physiology 19: 31-37.

Klein T (2014). The variability of stomatal sensitivity to leaf water potential across tree species indicates a continuum between isohydric and anisohydric behaviours. Functional Ecology 28: 1313-1320.

Klein T, Yakir D, Buchmann N,Grünzweig JM (2014). Towards an advanced assessment of the hydrological vulnerability of forests to climate change-induced drought. New phytologist 201: 712-716.

Klepsch M, Zhang Y, Kotowska MM, Lamarque LJ, Nolf M, Schuldt B, et al. (2018). Is xylem of angiosperm leaves less resistant to embolism than branches? Insights from microCT, hydraulics, and anatomy. Journal of Experimental Botany 69: 5611-5623.

Kolb KJ, Sperry JS (1999). Differences in drought adaptation between subspecies of sagebrush (*Artemisia tridentata*). Ecology 80: 2373-2384.

Konings AG, Gentine P (2017). Global variations in ecosystem-scale isohydricity. Global Change Biology 23: 891-905.

Kursar TA, Engelbrecht BMJ, Burke A, Tyree MT, El Omari B,Giraldo JP (2009). Tolerance to low leaf water status of tropical tree seedlings is related to drought performance and distribution. Functional Ecology 23: 93-102.

Lamy JB, Lagane F, Plomion C, Cochard H,Delzon S (2012). Micro-evolutionary patterns of juvenile wood density in a pine species. Plant Ecology 213: 1781-1792.

Lamy JB, Delzon S, Bouche PS, Alia R, Vendramin GG, Cochard H, et al. (2014). Limited genetic variability and phenotypic plasticity detected for cavitation resistance in a Mediterranean pine. New phytologist 201: 874-886.

Larter M, Pfautsch S, Domec JC, Trueba S, Nagalingum N,Delzon S (2017). Aridity drove the evolution of extreme embolism resistance and the radiation of conifer genus *Callitris*. New phytologist 215: 97-112.

Lavoie-Lamoureux A, Sacco D, Risse PA,Lovisolo C (2017). Factors influencing stomatal conductance in response to water availability in grapevine: a meta-analysis. Physiologia Plantarum 159: 468-482.

Lens F, Sperry JS, Christman MA, Choat B, Rabaey D,Jansen S (2011). Testing hypotheses that link wood anatomy to cavitation resistance and hydraulic conductivity in the genus *Acer*. New phytologist 190: 709-723.

Lenz TI, Wright IJ,Westoby M (2006). Interrelations among pressure-volume curve traits across species and water availability gradients. Physiologia Plantarum 127: 423-433.

Leuzinger S, Zotz G, Asshoff R,Körner C (2005). Responses of deciduous forest trees to severe drought in Central Europe. Tree physiology 25: 641-650.

Li L, McCormack ML, Ma C, Kong D, Zhang Q, Chen X, et al. (2015a). Leaf economics and hydraulic traits are decoupled in five species-rich tropical-subtropical forests. Ecology letters 18: 899-906.

Li S, Feifel M, Karimi Z, Schuldt B, Choat B,Jansen S (2016). Leaf gas exchange performance and the lethal water potential of five European species during drought. Tree physiology 36: 179-192.

Li X, Blackman C, Choat B, Rymer P, Medlyn B,Tissue D (2019a). Drought tolerance traits do not vary across sites differing in water availability in *Banksia serrata* (Proteaceae). Functional plant biology.

Li X, Blackman CJ, Choat B, Duursma RA, Rymer PD, Medlyn BE, et al. (2018a). Tree hydraulic traits are coordinated and strongly linked to climate-of-origin across a rainfall gradient. Plant, cell & environment 41: 646-660.

Li X, Blackman CJ, Rymer PD, Quintans D, Duursma RA, Choat B, et al. (2018b). Xylem embolism measured retrospectively is linked to canopy dieback in natural populations of Eucalyptus piperita following drought. Tree physiology 38: 1193-1199.

Li X, Blackman CJ, Peters JM, Choat B, Rymer PD, Medlyn BE, et al. (2019b). More than iso/anisohydry: Hydroscapes integrate plant water-use and drought tolerance traits in ten eucalypt species from contrasting climates. Functional Ecology.

Liu YY, Wang AY, An YN, Lian PY, Wu DD, Zhu JJ, et al. (2018). Hydraulics play an important role in causing low growth rate and dieback of aging *Pinus sylvestris* var. mongolica trees in plantations of Northeast China. Plant, cell & environment 41: 1500-1511.

Lobo A, Torres-Ruiz JM, Burlett R, Lemaire C, Parise C, Francioni C, et al. (2018). Assessing inter-and intraspecific variability of xylem vulnerability to embolism in oaks. Forest ecology and management 424: 53-61.

López R, Cano FJ, Choat B, Cochard H,Gil L (2016). Plasticity in vulnerability to cavitation of Pinus canariensis occurs only at the driest end of an aridity gradient. Frontiers in plant science 7: 769.

Maherali H,DeLucia EH (2000). Xylem conductivity and vulnerability to cavitation of ponderosa pine growing in contrasting climates. Tree physiology 20: 859-867.

Maherali H, Moura CF, Caldeira MC, Willson CJ,Jackson RB (2006). Functional coordination between leaf gas exchange and vulnerability to xylem cavitation in temperate forest trees. Plant, cell & environment 29: 571-583.

Maherali H, Pockman WT,Jackson RB (2004). Adaptive variation in the vulnerability of woody plants to xylem cavitation. Ecology 85: 2184-2199.

Manion PD (1981). Tree disease concepts, Prentice-Hall, Inc.

Maréchaux I, Bartlett MK, Sack L, Baraloto C, Engel J, Joetzjer E, et al. (2015). Drought tolerance as predicted by leaf water potential at turgor loss point varies strongly across species within an Amazonian forest. Functional Ecology 29: 1268-1277.

Markesteijn L, Poorter L, Paz H, Sack L,Bongers F (2011). Ecological differentiation in xylem cavitation resistance is associated with stem and leaf structural traits. Plant, cell & environment 34: 137-148.

Martin-StPaul N, Delzon S,Cochard H (2017). Plants resistance to drought relies on early stomata closure. bioRxiv: 099531.

Martínez-Vilalta J, Cochard H, Mencuccini M, Sterck F, Herrero A, Korhonen J, et al. (2009). Hydraulic adjustment of Scots pine across Europe. New phytologist 184: 353-364.

Martínez-Vilalta J,Garcia-Forner N (2017). Water potential regulation, stomatal behaviour and hydraulic transport under drought: deconstructing the iso/anisohydric concept. Plant, cell & environment 40: 962-976.

Martínez-Vilalta J, Poyatos R, Aguadé D, Retana J,Mencuccini M (2014). A new look at water transport regulation in plants. New phytologist 204: 105-115.

Martorell S, Diaz-Espejo A, Medrano H, Ball MC, Choat B (2014). Rapid hydraulic recovery in Eucalyptus pauciflora after drought: linkages between stem hydraulics and leaf gas exchange. Plant Cell and Environment 37: 617-626.

Matusick G, Ruthrof KX, Brouwers NC, Dell B, Hardy GSJ (2013). Sudden forest canopy collapse corresponding with extreme drought and heat in a mediterranean-type eucalypt forest in southwestern Australia. European Journal of Forest Research 132: 497-510.

McCulloh KA, Meinzer FC, Sperry JS, Lachenbruch B, Voelker SL, Woodruff DR, et al. (2011). Comparative hydraulic architecture of tropical tree species representing a range of successional stages and wood density. Oecologia 167: 27-37.

McDowell N, Pockman WT, Allen CD, Breshears DD, Cobb N, Kolb T, et al. (2008). Mechanisms of plant survival and mortality during drought: why do some plants survive while others succumb to drought? New phytologist 178: 719-739.

McDowell NG (2011a). Mechanisms linking drought, hydraulics, carbon metabolism, and vegetation mortality. Plant physiology 155: 1051-1059.

McDowell NG, Allen CD (2015). Darcy's law predicts widespread forest mortality under climate warming. Nature Climate Change 5: 669-672.

McDowell NG, Beerling DJ, Breshears DD, Fisher RA, Raffa KF, Stitt M (2011b). The interdependence of mechanisms underlying climate-driven vegetation mortality. Trends in ecology & evolution 26: 523-532.

McDowell NG, Fisher RA, Xu C, Domec J, Hölttä T, Mackay DS, et al. (2013a). Evaluating theories of drought-induced vegetation mortality using a multimodel-experiment framework. New phytologist 200: 304-321.

McDowell NG, Ryan MG, Zeppel MJ, Tissue DT (2013b). Feature: Improving our knowledge of drought-induced forest mortality through experiments, observations, and modeling. New phytologist 200: 289-293.

Meinzer FC, James SA, Goldstein G (2004). Dynamics of transpiration, sap flow and use of stored water in tropical forest canopy trees. Tree physiology 24: 901-909.

Meinzer FC, Johnson DM, Lachenbruch B, McCulloh KA, Woodruff DR (2009). Xylem hydraulic safety margins in woody plants: coordination of stomatal control of xylem tension with hydraulic capacitance. Functional Ecology 23: 922-930.

Meinzer FC, McCulloh KA (2013). Xylem recovery from drought-induced embolism: where is the hydraulic point of no return? Tree physiology 33: 331-334.

Meinzer FC, McCulloh KA, Lachenbruch B, Woodruff DR, Johnson DM (2010). The blind men and the elephant: the impact of context and scale in evaluating conflicts between plant hydraulic safety and efficiency. Oecologia 164: 287-296.

Meinzer FC, Woodruff DR, Marias DE, McCulloh KA, Sevanto S (2014). Dynamics of leaf water relations components in co-occurring iso-and anisohydric conifer species. Plant, cell & environment 37: 2577-2586.

Meinzer FC, Woodruff DR, Marias DE, Smith DD, McCulloh KA, Howard AR, et al. (2016). Mapping ‘hydroscapes’ along the iso-to anisohydric continuum of stomatal regulation of plant water status. Ecology letters 19: 1343-1352.

Mencuccini M, Grace J (1995). Climate influences the leaf area/sapwood area ratio in Scots pine. Tree physiology 15: 1-10.

Mitchell PJ, O'Grady AP (2015). Adaptation of leaf water relations to climatic and habitat water availability. Forests 6: 2281-2295.

Mitchell PJ, O'Grady AP, Hayes KR, Pinkard EA (2014). Exposure of trees to drought-induced die-off is defined by a common climatic threshold across different vegetation types. Ecology and Evolution 4: 1088-1101.

Mitchell PJ, O'grady AP, Pinkard EA, Brodribb TJ, Arndt SK, Blackman CJ, et al. (2016). An ecoclimatic framework for evaluating the resilience of vegetation to water deficit. Global Change Biology 22: 1677-1689.

Mott K, Franks P (2001). The role of epidermal turgor in stomatal interactions following a local perturbation in humidity. Plant, cell & environment 24: 657-662.

Munné-Bosch S, Alegre L (2004). Die and let live: leaf senescence contributes to plant survival under drought stress. Functional Plant Biology 31: 203-216.

Nadal M, Flexas J, Gulías J (2018). Possible link between photosynthesis and leaf modulus of elasticity among vascular plants: a new player in leaf traits relationships? Ecology letters 21: 1372-1379.

Nardini A, Battistuzzo M, Savi T (2013). Shoot desiccation and hydraulic failure in temperate woody angiosperms during an extreme summer drought. New phytologist 200: 322-329.

Nardini A, Salleo S (2000). Limitation of stomatal conductance by hydraulic traits: sensing or preventing xylem cavitation? Trees-Structure and Function 15: 14-24.

Nicholls N, Drosdowsky W, Lavery B (1997). Australian rainfall variability and change. Weather 52: 66-72.

Nicotra AB, Atkin OK, Bonser SP, Davidson AM, Finnegan E, Mathesius U, et al. (2010). Plant phenotypic plasticity in a changing climate. Trends in plant science 15: 684-692.

Niinemets Ü (2001). Global-scale climatic controls of leaf dry mass per area, density, and thickness in trees and shrubs. Ecology 82: 453-469.

Nolf M, Creek D, Duursma R, Holtum J, Mayr S, Choat B (2015). Stem and leaf hydraulic properties are finely coordinated in three tropical rain forest tree species. Plant Cell and Environment 38: 2652-2661.

O'Brien MJ, Ong R, Reynolds G (2017). Intra-annual plasticity of growth mediates drought resilience over multiple years in tropical seedling communities. Global Change Biology: 1-10.

O'Brien MJ, Leuzinger S, Philipson CD, Tay J, Hector A (2014). Drought survival of tropical tree seedlings enhanced by non-structural carbohydrate levels. Nature Climate Change 4: 710-714.

Ogasa M, Miki NH, Murakami Y, Yoshikawa K (2013). Recovery performance in xylem hydraulic conductivity is correlated with cavitation resistance for temperate deciduous tree species. Tree physiology 33: 335-344.

Oliveira RS, Costa FR, van Baalen E, de Jonge A, Bittencourt PR, Almanza Y, et al. (2019). Embolism resistance drives the distribution of Amazonian rainforest tree species along hydro-topographic gradients. New phytologist 221: 1457-1465.

Oren R, Sperry J, Katul G, Pataki D, Ewers B, Phillips N, et al. (1999). Survey and synthesis of intra-and interspecific variation in stomatal sensitivity to vapour pressure deficit. Plant, cell & environment 22: 1515-1526.

Pan Y, Birdsey RA, Fang J, Houghton R, Kauppi PE, Kurz WA, et al. (2011). A large and persistent carbon sink in the world's forests. science 333: 988-993.

Pfautsch S, Harbusch M, Wesolowski A, Smith R, Macfarlane C, Tjoelker MG, et al. (2016). Climate determines vascular traits in the ecologically diverse genus *Eucalyptus*. Ecology letters 19: 240-248.

Pfautsch S, Renard J, Tjoelker MG, Salih A (2015). Phloem as capacitor: radial transfer of water into xylem of tree stems occurs via symplastic transport in ray parenchyma. Plant physiology 167: 963-971.

Pivovaroff AL, Cook VM, Santiago LS (2018). Stomatal behavior and stem xylem traits are coordinated for woody plant species under exceptional drought conditions. Plant, cell & environment 41: 2617-2626.

Pivovaroff AL, Sack L, Santiago LS (2014). Coordination of stem and leaf hydraulic conductance in southern California shrubs: a test of the hydraulic segmentation hypothesis. New phytologist 203: 842-850.

Pockman WT, Sperry JS (2000). Vulnerability to xylem cavitation and the distribution of Sonoran desert vegetation. American journal of botany 87: 1287-1299.

Poorter H, Niinemets Ü, Poorter L, Wright IJ, Villar R (2009). Causes and consequences of variation in leaf mass per area (LMA): a meta-analysis. New phytologist 182: 565-588.

Powell TL, Galbraith DR, Christoffersen BO, Harper A, Imbuzeiro H, Rowland L, et al. (2013). Confronting model predictions of carbon fluxes with measurements of Amazon forests subjected to experimental drought. New phytologist 200: 350-365.

Powell TL, Wheeler JK, de Oliveira AA, da Costa L, Carlos A, Saleska SR, et al. (2017). Differences in xylem and leaf hydraulic traits explain differences in drought tolerance among mature Amazon rainforest trees. Global Change Biology 23: 4280-4293.

Pratt RB, Jacobsen AL (2017). Conflicting demands on angiosperm xylem: Tradeoffs among storage, transport and biomechanics. Plant, cell & environment 40: 897-913.

Quero JL, Sterck FJ, Martínez-Vilalta J,Villar R (2011). Water-use strategies of six co-existing Mediterranean woody species during a summer drought. Oecologia 166: 45-57.

Reich PB (2014). The world-wide 'fast-slow' plant economics spectrum: a traits manifesto. Journal of Ecology 102: 275-301.

Richards AE, Wright IJ, Lenz TI,Zanne AE (2014). Sapwood capacitance is greater in evergreen sclerophyll species growing in high compared to low-rainfall environments. Functional Ecology 28: 734-744.

Rogiers SY, Greer DH, Hatfield JM, Hutton RJ, Clarke SJ, Hutchinson PA, et al. (2011). Stomatal response of an anisohydric grapevine cultivar to evaporative demand, available soil moisture and abscisic acid. Tree physiology 32: 249-261.

Russo SE, Jenkins KL, Wiser SK, Uriarte M, Duncan RP,Coomes DA (2010). Interspecific relationships among growth, mortality and xylem traits of woody species from New Zealand. Functional Ecology 24: 253-262.

Ryan MG, Stape JL, Binkley D, Fonseca S, Loos RA, Takahashi EN, et al. (2010). Factors controlling Eucalyptus productivity: how water availability and stand structure alter production and carbon allocation. Forest ecology and management 259: 1695-1703.

Sack L,Holbrook NM (2006). Leaf hydraulics. Annu. Rev. Plant Biol. 57: 361-381.

Sala A, Piper F,Hoch G (2010). Physiological mechanisms of drought-induced tree mortality are far from being resolved. New phytologist 186: 274-281.

Salleo S, Nardini A, Pitt F,Gullo MAL (2000). Xylem cavitation and hydraulic control of stomatal conductance in laurel (*Laurus nobilis* L.). Plant, cell & environment 23: 71-79.

Salmon Y, Torres-Ruiz JM, Poyatos R, Martinez-Vilalta J, Meir P, Cochard H, et al. (2015). Balancing the risks of hydraulic failure and carbon starvation: a twig scale analysis in declining Scots pine. Plant, cell & environment 38: 2575-2588.

Santiago LS, De Guzman ME, Baraloto C, Vogenberg JE, Brodie M, Hérault B, et al. (2018). Coordination and trade-offs among hydraulic safety, efficiency and drought avoidance traits in Amazonian rainforest canopy tree species. New phytologist 218: 1015-1024.

Santiago LS, Goldstein G, Meinzer FC, Fisher JB, Machado K, Woodruff D, et al. (2004). Leaf photosynthetic traits scale with hydraulic conductivity and wood density in Panamanian forest canopy trees. Oecologia 140: 543-550.

Scholz FG, Bucci SJ, Goldstein G, Meinzer FC, Franco AC,Miralles-Wilhelm F (2007). Biophysical properties and functional significance of stem water storage tissues in Neotropical savanna trees. Plant Cell and Environment 30: 236-248.

Schuldt B, Knutzen F, Delzon S, Jansen S, Müller-Haubold H, Burlett R, et al. (2016). How adaptable is the hydraulic system of European beech in the face of climate change-related precipitation reduction? New phytologist 210: 443-458.

Schultz HR,Matthews MA (1993). Xylem development and hydraulic conductance in sun and shade shoots of grapevine (*Vitis vinifera* L.): evidence that low light uncouples water transport capacity from leaf area. Planta 190: 393-406.

Scoffoni C, Vuong C, Diep S, Cochard H,Sack L (2013). Leaf shrinkage with dehydration: coordination with hydraulic vulnerability and drought tolerance. Plant physiology 164: 1772-1788.

Sevanto S, McDowell NG, Dickman LT, Pangle R,Pockman WT (2014). How do trees die? A test of the hydraulic failure and carbon starvation hypotheses. Plant, cell & environment 37: 153-161.

Sevanto S, Xu C (2016). Towards more accurate vegetation mortality predictions. Tree physiology 36: 1191-1195.

Skelton RP, Brodribb TJ,Choat B (2017a). Casting light on xylem vulnerability in an herbaceous species reveals a lack of segmentation. New phytologist 214: 561-569.

Skelton RP, Brodribb TJ, McAdam SA,Mitchell PJ (2017b). Gas exchange recovery following natural drought is rapid unless limited by loss of leaf hydraulic conductance: evidence from an evergreen woodland. New phytologist 215: 1399-1412.

Skelton RP, Dawson TE, Thompson SE, Shen Y, Weitz AP,Ackerly D (2018). Low vulnerability to xylem embolism in leaves and stems of North American oaks. Plant physiology 177: 1066-1077.

Skelton RP, West AG,Dawson TE (2015). Predicting plant vulnerability to drought in biodiverse regions using functional traits. Proceedings of the National Academy of Sciences 112: 5744-5749.

Soudzilovskaia NA, Elumeeva TG, Onipchenko VG, Shidakov II, Salpagarova FS, Khubiev AB, et al. (2013). Functional traits predict relationship between plant abundance dynamic and long-term climate warming. Proceedings of the National Academy of Sciences 110: 18180-18184.

Sperry J, Adler F, Campbell G,Comstock J (1998). Limitation of plant water use by rhizosphere and xylem conductance: results from a model. Plant, cell & environment 21: 347-359.

Sperry JS, Donnelly JR,Tyree MT (1988). A Method for Measuring Hydraulic Conductivity and Embolism in Xylem. Plant Cell and Environment 11: 35-40.

Sperry JS, Venturas MD, Anderegg WR, Mencuccini M, Mackay DS, Wang Y, et al. (2017). Predicting stomatal responses to the environment from the optimization of photosynthetic gain and hydraulic cost. Plant, cell & environment 40: 816-830.

Tai X, Mackay DS, Anderegg WR, Sperry JS,Brooks PD (2017). Plant hydraulics improves and topography mediates prediction of aspen mortality in southwestern USA. New phytologist 213: 113-127.

Torres-Ruiz JM, Jansen S, Choat B, McElrone AJ, Cochard H, Brodribb TJ, et al. (2015). Direct X-ray microtomography observation confirms the induction of embolism upon xylem cutting under tension. Plant physiology 167: 40-43.

Trifilò P, Nardini A, Gullo MAL, Barbera PM, Savi T,Raimondo F (2015). Diurnal changes in embolism rate in nine dry forest trees: relationships with species-specific xylem vulnerability, hydraulic strategy and wood traits. Tree physiology 35: 694-705.

Trueba S, Pouteau R, Lens F, Feild TS, Isnard S, Olson ME, et al. (2017). Vulnerability to xylem embolism as a major correlate of the environmental distribution of rain forest species on a tropical island. Plant, cell & environment 40: 277-289.

Tsuda M,Tyree MT (1997). Whole-plant hydraulic resistance and vulnerability segmentation in *Acer saccharinum*. Tree physiology 17: 351-357.

Tyree M,Hammel H (1972). The measurement of the turgor pressure and the water relations of plants by the pressure-bomb technique. Journal of Experimental Botany 23: 267-282.

Tyree MT,Ewers FW (1991). The hydraulic architecture of trees and other woody plants. New phytologist 119: 345-360.

Tyree MT,Sperry JS (1988). Do woody plants operate near the point of catastrophic xylem dysfunction caused by dynamic water stress? Answers from a model. Plant physiology 88: 574-580.

Urli M, Porté AJ, Cochard H, Guengant Y, Burlett R,Delzon S (2013). Xylem embolism threshold for catastrophic hydraulic failure in angiosperm trees. Tree physiology 33: 672-683.

Venturas MD, MacKinnon ED, Dario HL, Jacobsen AL, Pratt RB,Davis SD (2016). Chaparral shrub hydraulic traits, size, and life history types relate to species mortality during California's historic drought of 2014. PloS one 11: e0159145.

Villagra M, Campanello PI, Bucci SJ,Goldstein G (2013). Functional relationships between leaf hydraulics and leaf economic traits in response to nutrient addition in subtropical tree species. Tree physiology 33: 1308-1318.

Wason JW, Anstreicher KS, Stephansky N, Huggett BA,Brodersen CR (2018). Hydraulic safety margins and air-seeding thresholds in roots, trunks, branches and petioles of four northern hardwood trees. New phytologist 219: 77-88.

Westoby M (1998). A leaf-height-seed (LHS) plant ecology strategy scheme. Plant and soil 199: 213-227.

Wheeler JK, Huggett BA, Tofte AN, Rockwell FE,Holbrook NM (2013). Cutting xylem under tension or supersaturated with gas can generate PLC and the appearance of rapid recovery from embolism. Plant, cell & environment 36: 1938-1949.

Wheeler JK, Sperry JS, Hacke UG, Hoang N (2005). Inter-vessel pitting and cavitation in woody *Rosaceae* and other vesselled plants: a basis for a safety versus efficiency trade-off in xylem transport. Plant, cell & environment 28: 800-812.

Williams AP, Allen CD, Macalady AK, Griffin D, Woodhouse CA, Meko DM, et al. (2013). Temperature as a potent driver of regional forest drought stress and tree mortality. Nature Climate Change 3: 292-297.

Wright IJ, Reich PB, Westoby M, Ackerly DD, Baruch Z, Bongers F, et al. (2004). The worldwide leaf economics spectrum. Nature 428: 821-827.

Xu C, McDowell NG, Sevanto S, Fisher RA (2013). Our limited ability to predict vegetation dynamics under water stress. New phytologist 200: 298-300.

Xu X, Medvigy D, Powers JS, Becknell JM, Guan K (2016). Diversity in plant hydraulic traits explains seasonal and inter-annual variations of vegetation dynamics in seasonally dry tropical forests. New phytologist 212: 80-95.

Zhang S, Zhang J, Cao K (2017). Divergent hydraulic safety strategies in three co-occurring anacardiaceae tree species in a Chinese savanna. Frontiers in plant science 7: 1-10.

Zhu S, Chen Y, Ye Q, He P, Liu H, Li R, et al. (2018). Leaf turgor loss point is correlated with drought tolerance and leaf carbon economics traits. Tree physiology 38: 658-663.

Zhu S, Liu H, Xu Q, Cao K,Ye Q (2016). Are leaves more vulnerable to cavitation than branches? Functional Ecology 30: 1740-1744.

Zimmermann MH, Brown CL (1971). Trees: structure and function. Springer-Verlag: Berlin.

Zimmermann M (1983). Xylem structure and the sscent of sap. Springer-Verlag: Berlin.